A Systematic Review of the Giant Alligatoroid Deinosuchus from the Campanian of North America and Its Implications for the Relationships at the Root of Crocodylia

Authors: Cossette, Adam P., and Brochu, Christopher A.

Source: Journal of Vertebrate Paleontology, 40(1)

Published By: The Society of Vertebrate Paleontology

URL: https://doi.org/10.1080/02724634.2020.1767638

Journal of Vertebrate Paleontology e1767638 (37 pages)
Published with license by the Society of Vertebrate Paleontology
DOI: 10.1080/02724634.2020.1767638

ARTICLE

A SYSTEMATIC REVIEW OF THE GIANT ALLIGATOROID *DEINOSUCHUS* FROM THE CAMPANIAN OF NORTH AMERICA AND ITS IMPLICATIONS FOR THE RELATIONSHIPS AT THE ROOT OF CROCODYLIA

ADAM P. COSSETTE*[,1,2] and CHRISTOPHER A. BROCHU[1]
[1]Department of Earth and Environmental Sciences, University of Iowa, Iowa City, Iowa 52241, U.S.A., chris-brochu@uiowa.edu;
[2]Department of Basic Sciences, New York Institute of Technology College of Osteopathic Medicine–Arkansas, Jonesboro, Arkansas 72401, U.S.A., acossett@nyit.edu

ABSTRACT—*Deinosuchus* is a lineage of giant (≥10 m) Late Cretaceous crocodylians from North America. These were the largest semiaquatic predators in their environments and are known to have fed on large vertebrates, including contemporaneous terrestrial vertebrates such as dinosaurs. Fossils have been found in units of Campanian age from northern Mexico to Montana in the west and Mississippi to New Jersey in the east. Three species have been named, and recent consensus suggests that they represent a single, widely ranging species. The authors studied newly collected material from western Texas and increased sampling from throughout North America to review species-level systematics of *Deinosuchus* and help refine its phylogenetic placement among crocodylians. *Deinosuchus* from eastern and western North America can be consistently differentiated and represent different species. A phylogenetic study is conducted including new character states. This work reinforces the identity of the 'terror crocodile' as an alligatoroid. Reference to the holotypes indicates that the generic name holder, *Deinosuchus hatcheri*, is extremely incomplete. As a result, the three known species of *Deinosuchus* cannot be differentiated. To ensure nomenclatural stability, the type species for *Deinosuchus* should be transferred to *Deinosuchus riograndensis*, a species known from multiple mostly complete individuals. Additionally, *Deinosuchus rugosus* is based on a holotype that is not diagnostic, and a new species, *Deinosuchus schwimmeri*, is named to encompass some specimens formerly assigned to *D. rugosus*.

http://zoobank.org/urn:lsid:zoobank.org:pub:E12E2DAE-C875-4721-9465-198721ED89E4

SUPPLEMENTAL DATA—Supplemental materials are available for this article for free at www.tandfonline.com/UJVP

Citation for this article: Cossette, A. P., and C. A. Brochu. 2020. A systematic review of the giant alligatoroid *Deinosuchus* from the Campanian of North America and its implications for the relationships at the root of Crocodylia. Journal of Vertebrate Paleontology. DOI: 10.1080/02724634.2020.1767638.

INTRODUCTION

Extant alligatorids represent the most speciose clade of New World crocodylians (Trutnau and Sommerland, 2006; Grigg and Kirshner, 2015). The oldest known crocodylians are alligatoroids (*Brachychampsa*, *Deinosuchus*, *Leidyosuchus*) from the Campanian of North America, suggesting that Alligatoroidea has long been the most speciose clade of North American crocodylians (Lambe, 1907; Gilmore, 1911; Williamson, 1996; Wu et al., 1996).

During the Campanian Age of the Late Cretaceous, North America was divided in two by the Western Interior Seaway. The 'terror crocodile' (Erickson and Brochu, 1999) lived along the extensive wetlands bordering the coasts. Fossils referred to species of *Deinosuchus* have been discovered in 10 states of the U.S.A. (New Jersey, North Carolina, Georgia, Alabama, Mississippi, Texas, New Mexico, Utah, Wyoming, Montana) and Coahuila, Mexico (Fig. 1). This semiaquatic ambush predator was the largest carnivore in its ecosystem, with some specimens likely approaching 10 m in length (Erickson and Brochu, 1999). Species of *Deinosuchus* are longer and heavier than their predatory competitors and are known to have fed upon dinosaurs through trace fossil analysis (Rivera-Sylva et al., 2009; Schwimmer, 2010).

Species of *Deinosuchus* share morphology diagnostic of Alligatoroidea but diverge from the hypothesized ancestral form in a number of ways. As such, its phylogenetic relationships have proven enigmatic.

Recently, a number of authors have suggested that *Deinosuchus* is monospecific (Schwimmer, 2002; Lucas et al., 2006; Irmis et al., 2013) and that the name should be restricted to *D. hatcheri* because it is the first published species bearing the name *Deinosuchus* (Irmis et al., 2013). Additional issues arise because the generic name holder, *D. hatcheri*, is based upon a type that has become undiagnostic with discovery of additional species attributable to *Deinosuchus*.

Here, the authors demonstrate that a more complete understanding of the clade reveals that *D. rugosus* is based on a type specimen that cannot be differentiated to the level of species. Additionally, a new species is named for a number of specimens that have been placed in *D. rugosus*. The type species for *Deinosuchus*, *D. hatcheri*, is extremely incomplete

*Corresponding author.

Color versions of one or more of the figures in the article can be found online at www.tandfonline.com/ujvp.

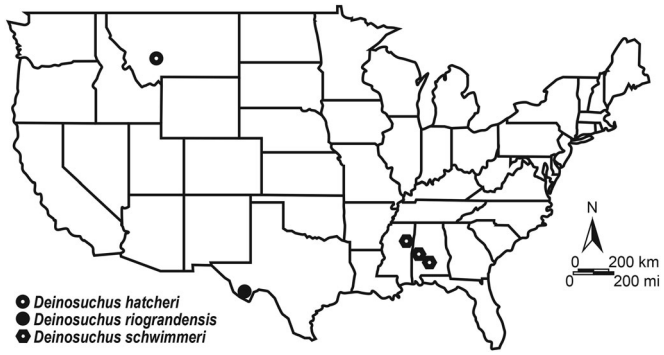

FIGURE 1. Map of *Deinosuchus* localities discussed in this study.

and is differentiated from *D. riograndensis* and *D. schwimmeri* on the basis of a single character state—diagnosis via this state may not be reliable because the other species do not preserve osteoderms of the lateral margin of the dorsal shield. *Deinosuchus hatcheri* shares little morphology in common with the other named species. The result is that *D. riograndensis* and *D. schwimmeri* collapse into a single species, although they may be differentiated from one another via morphology not preserved by the type species.

Alternative systematic approaches involve naming new genera, but the name *Deinosuchus* is historically important to professional systematists and the public alike and should be retained. Here, the authors propose that *D. riograndensis*, a species with several individuals known from its type locality, should form the type species for the genus. The result would allow for the differentiation of the three species of *Deinosuchus* that are evident in the fossil record of the United States and northern Mexico. To ensure nomenclatural stability and the maintenance of the name *Deinosuchus*, the authors will be petitioning the International Commission on Zoological Nomenclature (ICZN) to transfer the type species to *D. riograndensis*.

Previously published analyses generally recover species of *Deinosuchus* in a poorly resolved position at the base of Alligatoroidea (Brochu, 1999; Erickson and Brochu, 1999; Aguilera et al., 2006; Martin et al., 2015; Hastings et al., 2016). Here, the authors provide a reevaluation of the three named species of *Deinosuchus* through reference to an extensive collection of specimens referred to the clade. All character scoring was completed by the authors through direct observation. The phylogenetic analysis provides new characters and places the species among a well-resolved phylogeny.

HISTORY OF THE *DEINOSUCHUS* TYPE MATERIAL

Deinosuchus hatcheri

Currently, there are three recognized species of *Deinosuchus*, but their type specimens present numerous problems to the systematist. The generic name holder, *Deinosuchus hatcheri* Holland, 1909, was found in the Judith River Formation of Fergus County, Montana. The holotype specimen, CM 963, consists of two vertebrae, a pubis, one atlantal rib, one first dorsal rib, numerous osteoderms, and several hundred fragments of bones that cannot be identified to element (Figs. 2–4) (Holland, 1909). Subsequently, the atlantal rib, pubis, and most of the unidentified fragments have been lost.

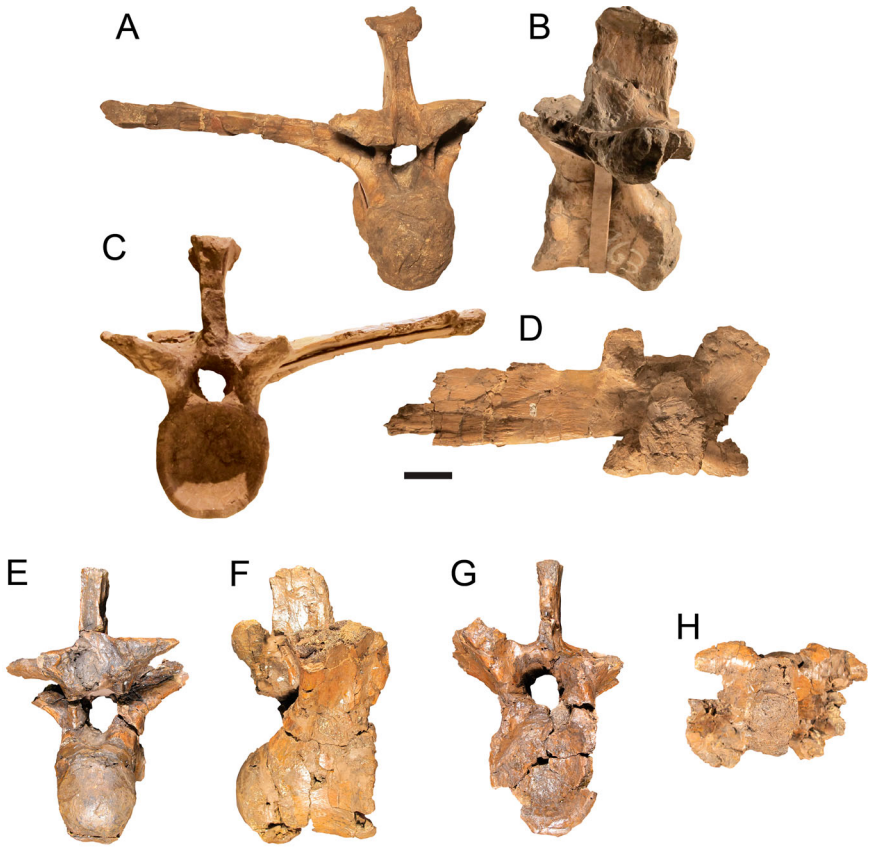

FIGURE 2. *Deinosuchus hatcheri* holotype specimen (CM 963) vertebrae. **A**–**D**, dorsal vertebra in **A**, posterior, **B**, lateral, **C**, anterior, and **D**, dorsal views. **E**–**H**, dorsal vertebra in **E**, posterior, **F**, lateral, **G**, anterior, and **H**, dorsal views. Scale bar equals 5 cm.

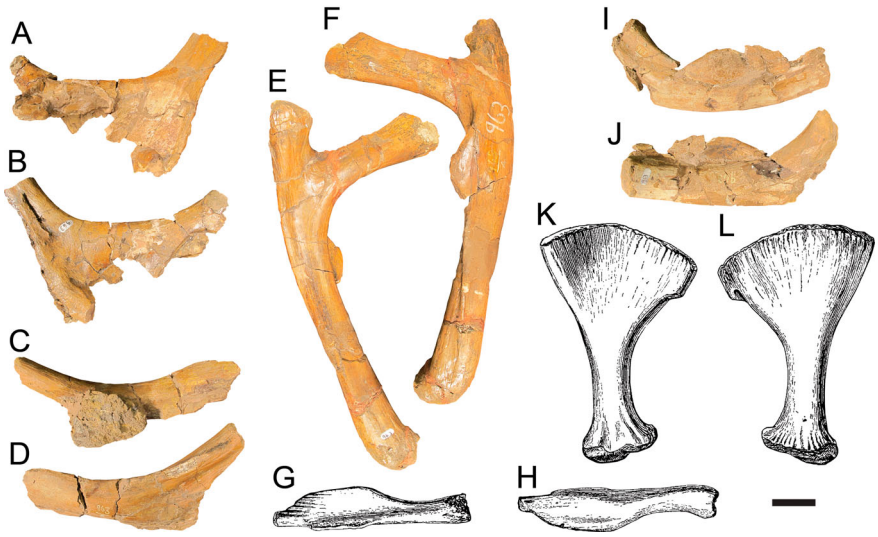

FIGURE 3. *Deinosuchus hatcheri* holotype specimen (CM 963) ribs and pubis. **A**, **B**, proximal end of dorsal rib. **C**, **D**, proximal end of dorsal rib. **E**, **F**, dorsal rib. **G**, **H**, atlantal rib. **I**, **J**, proximal end of dorsal rib. **K**, **L**, pubis. Scale bar equals 5 cm.

Diagnostic characters of *Deinosuchus hatcheri*, according to Holland (1909), consist of massive osteoderms with inflated keels, a pubis that is straighter and less deeply excavated posteriorly than that of extant crocodylians, dorsal-most extent of neural spines are transversely broad, and postzygapophyses lie nearly on the same plane as the transverse processes. Knowledge of crocodylian morphology has increased since the publication of the Holland specimen; accordingly, diagnostic characters were tested against an expanded sample of extinct and living taxa.

Characters diagnosing *D. hatcheri* are shared with specimens referable to other species of *Deinosuchus*, themselves diagnosed by features not preserved in the holotype of *D. hatcheri*. Specimens from Texas and the Western Interior localities bear massive, inflated dorsal osteoderms, whereas specimens that were referable to *Deinosuchus* from Texas and Alabama (TMM 43632-1, TMM 43620-1, ALMNH 1002) preserve dorsal vertebrae whose postzygapophyses are nearly on the same plane as the transverse processes and bear a transversely broad terminal dorsal spine (Fig. 5). Holland (1909) also diagnosed the species on the basis of pubic morphology; the pubis is straighter and less deeply excavated posteriorly than extant crocodylians. TMM 43620-1 and ALMNH 1002 preserve pubes that bear diagnostic characters in common with the *D. hatcheri* holotype specimen (Fig. 6).

The *D. hatcheri* type was diagnostic when it was named. Some authors have argued that *Deinosuchus* is monotypic (Schwimmer, 2002; Irmis et al., 2013) because discovery of more complete material indicated that *D. hatcheri* could not be distinguished from *D. riograndensis* or *D. rugosus*. Here, the authors revise the diagnosis of *D. hatcheri*—the lateral shield osteoderms preserve an indentation along a single edge—and show that it may be differentiated from the other species. However, *D. riograndensis* and *D. schwimmeri* do not preserve osteoderms of the lateral margin of the dorsal shield, and future discoveries may indicate that the state is shared among the species.

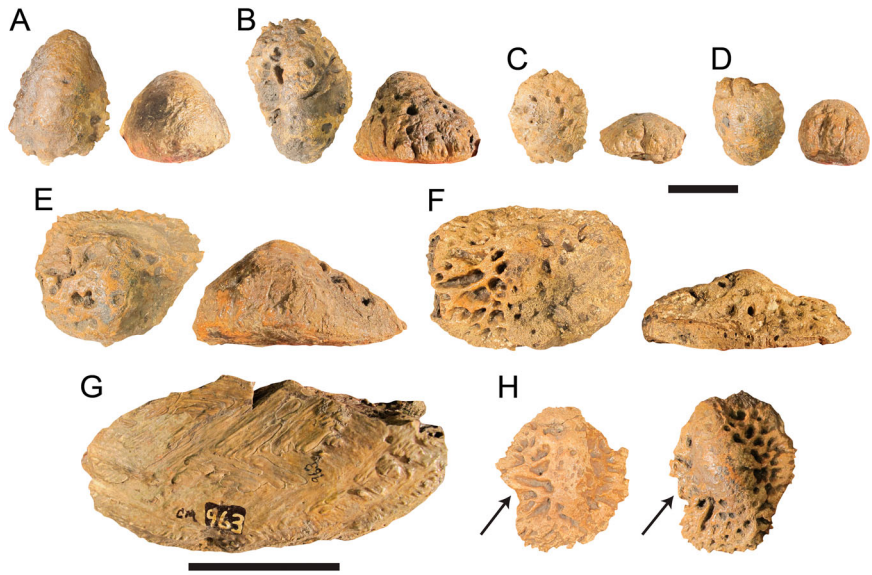

FIGURE 4. *Deinosuchus hatcheri* holotype specimen (CM 963) osteoderms. **A**–**D**, nuchal osteoderms in dorsal and anterior views. **E**, **F**, dorsal osteoderms in dorsal and anterior views. **G**, dorsal osteoderm in ventral view. **H**, nuchal osteoderms in dorsal view showing indentations along margin (arrows). Scale bars equal 5 cm. Large scale bar corresponds to **G** only.

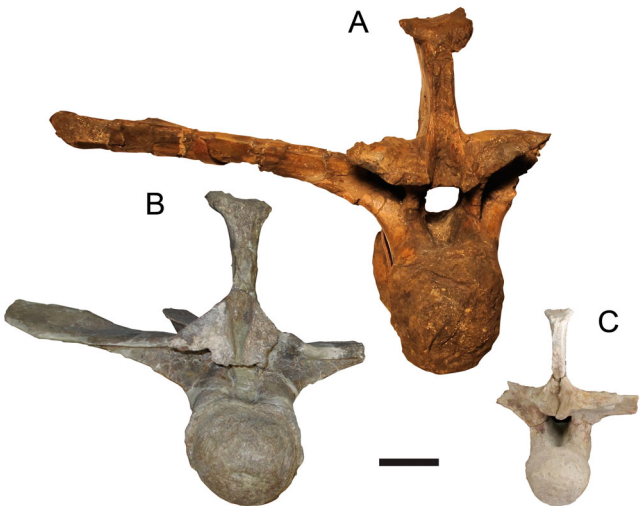

FIGURE 5. Comparison of dorsal vertebrae. **A**, *Deinosuchus hatcheri*, CM 963, posterior view. **B**, *Deinosuchus riograndensis*, TMM 43620-1, posterior view. **C**, *Deinosuchus schwimmeri*, ALMNH 1002, posterior view. Scale bar equals 5 cm.

Deinosuchus rugosus

Emmons (1858) published figures of two teeth attributed to a new species, '*Polyptchodon*' *rugosus*. Although not explicitly stated, these teeth form the syntype series of *Deinosuchus rugosus* (Emmons, 1858). Currently, USNM PAL 535447, a single tooth, forms the type specimen of *D. rugosus* (Fig. S1). The location of the second tooth forming the type series is unknown. The type material was discovered in a Miocene marl bed near Elizabethtown, Bladen County, North Carolina, in 1852–1853 (Emmons, 1858).

Initially, the type material was referred to *Polyptchodon*, a name commonly used during the 19th century for the Late Cretaceous crocodylian fauna of southern England and whose type specimen was subsequently determined to be a pliosaur (Schwimmer, 2002). Later, Cope (1871) assigned the material to '*Thecachampsa*,' a junior synonym of *Crocodylus*, and Hay (1902) reassigned the specimen as '*Crocodylus*' *rugosus*. Baird and Horner (1979) reevaluated the Emmons type material, determining it to be a species of *Deinosuchus*.

The specific epithet refers to the thick, vertically striated enamel of the teeth used by Emmons to diagnose the species. More complete eastern *Deinosuchus* material indicates that the teeth comprising the type specimen are likely from the mid-jaw region. Reference to other species of *Deinosuchus* indicates that the teeth are not diagnostic to the level of species, nor to the level of higher taxa.

Although recovered in a Miocene marl bed, stratigraphic placement of the holotype specimen is complicated because the teeth were likely reworked from the middle Campanian Black Creek Formation (Miller, 1967; Baird and Horner, 1979; Schwimmer, 2002). The type locality has yielded other very incomplete specimens, often found reworked into geologically younger strata. Here, the authors, in agreement with Irmis et al. (2013), assert that the combination of the uncertain stratigraphic placement of the type, undiagnostic morphology, and lack of more complete material from the type locality renders *D. rugosus* a nomen dubium.

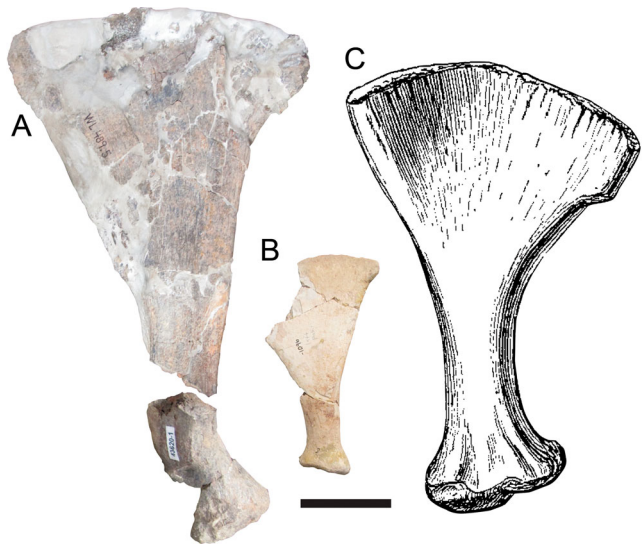

FIGURE 6. Comparison of pubes. **A**, *Deinosuchus riograndensis*, TMM 43620-1, left pubis, medial view. **B**, *Deinosuchus schwimmeri*, ALMNH 1002, left pubis, medial view. **C**, *Deinosuchus hatcheri*, CM 963, left pubis, medial view, as figured by Holland (1909), scaled to original measurements. Scale bar equals 5 cm.

Deinosuchus riograndensis

Deinosuchus riograndensis (Colbert and Bird, 1954) was originally assigned to *Phobosuchus* (Nopsca, 1924), a polyphyletic assemblage of South American crocodylians. The species was named upon a mostly incomplete skull, mandible, dorsal vertebra, right scapula, superior portion of a right ilium, osteoderms, and other indeterminate fragments from the Campanian-age Aguja Formation of Big Bend National Park, Brewster County, Texas. Colbert and Bird (1954) diagnosed the species on the basis of its large size, robust teeth, inflated osteoderms, and large premaxillary fenestrae lateral to the bony narial aperture. Save the premaxillary fenestration, these features do not adequately differentiate *D. riograndensis* from the types of *D. hatcheri* or *D. rugosus*.

Preservation of the holotype, as all of the Texas *Deinosuchus*, is via calcium carbonate salts, as opposed to the eastern *Deinosuchus* specimens, which are preserved via calcium phosphate salts (Schwimmer, 2002). As such, they are prone to extensive cracking, obscuring morphology and sutural contacts. In many specimens, otherwise adequately preserved and mostly free of cracks, sutures are hard to see. The large size of all specimens and relative obscurity of sutural marks may indicate maturity; in late ontogenetic stages, bones are fully coossified and morphology present in the form of sutural contacts may be lost.

Deinosuchus sp.

Two specimens described in earlier works from the Fruitland Formation of New Mexico (Lucas et al., 2006) and the Kaiparowits Formation of Utah (Irmis et al., 2013) bear characters diagnostic of species of *Deinosuchus*. These specimens are found near the western paleoshores of the Western Interior Seaway.

The Fruitland Formation *Deinosuchus* specimen consists of a mandible, osteoderms, and vertebrae. The specimen is identified by Lucas et al. (2006) as *Deinosuchus* due to the large size of the specimen, confluent third and fourth dentary alveoli, and inflated, deeply pitted osteoderms. Lucas et al. (2006), prior to the revised taxonomy presented here, attributed the specimen to *D. rugosus*, considering *D. hatcheri* and *D. riograndensis* to be indistinct from the species. Because it does not preserve

character states diagnostic of any particular species of *Deinosuchus*, the authors do not assign this specimen to species level.

The Kaiparowits Formation *Deinosuchus* specimens consist of a partial rostrum and a number of unassociated osteoderms. These specimens are identified by Irmis et al. (2013) as *D. hatcheri* based on a taxonomic argument and the preservation of large, inflated, deeply pitted osteoderms. They correctly indicate that *D. rugosus* is a nomen dubium. Further, Irmis et al. (2013) state that it is difficult to refer the material to *Deinosuchus* owing to a lack of cranial elements preserved by the *D. hatcheri* holotype specimen and, until now, few described specimens from the type locality of *D. riograndensis*. Here, the authors attribute this specimen to *Deinosuchus* but not to the level of species.

Institutional Abbreviations—**ALMNH**, Alabama Museum of Natural History, Tuscaloosa, Alabama, U.S.A.; **AMNH**, American Museum of Natural History, New York, New York, U.S.A.; **CM**, Carnegie Museum of Natural History, Pittsburgh, Pennsylvania, U.S.A.; **MMNS**, Mississippi Museum of Natural Sciences, Jackson, Mississippi, U.S.A.; **NCSM**, North Carolina Museum of Natural Sciences, Raleigh, North Carolina, U.S.A.; **TMM**, Texas Memorial Museum, Austin, Texas, U.S.A.; **USNM**, United States National Museum, Washington, D.C., U.S.A.

SYSTEMATIC PALEONTOLOGY

CROCODYLIA Gmelin, 1789, sensu Benton and Clark, 1988
ALLIGATOROIDEA Gray, 1844
DEINOSUCHUS HATCHERI Holland, 1909
(Figs. 2–6)

Holotype—CM 963, two vertebrae, cervical rib, dorsal rib, fragments of dorsal ribs, pubis, 27 complete or nearly complete osteoderms, and several dozen fragments likely from the vertebrae, ribs, and skull (Figs. 2–4).

Occurrence—Judith River Formation, middle Campanian, Late Cretaceous, three miles west of Nolan and Archer's ranch along the Willow Creek, Fergus County, Montana, U.S.A.

Referable Specimens—None.

Diagnosis—"Great size, exceeding that of any other representative of the Crocodilia thus far described from North America. Scutes massive and possessing great vertical height in comparison with their breadth, many of the smaller scutes being almost hemispherical, and some of the smallest subglobose. Pubis straighter and less deeply excavated posteriorly than in recent Crocodilia Extremities of dorsal spines of vertebrae broad transversely and thickened for attachments, much more than in existing genera. The postzygapophyses of the vertebrae more nearly on the same plane as the transverse processes and not looking outwardly as much as in other crocodiles" (Holland, 1909:282). Additionally, the osteoderms of the lateral margin of the dorsal shield preserve indentations along a single edge.

Description—Some elements indicated by Holland (1909) are missing. Historically, the atlantal rib, pubis, and several hundred indeterminate fragments were preserved. Missing elements were coded into the matrix using figures from Holland (1909). Currently, the atlantal rib, pubis, and most of the indeterminate fragments are missing. The collections manager at CM (A. Henrici, pers. comm.) indicates that they were lost long ago.

The most striking feature of the specimen is its incredible size. Preserved elements shared with other species of *Deinosuchus* may be compared to indicate relative sizes. Osteoderms and vertebrae indicate that CM 963 is among the largest individuals of all species previously attributed to *Deinosuchus*, although some of the largest *D. riograndensis* specimens approach or equal its immense size.

Two very large dorsal vertebrae are preserved; they are procoelous and preserve long transverse processes and neural spines (Fig. 2). The neural spines end in a dorsally flat, mediolaterally expanded tuberosity, likely for the attachment of epaxial musculature. As indicated by Holland (1909), the postzygapophyses are nearly on the same plane as the transverse processes.

The most complete vertebra was determined by Holland (1909) to be the seventh in the dorsal series. Comparison with modern taxa indicates that the vertebra was likely between positions 6 and 10 in the thoracic series. The element is nearly complete save the right transverse process. The left transverse process bears attachment sites for the dorsal ribs and establishes the identity of the vertebra as belonging to the dorsal series. The neural spine is very long and ends in a large flattened tuberosity. The less complete of the two vertebrae was tentatively assigned by Holland (1909) as the last vertebra of the lumbar series. The authors agree that the vertebra is part of the lumbar series but do not assign a position. This vertebra preserves a left transverse process; the right side is missing. Both the transverse process and neural spines are shorter than those of the thoracic vertebra. In addition, the transverse process is narrow relative to the thoracic vertebra. The extremity of the neural spine is largely incomplete, but proportions of preserved bone indicate that it was mediolaterally expanded.

A complete left dorsal rib is preserved (Fig. 3). Additionally, one midshaft, three proximal, and four distal rib fragments are present; they likely represent dorsal ribs as indicated by size, proportion, and preserved morphology.

Thirty-seven osteoderms, in various states of completeness, are preserved (Fig. 4). Elements of the nuchal, dorsal, and sacrocaudal shields are preserved. Most osteoderms are deeply pitted with inflated parasagittal keels—the result is an osteoderm that is lumpy in appearance when viewed anteriorly or posteriorly. Some osteoderms, presumably postoccipitals or the superior-most osteoderms of the lateral shield along the animal's flank, are subglobose—pitting is highly reduced in these elements, with one preserving no pitting whatsoever. Striations intersecting at 45° angles and approximating the shape of a chevron cover the ventral surfaces; this morphology is especially evident in dorsal shield osteoderms. Comparison with *Alligator mississippiensis* indicates that the striations are surface markings for tendinous deep fascia connecting to the underlying epaxial musculature (Seidel, 1979). Some osteoderms show indentations along a single margin, presumably indicating contact with a neighboring osteoderm. These osteoderms are tentatively identified as belonging to the lateral margin of the dorsal shield.

SYSTEMATIC PALEONTOLOGY

CROCODYLIA Gmelin, 1789, sensu Benton and Clark, 1988
ALLIGATOROIDEA Gray, 1844
DEINOSUCHUS RIOGRANDENSIS, Colbert and Bird, 1954
(Figs. 5–19)

Holotype—AMNH 3073 (Figs. 7–11), premaxillae and part of a right maxilla, portions of the left articular, angular, and surangular, left and right splenials and dentaries, six loose teeth, one thoracic vertebra (tentatively the 12th vertebra of the presacral series), right scapula, a possible portion of a superior right ilium, as well as osteoderms and other indeterminate fragments. The International Commission of Zoological Nomenclature will be petitioned to change the type species of *Deinosuchus* to *Deinosuchus riograndensis*.

Occurrence—Campanian, Late Cretaceous, Aguja Formation west of Glenn Spring, Big Bend National Park, Brewster County, Texas, U.S.A.

Referable Specimens—TMM 40571-1 (Fig. S2) consists of the left side of an upper jaw and left hemimandible from Brewster County, Texas, U.S.A. TMM 43538-1 (Fig. S3) consists of the left side of a skull from Brewster County, Texas, U.S.A. TMM 43620-1 (Figs. 12, 13A, 16, 18, S4, S5) consists of a skull, mandible, and postcranial elements from Brewster County, Texas, U.S.A. TMM 43632-1 (Figs. 13C, 14, 15, 17, 19) consists of a skull,

lower jaw, and postcranial elements from Brewster County, Texas, U.S.A.

Diagnosis—"A eusuchian crocodile of tremendous size, the lower jaw being about 1800 mm (approximately 6 feet) in length. The bones of the skull and lower jaw are heavy and the teeth are robust. In each premaxilla there is a large fenestra lateral to the external narial opening—a distinctive feature not seen in any other known crocodilian. The single known vertebra is strongly procoelous. The broad scapula indicates that the limbs may have been comparatively heavy. Scutes very heavy" (Colbert and Bird, 1954:13).

Amended Diagnosis—Bulbous premaxillae bear large, dorsally displaced fenestrae anterolateral to the bony narial aperture; bony narial aperture opens posterodorsally and is wider than long; shallow occlusal marks present on the premaxilla between the first and second alveoli and lingual to the third and fourth alveoli; premaxilla-maxilla notch is posteromedial to the fifth premaxillary tooth; anterior margin of suborbital fenestra acute and extends to the posterior margin of the 12th maxillary alveolus from the end of the tooth row; ophthalmic groove trends anteroposteriorly; osteoderms are very large and bear inflated parasagittal keels.

Description

Deinosuchus riograndensis AMNH 3073 represents a very large alligatoroid from the Campanian Aguja Formation of the Big Bend region of Texas. It was discovered in 1940 by an expedition of the American Museum of Natural History and excavated by Barnum Brown and Roland Bird.

Many bones are adequately preserved, but others such as the premaxillae are composed of many cracked pieces held together by plaster. Often, bones that are proximal to one another, such as the articular and the surangular, do not fit together. The intervening bone is missing either as a product of diagenesis or a result of the fossil preparation process.

Premaxilla—The premaxillae are very large and particularly deep relative to their length and width (Fig. 7). AMNH 3073 has the largest and most bulbous premaxillae of all specimens referred to species of *Deinosuchus*. The elements do not fit together; it is unknown whether this is due to diagenesis or as a result of preparation. The edges of the premaxillae, especially along the dorsal midline and the dorsal premaxillary processes, are smooth and indicate that the polished edges may have been created via preparation of the specimen.

The anterior and anterolateral margins of the external naris are formed by the premaxillae. The margins of the bony narial aperture are smooth; considerable breakage and reconstruction is present along the margins formed by the premaxilla. Preserved portions of the bony narial aperture on the premaxillae and the maxillary fragment suggest that the aperture opened posterodorsally.

The dorsal processes of the premaxillae are short relative to the large size of the elements. Their posterior extent comes to a blunt point when viewed from a lateral aspect. Colbert and Bird (1954:6) describe the dorsal processes of the premaxillae as "… barely reaching back to the level of the space between the first and second maxillary teeth, for which reason they embrace only the anterior border of the external nares." Additional *D. riograndensis* specimens from Texas agree with this assertion, but at the time of their description this could not be verified; the right premaxilla does not fit with the maxillary fragment because there is bone missing between the elements. Laterally, the dorsal processes would have wrapped around the posterior of the dome-like anterior-most snout. However, as isolated elements, this interpretation is dependent on how the premaxillae are posed; comparisons with more complete specimens indicate that this is the case.

Undocumented among eusuchians is the presence of large fenestrae anterolateral to the bony narial aperture. The extreme depth of the premaxillae, dorsal placement of the fenestrae, and lack of holes in the palatal processes of the premaxillae suggest that they were not for receiving the first dentary teeth as is found in modern forms such as *Caiman crocodilus*. This feature is preserved in both premaxillae, but the margins of the fenestrae are incomplete; in life, they were likely somewhat smaller than currently preserved.

The fenestrae lead to an internal hollow space within the premaxillae and appear to have connected with a paranasal air sinus in the interior of the element. The anterior wall of the premaxilla bears a dorsoventrally oriented, mediolaterally thin ridge extending from the roof of the element to the middle of the anterior wall (Fig. 7I). It is approximately 3 cm long and projects posteriorly into the hollow of the premaxilla. Although likely, it is unknown whether the feature extended further to the posterior to

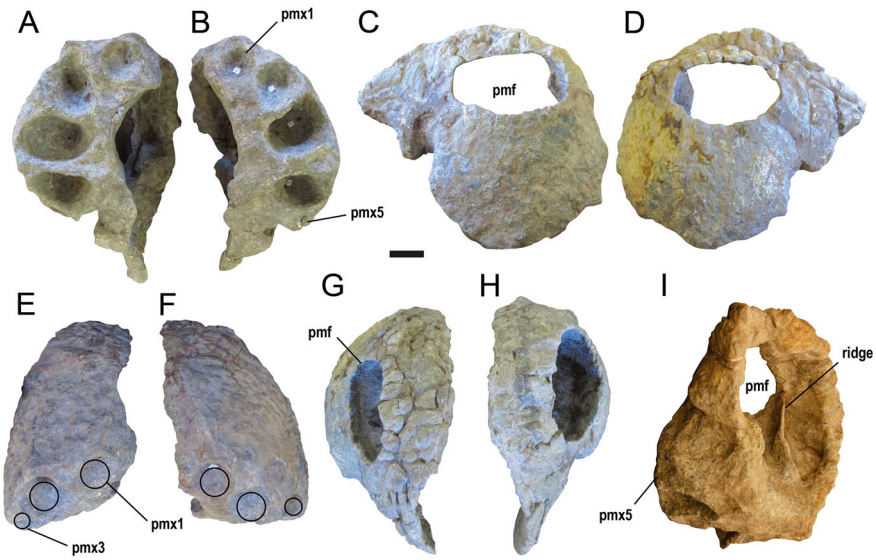

FIGURE 7. *Deinosuchus riograndensis* holotype specimen (AMNH 3073) premaxillae. **A**, right premaxilla in ventral view. **B**, left premaxilla in ventral view. **C**, right premaxilla in lateral view. **D**, left premaxilla in lateral view. **E**, right premaxilla in anterior view. **F**, left premaxilla in anterior view. **G**, left premaxilla in dorsal view. **H**, right premaxilla in dorsal view. **I**, left premaxilla in posteroventral view. **Abbreviations**: **pmf**, premaxillary fenestra; **pmx1**, premaxillary tooth 1; **pmx3**, premaxillary tooth 3; **pmx5**, premaxillary tooth 5. Scale bar equals 5 cm.

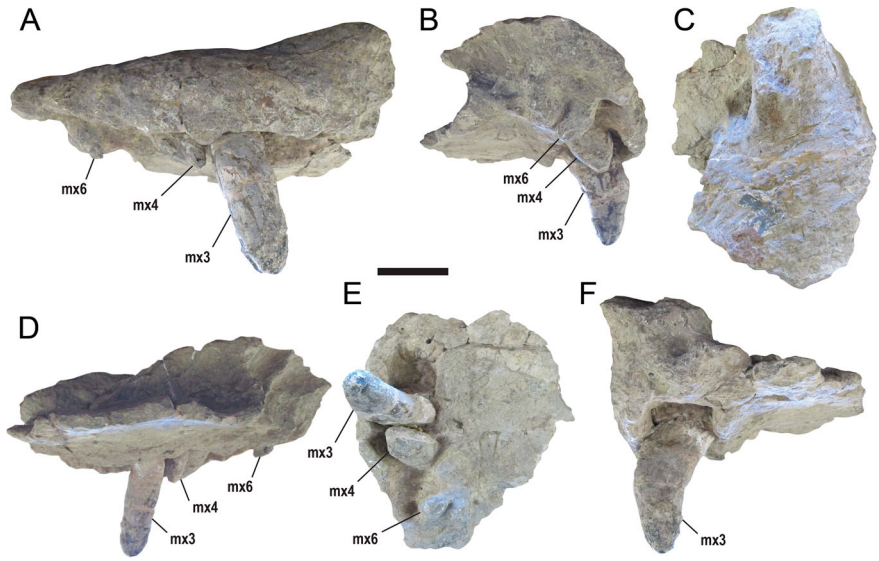

FIGURE 8. *Deinosuchus riograndensis* holotype specimen (AMNH 3073) right anterior maxillary fragment. **A**, lateral view. **B**, posterior view. **C**, dorsal view. **D**, medial view. **E**, ventral view. **F**, anterior view. **Abbreviations**: **mx3**, maxillary tooth 3; **mx4**, maxillary tooth 4; **mx6**, maxillary tooth 6. Scale bar equals 5 cm.

form a wall separating the nasal passage from the paranasal air sinus.

There are large bumps on the floor of the premaxillary cavity where the roots of the premaxillary teeth are encased in bone. The bone forming the floor of the external naris is not preserved; the incisive foramen is missing.

Each premaxilla preserves five closely spaced alveoli. Alveoli 1–3 get progressively larger from mesial to distal, the third and fourth are large, and the fifth is the smallest among the premaxillary arcade. The largest alveolus in the left premaxilla is the third, but the third and fourth alveoli are approximately the same size on the right side. A pronounced difference in the

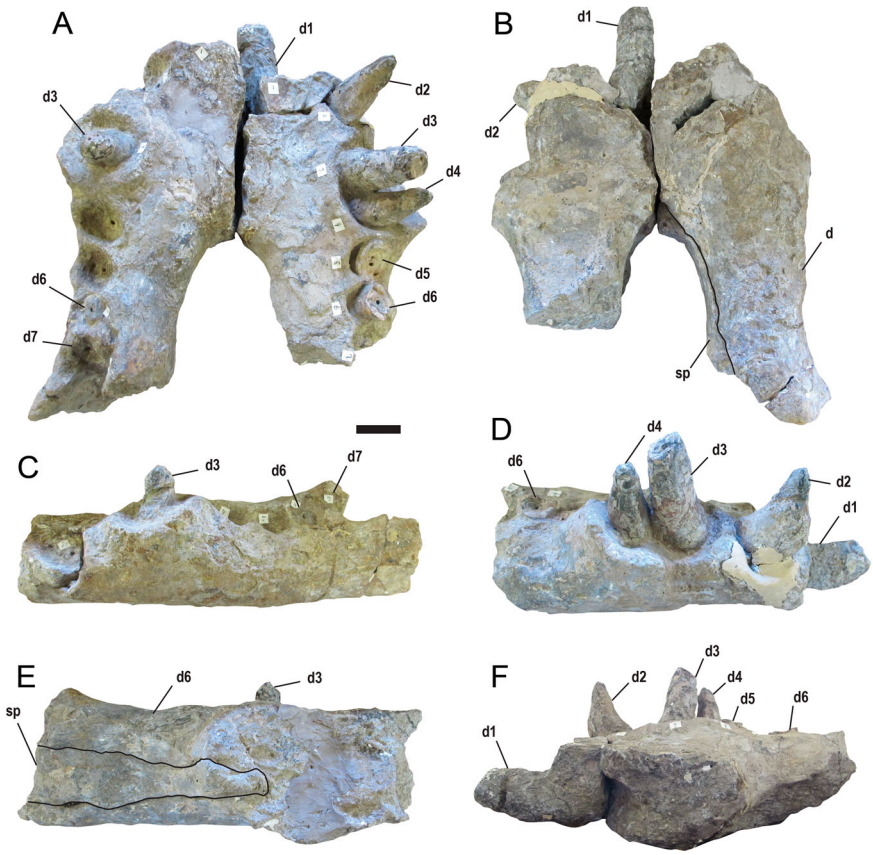

FIGURE 9. *Deinosuchus riograndensis* holotype specimen (AMNH 3073) anterior mandible. **A**, anterior mandible in dorsal view. **B**, anterior mandible in ventral view. **C**, left anterior mandibular ramus in lateral view. **D**, right anterior mandibular ramus in lateral view. **E**, left anterior mandibular ramus in medial view. **F**, right anterior mandibular ramus in medial view. **Abbreviations**: **d**, dentary; **d1**–**d7**, dentary teeth corresponding to positions in the mandibular dental arcade; **sp**, splenial. Scale bar equals 5 cm.

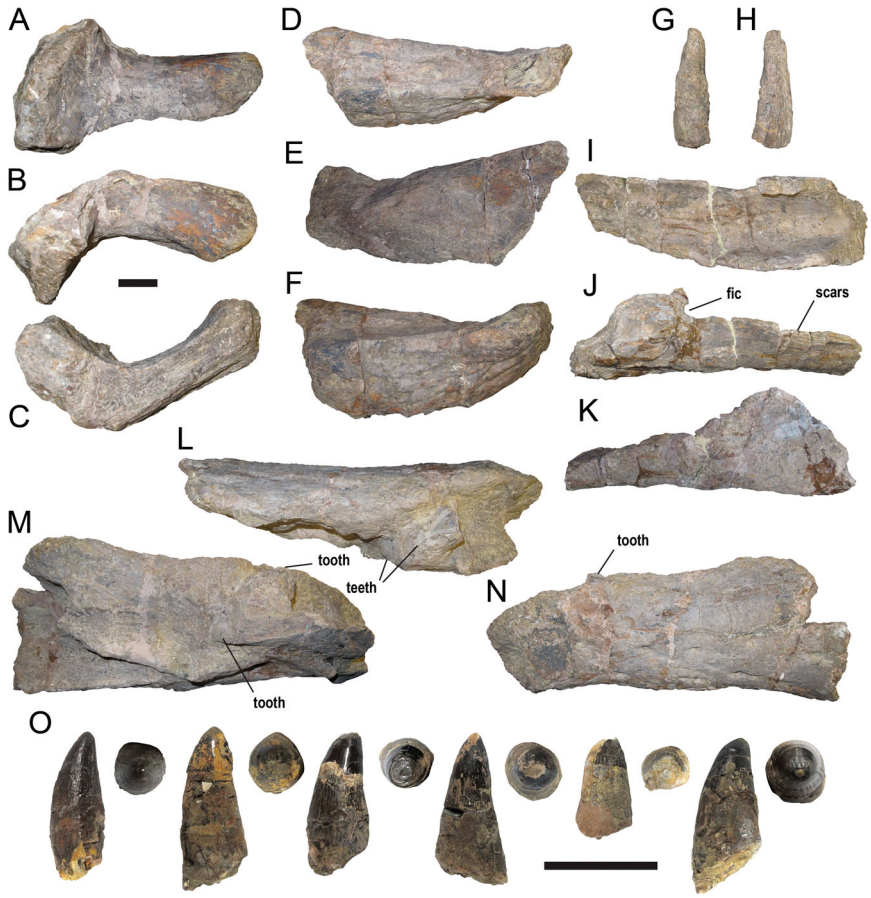

FIGURE 10. *Deinosuchus riograndensis* holotype specimen (AMNH 3073) mandibular elements. **A**, left articular in dorsal view. **B**, left articular in medial view. **C**, left articular in lateral view. **D**, left surangular in dorsal view. **E**, left surangular in medial view. **F**, left surangular in lateral view. **G**, left dorsal surangular in lateral view. **H**, left dorsal surangular in medial view. **I**, left angular in dorsal view. **J**, left angular in medial view. **K**, left angular in lateral view. **L**, mid-jaw fragment in dorsal view. **M**, mid-jaw fragment in dorsal view. **N**, mid-jaw fragment in dorsal view. **O**, loose teeth in medial/lateral view and occlusal view. **Abbreviation**: **fic**, foramen intermandibularis caudalis. Scale bars equal 5 cm.

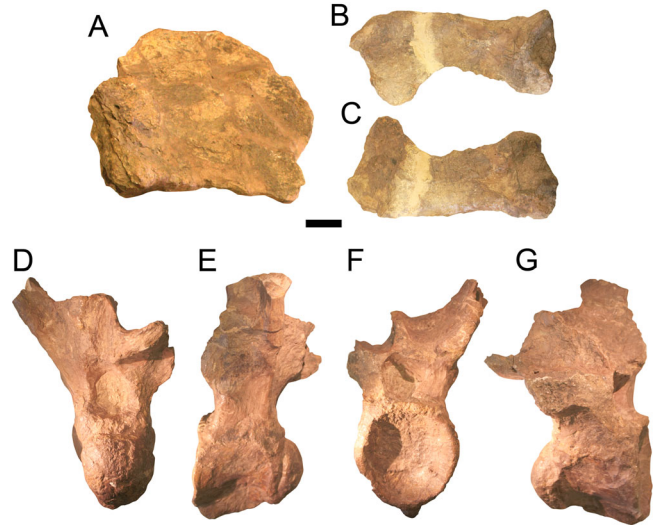

FIGURE 11. *Deinosuchus riograndensis* holotype specimen (AMNH 3073) postcrania. **A**, fragment of (right?) ilium. **B**, right scapula in medial view. **C**, right scapula in lateral view. **D**–**G**, dorsal vertebra in **D**, posterior, **E**, left lateral, **F**, anterior, and **G**, right lateral views. Scale bar equals 5 cm.

amount of bone separating the third and fourth alveoli among the premaxillae is present; the left side preserves more intervening bone. It is unknown whether these differences are pathological, taphonomic, normal morphological variation, or the result of preparation. The fifth alveolar position of the left premaxilla preserves a partially broken crown of an erupting tooth. Posterior to the fifth alveolus is a large notch for receiving the third and fourth dentary teeth, as is present in the alligatoroid *Leidyosuchus canadensis* Lambe, 1907.

Maxilla—The anterior portion of the right maxilla is preserved (Fig. 8). Its lateral margin is complete; the medial margin is damaged. Sutural contacts between the right premaxilla and maxilla fragments are missing. However, the outline of their margins in dorsal and lateral views suggests that they were nearly contiguous. The anterior end of the maxillary fragment bears a large dorsal inflation. Medial to the inflation, the bone has been destroyed; preserved portions indicate that the maxilla contributes to the nasal canal and the posterolateral margin of the bony narial aperture.

Six alveoli and part of a seventh are preserved on the maxillary fragment (Fig. 8E). The identities of the alveoli are unknown, but comparison with referred specimen TMM 43620-1, a nearly complete *D. riograndensis* skull from the holotype locality, suggests that the fragment preserves maxillary alveoli 1–7. Alveoli in positions 3, 4, and 6 preserve teeth. The tooth in the third alveolus is very large and robust; it is anteroposteriorly compressed and bears a lengthwise groove on its distal side. The fourth and sixth alveoli contain partially erupted teeth. The maxilla is laterally expanded in the region of the first to seventh alveoli.

Lingual to the sixth alveolus are indentations for receiving the teeth of the mandible. The taxon had an overbite in this region.

Colbert and Bird (1954) suggest that a fragment of the right nasal is attached to the maxillary fragment and the nasals are broad. However, the nasal fragment is not evident. Comparison with more complete specimens indicates that a nasal may be present in this region.

When viewed from a posterior aspect, the maxilla fragment preserves a matrix-filled cavity lateral to the nasal passage interpreted as a paranasal air sinus. Additionally, a moderately deep, 'U'-shaped indentation is present ventral to the paranasal sinus. Colbert and Bird (1954) suggest that this indentation is the anterior-most margin of the suborbital fenestra and that it is unexpectedly positioned to the extreme anterior of what is usually encountered in crocodylians. However, when viewed ventrally, the anterior margins of most crocodylian suborbital fenestrae give way to an open space occupied by the adductor muscles. In AMNH 3073, the anterior of the proposed suborbital fenestra has a bony floor. Comparison with more complete specimens (TMM 40571-1, TMM 43538-1, TMM 43620-1, TMM 45973-1) indicates that this feature cannot be related to the suborbital fenestra due to its unusual morphology and its extreme anterior placement.

Dentary—The anterior-most portions of the dentaries are preserved (Fig. 9). The right dentary preserves alveoli 1–7. Alveoli 1–6 are complete and preserve teeth. The floor of the first alveolus, along with the deeper walls of the second alveolus, is preserved. Apically, the first tooth curves toward the midline, likely as a result of deformation during burial; preserved alveolar margins suggest that in life the tooth projected somewhat laterally away from the midline. Along the midline is a space separating the first teeth of the hemimandibles; these teeth would have occluded with the premaxillae behind the space for the first and second premaxillary teeth. The alveoli for teeth 3 and 4 are confluent on the right side; the teeth themselves lie next to one another with moderate and slight anteroposterior compression of teeth 3 and 4, respectively.

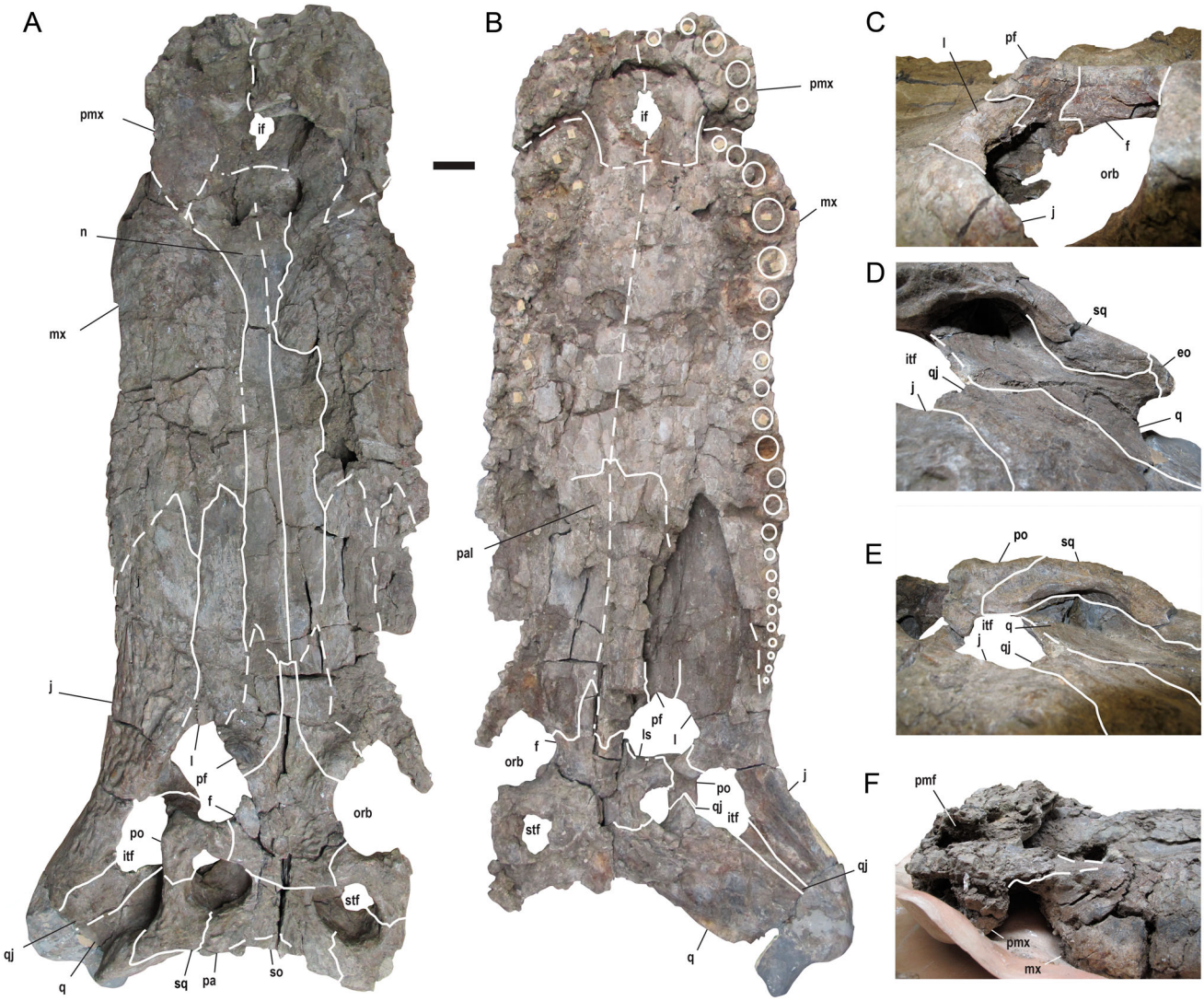

FIGURE 12. *Deinosuchus riograndensis* (TMM 43620-1) skull with elements illustrated. **A**, skull in dorsal view. **B**, skull in ventral view. **C**, left orbit in lateral view. **D**, left posterior-most skull in lateral view. **E**, left otic region in lateral view. **F**, left anterior-most snout in lateral view. **Abbreviations**: **eo**, exoccipital; **f**, frontal; **if**, incisive foramen; **itf**, infratemporal fenestra; **j**, jugal; **l**, lacrimal; **ls**, laterosphenoid; **mx**, maxilla; **n**, nasal; **orb**, orbit; **pf**, prefrontal; **pmf**, premaxillary fenestra; **pmx**, premaxilla; **pa**, parietal; **pal**, palatine; **po**, postorbital; **q**, quadrate; **qj**, quadratojugal; **sq**, squamosal; **so**, supraoccipital; **stf**, supratemporal fenestra. Scale bar equals 5 cm.

This condition is not present on the left side where the alveoli are widely spaced, and no teeth are present (Fig. 9A). Differences in morphology may be a product of taphonomy, pathology, or normal variation. When present, enamel on the teeth is thick. The mandibular symphysis extends posteriorly to the space between the fourth and fifth dentary teeth when viewed dorsally.

The left dentary fragment has spaces for seven alveoli; the posterior portion of the seventh alveolus is missing. Teeth are present in alveoli 3, 6, and 7. The left fragment shows that the splenial reaches the symphysis. The sutural portion of the dentary symphysis encloses an anterior projection of the splenial that cannot be viewed unless the hemimandibles are separated (Fig. 9E). The anterior projection of the splenial extends for no more than one alveolus length (stops before the position of the third alveolus). The left side suggests a splenial that thins dorsoventrally as it proceeds to its anterior-most extent.

A large left dentary fragment preserves two teeth (Fig. 10L–N). Curvature of the lateral side of the fragment suggests that it came from the mid-jaw region of the mandible. The medial portion is not preserved. The fragment is contiguous with the left dentary fragment containing the symphysis. There are large, deep pits on the lateral side for the passage of nerves and blood vessels. No discernible alveoli are present save one that bears a tooth that is missing its crown, is nearly round in cross-section, and has very thick enamel. Deep in the mandible, ventral to the erupted tooth, is a developing tooth.

Colbert and Bird (1954) suggest that nine alveoli are preserved on the left side of the mandible, but there is no evidence for discernible alveoli beyond the anterior portion of the seventh in the anterior fragment and a single alveolus in the mid-jaw fragment.

Angular—Both angulars are preserved (Fig. 10I–K). Medially, the mandibular fossa and posterior margin of the foramen intermandibularis caudalis are preserved. The mandibular fossa is extensive anteroposteriorly and mediolaterally for the accommodation of presumably large m. adductor mandibulae externus posterior and m. intramandibularis necessary in order to close the massive jaws. The medial side of the left angular preserves sutural scars where the element likely contacted the splenial, which itself may have extended posteriorly to the anterior margin of the foramen intermandibularis caudalis.

Surangular—The posterior portion of the left mandible preserves the surangular (Fig. 10 D–H). At the point of the glenoid fossa, there is a lateral expansion of the surangular, producing a swelling along the dorsolateral portion of the posterior mandible. An anteroposteriorly oriented groove is present on the dorsal side, confluent with the swollen region of the surangular (Fig. 10F). This portion of the element does not contact the articular fragment bearing the posterior wall of the glenoid fossa. The ascending ramus of the left surangular, forming the lateral face of the retroarticular process, is preserved and fits into a groove on the lateral side of the left articular.

Articular—A partial left articular preserves the retroarticular process and the posterior wall of the glenoid fossa; anteroventral portions of the articular are not preserved (Fig. 10A–C). The ridge forming the posterior wall of the glenoid fossa does not bear signs of the foramen aereum. Although incompletely preserved, sutural scars on the lateral side of the articular suggest that the surangular and angular may have extended to the dorsal-most tip of the retroarticular process.

Teeth—Six loose teeth are preserved (Fig. 10O), but it is of note that seven teeth are figured by Colbert and Bird (1954). Associated notes from the AMNH reconstruction suggest that they are left dentary teeth 2, 3, 5, and 6 as well as right dentary teeth 2 and 8, but this suggestion cannot be verified. The best-preserved teeth demonstrate modest mesiodistal carinae. Distal to the second and third teeth, crowns get progressively lower and less dagger-like. The dagger-like and low-crowned teeth likely functioned for holding (or tearing) and crushing, respectively (Erickson et al., 2003, 2012).

Postcrania—Postcranial elements consist of a single dorsal vertebra, right scapula, a possible fragment of a dorsal right ilium (Fig. 11), and osteoderms. Colbert and Bird (1954) suggest that the strongly procoelous dorsal vertebra is the 12th or 13th in the presacral series because both rib articulations are present on the transverse process, articular surfaces on the centrum are absent, and the centrum has a ventral keel (Fig. 11D–G). The vertebra is well preserved save the right transverse process and neural spine, which are missing. The left transverse process has been displaced by crushing and is bent superiorly where it contacts the intersection of the left pedicle and lamina. The scapula is shorter than expected for such a large animal and is very robust (Fig. 11B, C). The articular end of the element is less flared, and constriction of the neck is reduced relative to extant alligatorids. The result of this morphology is an articular end that gently grades into the inferior portion of the scapular blade. The margins of the inferior two-thirds of the blade are nearly parallel. The superior third of the blade is strongly flared. A partial right ilium demonstrates that the element was very robust (Fig. 11A).

TMM 43620-1 and Associated Material

This specimen (Figs. 12, 13A, 16, 18, S4, S5) represents a very large individual from the Big Bend region of western Texas. It is similar in size to the AMNH holotype specimen and is the most complete cranial specimen known for any species of *Deinosuchus*. Preservation is via calcium carbonate salts (Schwimmer, 2002); extensive cracking is present, and sutures are difficult to discern.

Premaxilla—Both premaxillae are preserved (Figs. 12A, B, 13A, S4). Although some dorsoventral crushing is present, the amount of compressed bone in the region suggests that they were as bulbous as the AMNH holotype specimen. When viewed laterally, the premaxillary region is the deepest portion

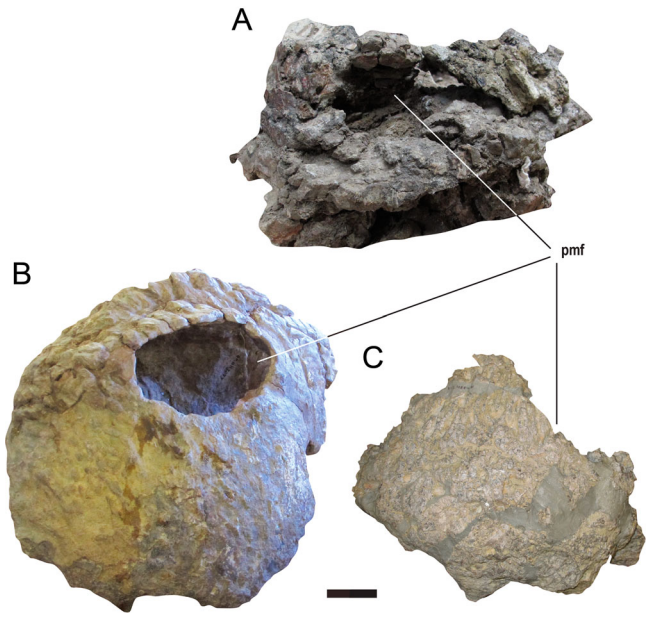

FIGURE 13. *Deinosuchus riograndensis* left premaxillae in anteromedial view demonstrating premaxillary fenestrae. **A**, TMM 43620-1. **B**, AMNH 3073. **C**, TMM 43632-1. **Abbreviation**: **pmf**, premaxillary fenestra. Scale bar equals 5 cm.

of the anterior snout. The anterior margin of the bony narial aperture, formed by the premaxilla, would have been situated dorsal to the posterior margin formed by the maxilla and nasals; the bony narial aperture opens posterodorsally and is mediolaterally wider than it is anteroposteriorly long.

Premaxillary fenestrae are preserved (Fig. 12F). Relative to the holotype (AMNH 3073), they are more immediately proximal to the tooth row. This variation in morphology is likely due to crushing in TMM 43620-1. The dorsal processes of the premaxillae are poorly preserved. However, the anterodorsal maxilla preserves marks where it contacts the dorsal processes of the premaxillae and indicates that they are short and extend to the posterior margin of the bony narial aperture. The dorsolateral margins of the bony narial aperture are formed by the premaxillae.

Ventrally, the premaxillae each preserve five alveoli—the first two alveolar positions are small and nearly equal in size, the third position is the largest, the fourth position is nearly as large as the third, and the fifth is the smallest among the premaxillary dental arcade. All premaxillary teeth are preserved, although the crowns are missing. The first and second premaxillary alveoli are separated by marks that were likely formed through occlusal contact with the first dentary teeth. These features are relatively shallow and are nearly equal to the diameters of the alveoli they separate.

Very shallow occlusal marks are present medial to the junction of the third and fourth alveoli; they were likely formed by the second dentary tooth. TMM 40571-1 (Fig. S2), a smaller individual from the same unit, may demonstrate similar morphology. The incisive foramen is small, mediolaterally narrow, shaped like a teardrop, and extends anteroposteriorly from the fourth premaxillary alveolus to the level of the posterior margin of the premaxillary-maxillary notch (Fig. 12B). Ventrally, the premaxilla is mediolaterally constricted at the point of the notch. The posterior premaxillary margin on the ventral surface of the snout is suggested by faint sutures and separation of bone—it extends to the anterior margin of the third maxillary tooth.

A large notch for reception of the third and fourth dentary teeth during occlusion is present at the point of premaxillomaxillary contact. The effect of this morphology is a mediolateral constriction of the snout at the juncture of the premaxilla and maxilla. The anterior and medial margins, as well as the anterior roof of the notch, are composed of the premaxilla. The posterior margin and roof are formed by the maxilla. Tooth crowns would have been covered by the roof of the notch formed by the maxilla.

Nasal—Nasals are broad along the length of the snout and are particularly wide at their anterior-most extent. Sutural margins are obscured at points, but the general outline is confidently determined (Fig. 12A). As preserved, the anterior tips of the nasals form a blunt point along the midline where they contribute to the posterior margin of the bony narial aperture, but it is unknown whether they continued anteriorly to bisect it as in *Alligator*. Laterally, the anterior nasals expand and form the posterior and posterolateral margins of the bony narial aperture. TMM 40571-1 appears to share this morphology. At midsnout, deformation of the right side has caused the medial margin of the maxilla to fold over the lateral margin of the nasals. Tentatively it is interpreted that the posterior extent of the nasals separates the anterior processes of the prefrontals from contacting the frontals; sutures are faint and cross-cut by many cracks.

Maxilla—Viewed through the bony narial aperture, the lateral walls of the nasal canal are formed by the maxilla (Fig. 12A). In dorsal view, the outline of the maxilla demonstrates pronounced mediolateral constriction at the first maxillary tooth, immediately behind the notch for receiving the third and fourth dentary teeth. Conversely, there are two associated areas of mediolateral expansion along the tooth row. The first corresponds to the area between the first and seventh alveoli, and the second corresponds to the area between the 10th and 14th alveoli. In the expanded regions, the diameter of the teeth increases from the anterior-most alveolus to the alveoli at the midpoint of the swelling and then decreases toward the posterior. There are 23 teeth in the maxillary tooth row; including the five premaxillary teeth, there are 28 teeth per side of the upper jaw. The largest maxillary tooth is in the fourth position; the fifth maxillary tooth is nearly as large. Lingual to the maxillary tooth row are depressions caused by the occlusion of the dentary tooth row; the taxon had an overbite.

The posterodorsal portion of the maxilla bears two posterior projections; the first separates the anterior-most jugal from the lacrimal, and the second separates the anterior-most lacrimal from the nasals. In palatal view, the maxilla terminates anterior to the lower temporal bar.

Suborbital Fenestra—The left suborbital fenestra is preserved (Fig. 12B); its posterior margin is missing. The anterior-most, anteromedial, and much of the lateral margin is formed by the maxilla. The anterior margin ends in an acute point roughly equal to the posterior margin of the 12th maxillary alveolus from the end of the tooth row. Although some breakage is present along the medial margin of the fenestra, the anterior margin appears to be smooth and unbroken.

The shape of the fenestra is reconstructed as teardrop-like. The medial and lateral margins are linear and traverse diagonally toward the anterior margin, which ends in an acute point. Although missing, preserved proportions suggest that the fenestra is widest at its posterior.

TMM 43632-1 (Fig. 14O, P) also preserves the anterior margin of the suborbital fenestra. Cracking is present, and the element has been split and folded at the tooth row. The reconstruction indicates that the anterior margin may not have been as acute as suggested by TMM 43620-1. Because the tooth row is incomplete in TMM 43632-1, the anterior extent of the fenestra cannot be determined. TMM 43538-1 demonstrates that posterior processes of the maxillae extend along the lateral margins of the palatines and form much of the medial margin of the fenestra.

Palatine—Palatines, save the posterior-most margins, are preserved (Fig. 12B). Additionally, TMM 43538-1 also preserves an anterior left palatine (Fig. S3). Extensive cracking obscures their morphology. At the midline, the anterior-most palatine forms a blunt projection. The palatines are interpreted to form the anterior and medial margins of the suborbital fenestrae; the medial margin of the left suborbital fenestra, formed by the lateral portion of the palatine, is incomplete. The lateral edges of the elements appear to be parallel from anterior to posterior. It is unlikely that they produced a shelf extending into the suborbital fenestra; this character (Char. 112) was left as uncoded in the phylogenetic analysis.

Pterygoid and Ectopterygoid—TMM 43620-1 does not preserve pterygoids or ectopterygoids, but TMM 43632-1 (Fig. 14A–C, I, J), a very large individual from the same unit, does. Left and right ectopterygoids are preserved; the left is complete. The posterior flange of a right pterygoid is preserved. The elements are extremely robust. Sutural marks on the right pterygoid suggest that the ectopterygoid did not extend to the posterior tip of the lateral pterygoid flange. The pterygoid ramus of the ectopterygoid is bowed; the posterolateral margin of the suborbital fenestra formed by the ectopterygoid would have been concave. TMM 40571-1 demonstrates that the maxilla broadly separates the ectopterygoid from contacting the maxillary tooth row (Fig. S2).

Frontal—The anterior extent of the frontal terminates in a broad sutural contact with the nasals posterior to the anterior extent of the prefrontals (Fig. 12A). The lateral edges of the anterior process of the frontal are linear. The medial margin of the left prefrontal is broken, giving the left lateral portion of the frontal an asymmetrical appearance relative to the right. The lateral edge

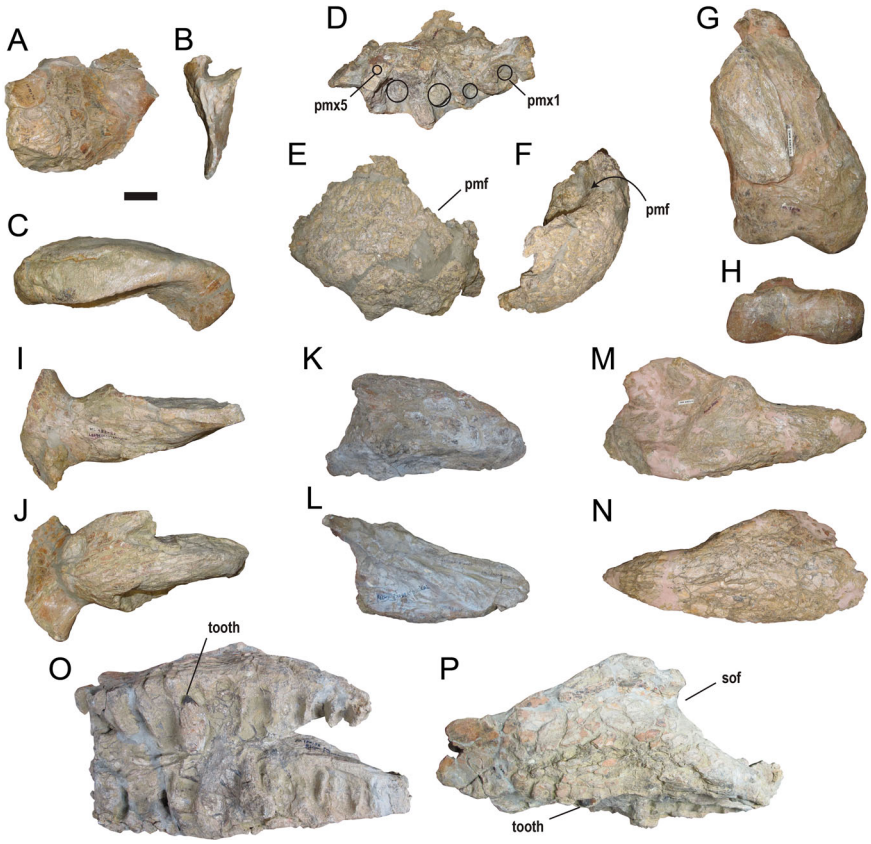

FIGURE 14. *Deinosuchus riograndensis* (TMM 43632-1) selected cranial elements. **A**, right pterygoid in ventral view. **B**, right pterygoid in posterior view. **C**, right pterygoid in lateral view. **D**, left premaxilla in ventral view. **E**, left premaxilla in lateral view. **F**, left premaxilla in dorsal view. **G**, right quadrate in dorsal view. **H**, right quadrate in posterior view. **I**, left ectopterygoid in medial view. **J**, left ectopterygoid in lateral view. **K**, right quadratojugal in dorsal view. **L**, right quadratojugal in ventral view. **M**, right jugal in medial view. **N**, right jugal in lateral view. **O**, right maxilla in occlusal view. **P**, right maxilla in dorsal view. **Abbreviations**: **pmf**, premaxillary fenestra; **pmx1**, premaxillary tooth 1; **pmx5**, premaxillary tooth 5; **sof**, suborbital fenestra. Scale bar equals 5 cm.

of the frontal, forming the medial margin of the orbit, is upturned and confluent with the upturned portion of the prefrontal. The frontoparietal suture is curved, the concave side facing anteriorly. Posteriorly, the lateral extent of the frontoparietal suture participates in the supratemporal fenestrae where it likely prevents the parietal from contacting the postorbital.

Prefrontal—In dorsal view, the anterior margins of the prefrontals are obscured, although the most likely position of the sutures is indicated (Fig. 12A). Anteriorly, the prefrontals end in a moderately blunt point. Dorsoventrally oriented swellings are present on the prefrontal and form the medial orbital margin. The swelling of the prefrontal forms the anterolateral extent of a continuous ridge that forms the medial margin of the orbit. On the ventral side of the skull, the dorsal-most prefrontal pillars are preserved; the medial processes of the pillars are anteroposteriorly expanded. Anterior to the pillars lie anteroposteriorly oriented elliptical recesses on the ventral side of the prefrontal.

Lacrimal—Lacrimals are incomplete. A composite morphology is known using information from both sides (Fig. 12A). The anterior-most portions of both lacrimals are obscured due to cracking but likely extended slightly to the anterior of the jugals; the anterior extent of the lacrimals is much greater than that of the frontal and prefrontals. The medial and lateral margins are linear for much of their length. The posteromedial margin makes a lateral excursion starting just posterior to the anterior extent of the frontal and continues to the orbital margin—along this length, the lacrimal makes broad contact with the lateral margin of the prefrontal. The posterior extent of the lacrimal forms the anterior margin of the orbit. A dorsoventrally oriented, 'V'-shaped notch is present on the lacrimal along the anterior border of the orbit.

Jugal—The left jugal is preserved in its entirety; the right jugal is largely absent (Fig. 12A, B). Laterally, the maxillojugal suture trends anteromedially from the lateral margin of the posterior snout toward the midline where it ends in a point. When viewed laterally, the anterior ramus of the element is widest immediately rostral to the orbit. The jugal forms a dorsoventral inflation along the lateral margin of the orbit.

The ventral and ventrolateral portions of the postorbital bar are formed by the jugal. The bar is relatively robust and is inset from the external lamina of the jugal. When viewed from an anterior aspect, the bar is 'L'-shaped and bows toward the midline at the midpoint of its body.

The lower temporal bar is formed entirely by the posterior ramus of the jugal. The posterior ramus of the jugal flattens dorsoventrally. The posterior-most left jugal is missing; a plaster reconstruction is in its place. Remaining margins suggest that the posterior-most portion of the ramus likely tapered to a point lateral to the lateral condyle of the quadrate. When viewed ventrally, the medial jugal foramen cannot be located due to poor preservation and the presence of matrix.

Orbit—The margins of the orbits are partially 'telescoped,' or elevated above the dorsal surface of the rostrum. Elements contributing to this morphology are the prefrontals, lacrimals, and jugals. The medial margins of the orbits, formed by the frontal, are gently upturned and are confluent with the 'telescoped' anterior and lateral margins formed by the prefrontal, lacrimal, and jugal. At the anterior-most margin lies a ventrally displaced 'V'-shaped depression of the lacrimal. The result is a cup-like morphology formed by the anterior and medial margins of the orbit due to contributions of the frontal, prefrontal, lacrimal, and jugal.

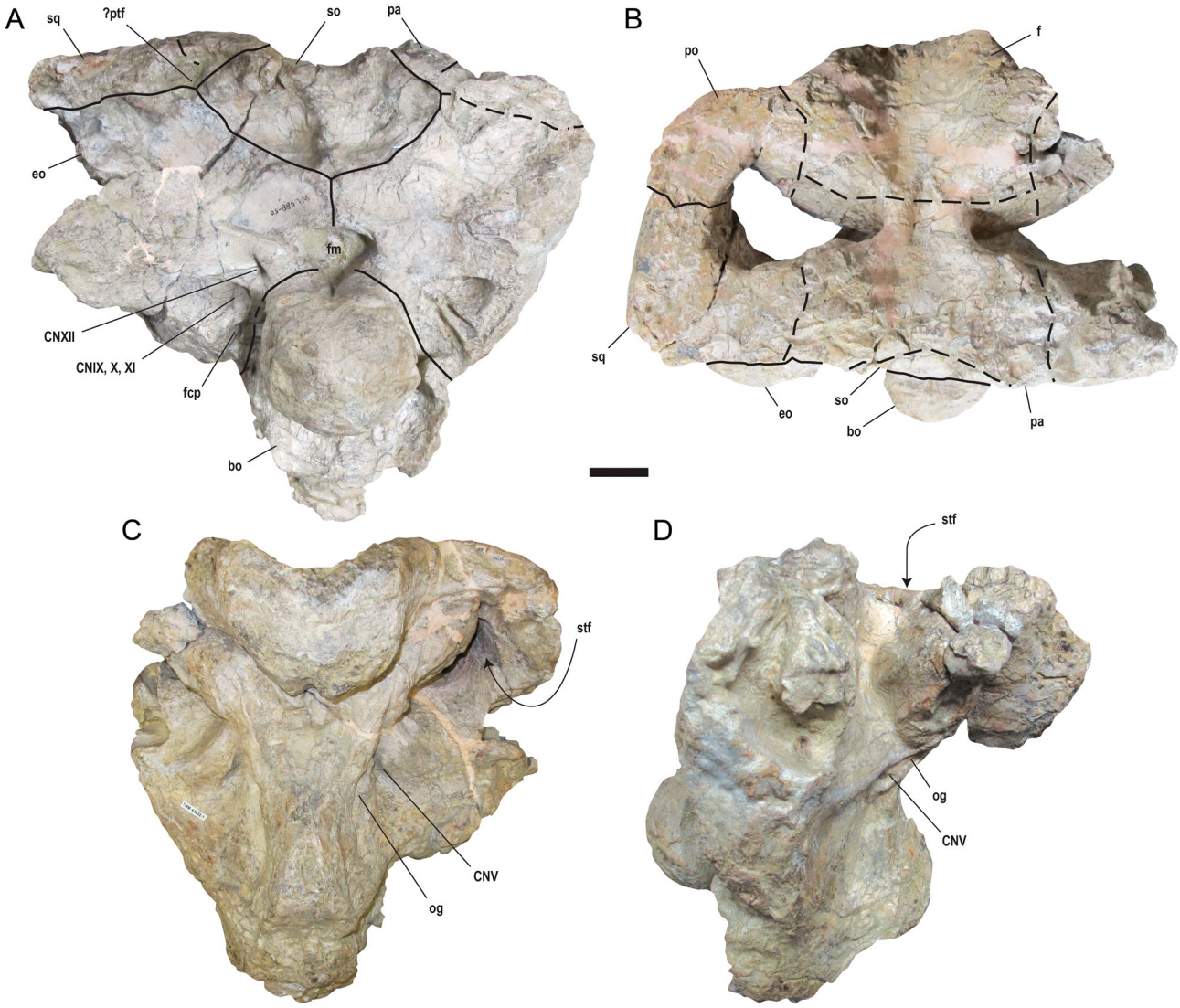

FIGURE 15. *Deinosuchus riograndensis* (TMM 43632-1) posterior skull. **A**, posterior view. **B**, dorsal view. **C**, anterior view. **D**, lateral view. **Abbreviations**: **bo**, basioccipital; **CNV**, cranial nerve V; **CNIX**, cranial nerve IX; **CNX**, cranial nerve X; **CNXI**, cranial nerve XI; **CNXII**, cranial nerve XII; **eo**, exoccipital; **f**, frontal; **fcp**, foramen caroticum posterius; **fm**, foramen magnum; **og**, ophthalmic groove; **pa**, parietal; **po**, postorbital; **ptf**, posttemporal fenestra; **so**, supraoccipital; **sq**, squamosal; **stf**, supratemporal fenestra. Scale bar equals 5 cm.

Skull Table—Skull table and otic region sutures are obscured on the right side but obvious on the left (Fig. 12A). The skull table slopes ventromedially toward the sagittal axis. The frontals, parietals, and supraoccipital form the floor of a midline furrow, the lateral margins of these elements raised relative to the midline. Elements forming the lateral margins of the skull table, the postorbitals and squamosals, are on a single plane dorsal to the midline furrow. The effect of this morphology is a skull table the midline of which is ventrally depressed relative to the lateral margins.

Postorbital—The postorbital is boomerang-shaped in dorsal view, its anterolateral corner approximating a 90° angle (Fig. 12A). The element forms the posterior margins of the orbits and the anterolateral margins of the large supratemporal fenestrae. Along the dorsal angle of the infratemporal fenestra, the postorbital contacts the quadrate and the quadratojugal. The element forms much of the postorbital bar; the postorbital process of the postorbital extends along the dorsolateral face of the bar. Although broken on the right side, the anterolateral side of the postorbital, immediately ventral to the skull table, bears a shallow, pit-like indentation for a foramen, allowing for the passage of the postorbital vein (Porter et al., 2016). The anteroventral portion of the postorbital, when viewed laterally, bears an anteroposteriorly oriented groove near the suture with the anterior process of the squamosal; posteroventral to the groove on the postorbital is a confluent groove on the squamosal for attachment of a muscular ear flap (Iordansky, 1973).

Parietal—In dorsal view, the parietal is hourglass-shaped between the supratemporal fenestrae, the constriction present at the point of the medial margin of the supratemporal fenestra (Fig. 12A). The parietal possesses ventral processes in the supratemporal fenestra. However, sutural margins are difficult to interpret and appear to differ bilaterally. The parietal sends posterior processes to each side of the supraoccipital, reaching the posterior margin of the skull table. When viewed from the posterior aspect, the parietal comprises the dorsomedial margin of the left posttemporal fenestra, which is preserved in its entirety.

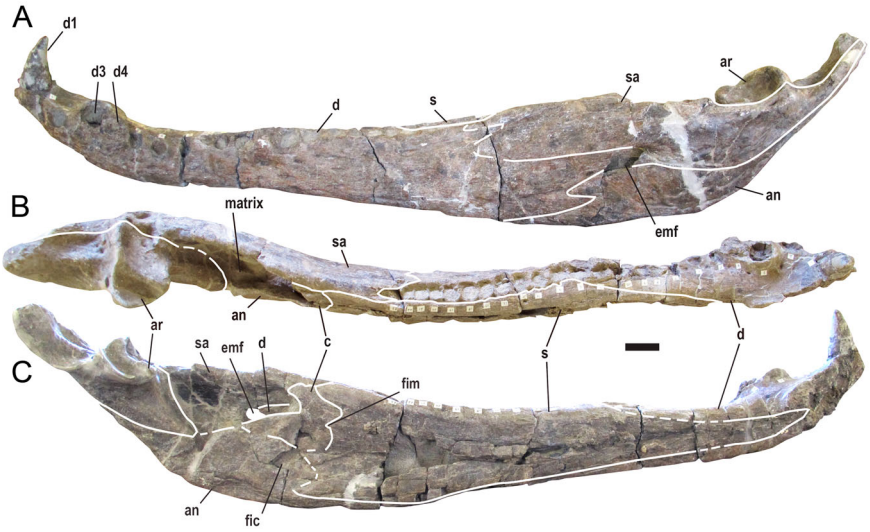

FIGURE 16. *Deinosuchus riograndensis* (TMM 43620-1) left hemimandible. **A**, lateral view. **B**, dorsal view. **C**, medial view. **Abbreviations**: **an**, angular; **ar**, articular; **c**, coronoid; **d**, dentary; **d1**, **d3**, **d4**, dentary teeth 1, 3, and 4; **emf**, external mandibular fenestra; **fic**, foramen intermandibularis caudalis; **fim**, foramen intermandibularis medius; **s**, splenial; **sa**, surangular. Scale bar equals 5 cm.

Supraoccipital—The supraoccipital is incompletely preserved; the posterior portion of the element is missing (Fig. 12A). However, other specimens (TMM 43538-1, TMM 43632-1) from the same unit preserve the element in its entirety (Fig. 15). The element is broadly exposed on the dorsal skull table; its anteroposterior length is abbreviated. The result is a half-moon-shaped exposure that culminates in a blunt point at its anterior extent. When viewed posteriorly, the supraoccipital is shaped like a cut diamond gemstone; its dorsolateral extent on the posterior skull forms the ventromedial margin of the posttemporal fenestrae. Posteriorly, the body of the supraoccipital bears mediolaterally trending indentations separated by a dorsoventrally oriented medial ridge.

Squamosal—The squamosal forms the posterolateral corner of the skull table (Fig. 12A). The postorbital-squamosal suture is concave anteriorly when viewed from a dorsal perspective and is located at the midpoint of the lateral margin of the supratemporal fenestra. The parietal-squamosal suture trends anteromedially from the posterior margin of the skull table and intersects the supratemporal fenestra at the midpoint of its posterior margin. Along the posterior wall of the supratemporal fenestra, the parietal-squamosal suture makes a lateral excursion and intersects the anterior opening of the posttemporal fenestra within the supratemporal fenestra. Laterally, the squamosal forms the roof of the otic aperture and the dorsal-most margin of the infratemporal fenestra. Along the dorsolateral surface of the element, the dorsal and ventral rims of the squamosal groove flare anteriorly. The posterolateral ramus of the squamosal is short and at its posterior-most extent contacts the paroccipital process of the exoccipital (Fig. 12D). When viewed posteriorly, the squamosal forms the dorsolateral margin of the posttemporal fenestra.

Quadratojugal—The left quadratojugal is incompletely preserved; the posterior-most extent has been reconstructed with clay; the right quadratojugal is missing entirely (Fig. 12A, B). The dorsal exposure of the quadratojugal is approximately twice the mediolateral width of the ventral exposure. The quadratojugal forms the posterior margin of the infratemporal fenestra. The suture joining the jugal and quadratojugal lies at the posterior angle of the infratemporal fenestra. TMM 43538-1 demonstrates that a quadratojugal spine projects into the infratemporal fenestra along the posterior wall between the posterior and superior angles. A dorsal process of the quadratojugal reaches the dorsal corner of the infratemporal fenestra and contacts the squamosal.

Quadrate—The left quadrate is mostly complete (Fig. 12A, B). The dorsal-most portions of the quadrate underlying the skull table are preserved, but the ventral portions in this area have been lost. Like the left quadratojugal, the posterior-most extent has been reconstructed. The quadrate forms the floor of the otic aperture and the ventral portion of the anterior wall along the external auditory meatus. Ventrally, the quadrate bears modest anteroposteriorly oriented crests for the attachment of the posterior adductor mandibulae muscle. Although incompletely preserved, the anterodorsal-most extent of the left quadrate underlying the supratemporal fenestra approaches the capitate process of the laterosphenoid; the elements may have contacted in life. Along the lateral braincase wall, the quadrate forms the posterior roof of the trigeminal foramen. TMM 43632-1 preserves an incomplete ventromedial portion of the quadrate. The quadrate forms the floor of the cranioquadrate passage and recess; the roof is formed by the paroccipital process of the exoccipital. TMM 43632-1 preserves both hemicondyles; the medial hemicondyle is smaller than its lateral counterpart (Fig. 14).

Laterosphenoid—The laterosphenoids are incompletely preserved in TMM 43620-1; the ventral-most portions are missing (Fig. 12B). The laterosphenoid forms the anterior margin of the trigeminal foramen. TMM 43632-1 also preserves dorsal portions; less bone is missing relative to TMM 43620-1, but sutures separating braincase elements are obscured. A pronounced anteroposteriorly trending ophthalmic groove is present on the laterosphenoid anterior to the roof of the trigeminal foramen.

Exoccipital—The exoccipital forms the ventrolateral margin of the posttemporal fenestra. Posteriorly, the paroccipital process of the exoccipital is laterally expansive and dorsoventrally deep. The lateral-most extension of the paroccipital process lies posteroventral to the posterior squamosal prong and forms an extensive sutural contact with the quadrate. Ventrally, the roof of the cranioquadrate recess is preserved on the posterolateral exoccipital. The ventral-most portion along the midline preserves the roof of the foramen magnum. When viewed from a ventral aspect, this region is posteriorly expanded. TMM 43632-1 preserves an unaltered foramen magnum (Fig. 15A). The dorsal and lateral walls are formed by the exoccipital. The floor is formed by the basioccipital. The foramen is heart-shaped in outline when viewed posteriorly.

TMM 43632-1 preserves the ventral exoccipital (Fig. 15). The robust ventral process of the element terminates dorsal to the

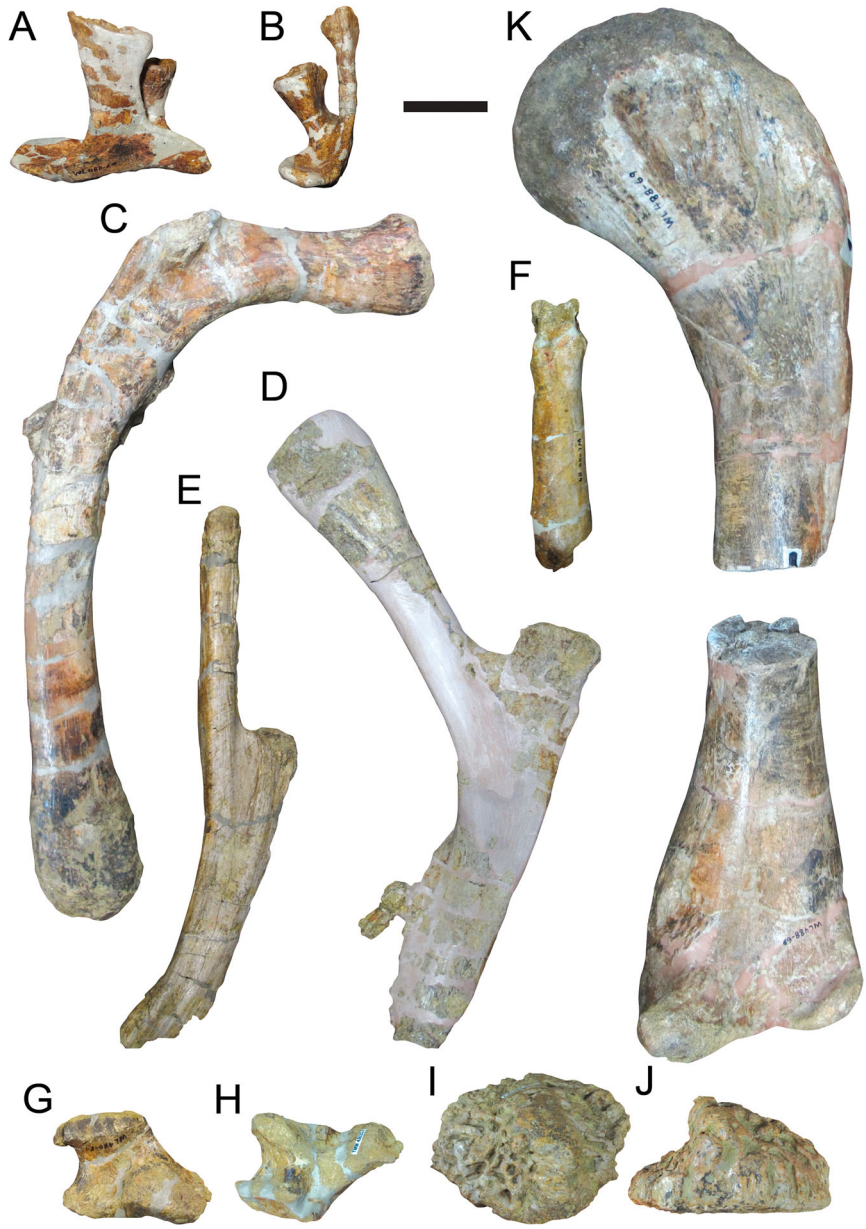

FIGURE 17. *Deinosuchus riograndensis* (TMM 43632-1) selected postcrania. **A**, right cervical vertebra in lateral view. **B**, right cervical vertebra in posterior view. **C**, proximal fragment of dorsal rib medial view. **D**, proximal fragment of dorsal rib in posterior view. **E**, proximal fragment of dorsal rib in anterior view. **F**, metatarsal in dorsal view. **G**, calcaneum in ventral view. **H**, calcaneum in dorsal view. **I**, dorsal osteoderm in dorsal view. **J**, dorsal osteoderm in anterior view. **K**, left femur in posterior view. Scale bar equals 5 cm.

basioccipital tubera and preserves openings for cranial nerves and blood vessels. Four depressions, likely representing infilled foramina for the passage of cranial nerves, are present on each ventral process of the exoccipital. The dorsal-most depression, presumably for the passage of cranial nerve XII, is lateral to the foramen magnum and is separated from the other depressions by a short distance. The other depressions are separated by mediolaterally trending ridges. The dorsal-most and deepest of the contiguous depressions, ventral to the depression for the conveyance of cranial nerve XII, is roughly triangular in shape. This depression is lateral to the ventral margin of the foramen magnum, has what appear to be small foramina inside its margins, and conveyed branches of cranial nerves IX, X, and XI as well as the jugular vein. Below it is the smallest depression, whose sides are nearly parallel and bordered by pronounced mediolaterally trending ridges. This depression likely corresponds to the carotid foramen. The ventral-most opening is nearly the same size as the dorsal-most opening but is very shallow. No obvious foramina are present within its borders; its function is unknown.

Basioccipital—TMM 43620-1 does not preserve a basioccipital, although it is preserved in TMM 43538-1 and TMM 43632-1. Preservation is best in TMM 43632-1 (Fig. 15). The element forms the floor of the foramen magnum and the occipital condyle. TMM 43632-1 best preserves the occipital condyle. The articular surface of the structure is bulbous and resembles a half sphere. A pronounced indention, separating the articular surface from the anterior portion of the structure, is present on all surfaces save the dorsal margin. Ventrally, the occipital condyle bears a large depression separating the articular surface from the basioccipital tubera.

Ventral to the occipital condyle, the external surface of the basioccipital is posteriorly oriented. Along the midline, directly below the condyle, lies a relatively large, unpaired foramen.

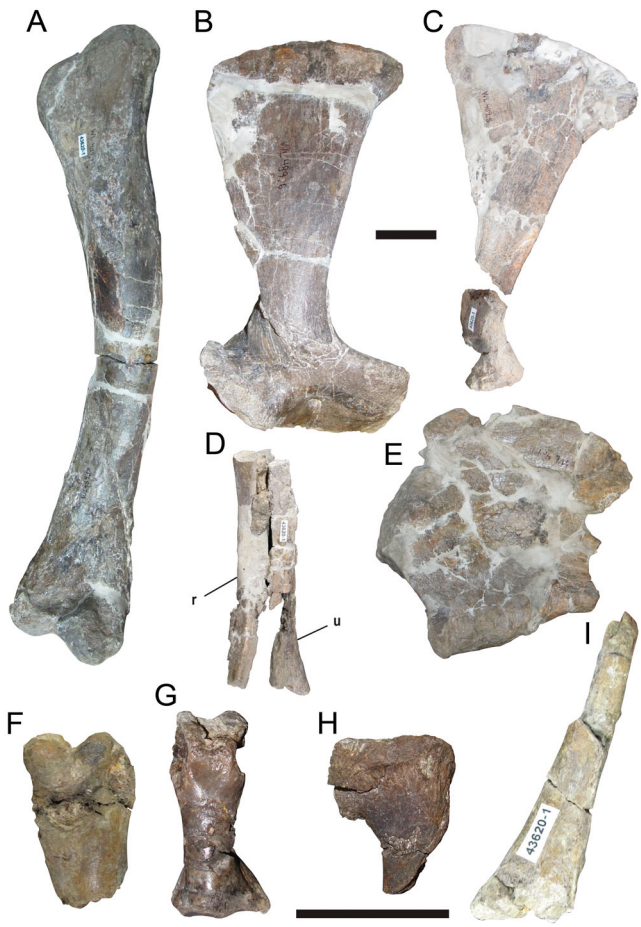

FIGURE 18. *Deinosuchus riograndensis* (TMM 43620-1) selected postcrania. **A**, right humerus in posterior view. **B**, left coracoid in lateral view. **C**, left pubis in medial view. **D**, left radius and ulna in posterior view. **E**, fragment of an ilium. **F**, distal end of a metapodial in anterior view. **G**, phalanx in anterior view. **H**, right proximal radiale. **I**, second cervical rib. **Abbreviations**: **r**, radius; **u**, ulna. Scale bars equal 5 cm. Top scale bar corresponds to **A**–**E**; bottom scale bar corresponds to **F**–**I**.

Ventral to the midline foramen, an acute ridge separates dorsoventrally trending depressions of the posterior basioccipital tubera. The edges of the ventral and ventrolateral basioccipital tubera have been chipped away; the external openings of the medial and lateral eustachian foramina are not preserved. A pronounced wing-like ridge lies lateral to the ventral-most occipital condyle. The ridge trends dorsoventrally and is expanded anteroposteriorly, resulting in a structure that projects outward from the posterolateral surface of the basioccipital tubera. TMM 43632-1 likely preserves the posteroventral basisphenoid, but sutures are obscured, and the morphology cannot be determined.

Mandible—A complete mandible is preserved for TMM 43620-1 (Fig. 16); it is separated at the mandibular symphysis, but the left side is largely intact and shows little to no evidence of deformation. The mandible is robustly built and nearly 1.5 m in length. The mandibular symphysis is short and does not extend posteriorly beyond the fourth dentary alveoli. The anterior-most alveoli lateral to the mandibular symphysis are oriented subparallel to one another. Posterior to the mandibular symphysis, the mid-dentary alveoli gradually curve medially. When viewed laterally, the dentary forms the anterior margin of the mandibular fenestra. Two posterior projections of the dentary are present. The dorsal-most of the two projects between the anterior processes of the surangular, whereas the ventral one projects into the anterior angular. The dorsal projection bears the anterior portion of a longitudinal depression that is confluent with a posterior depression on the surangular that forms the posterior portion of this depression. The longitudinal depression spans the distance from the juncture of the 17th and 18th alveoli to a point nearly in line with the dorsal projection of the anterior angular.

The third and fourth dentary alveoli are confluent; their shared margin is ovoid in dorsal view and raised relative to the body of the anterior dentary. Anterior teeth appear to project somewhat more buccally than teeth further posteriorly. The left hemimandible preserves a complete lower tooth row; there are spaces for 23 alveoli. The posterior-most alveoli are incompletely preserved on the right side. The right dentary preserves teeth in alveoli 2, 4, 12, 13, 15, and a posterior alveolus of unknown identity. Teeth are present in alveoli 1 and 4 on the left side; the first tooth is complete; the fourth tooth is missing its crown. The first tooth projects anterodorsally and would have occluded into a space between the first and second teeth of the premaxilla. Although missing in both dentaries, the margin of the third alveolus suggests that the third tooth was the largest in the mandible; the fourth dentary tooth was nearly as large as the third.

Teeth are large in two regions of the mandible. Anteriorly, the third and fourth alveoli are large; in the mid-dentary, the 11th and 12th alveoli are large. The 12th and 15th teeth have depressions on the medial sides near the base of the crown. These depressions were likely caused by replacement teeth growing under the teeth. Because the maxilla preserves evidence of an overbite in this region, the depressions were not caused by occlusion of the upper jaw dentition.

Splenial—The left splenial is nearly complete (Fig. 16). Anteriorly, it tapers along the body of the mandible where it reaches the mandibular symphysis but does not touch its counterpart. The splenial overlies the medial side of the anterior dentary until the space between dentary alveoli 11 and 12 where it then contributes to the dorsal exposure of the mandible and follows medially along the tooth row. The posterodorsal portion of the element extends past the tooth row and continues to the anterodorsal margin of the coronoid. The splenial bounds the anterior half of the foramen intermandibularis medius. Although the sutures with the angular and coronoid are indistinct, the splenial likely formed part of the anterior margin of foramen intermandibularis caudalis.

Coronoid—The coronoid is preserved; its anterior margin is somewhat damaged (Fig. 16). The superior margin of the element slopes anteriorly. The coronoid bounds the posterior half of the foramen intermandibularis medius and forms the dorsal margin of the foramen intermandibularis caudalis. The two short, blunt projections of the coronoid extend anterior to the foramen intermandibularis caudalis. They are positioned dorsal and ventral to the foramen.

Surangular—The anterior processes of the surangular extend along the medial margin of the 23rd alveolus but are incompletely preserved on both sides of the mandible (Fig. 16). Preservation is best for the left element, which preserves both processes save the anterior-most portion of the ventral process. Sutural marks on the dentary suggest that they were equal to subequal—this is confirmed by TMM 40571-1, which preserves the anterior processes. The notch between the two anterior projections bears a foramen. This structure is the posterior-most feature in a lengthwise groove that trends anteriorly along the dentary to the space between the 17th and 18th alveoli. The surangular forms the dorsal and posterior margins of the external mandibular fenestra. The lateral wall of the glenoid fossa is formed by the surangular. The lateral portion of the element, ventral to the glenoid, bears a mediolaterally oriented swelling as seen in AMNH 3073. Posteriorly,

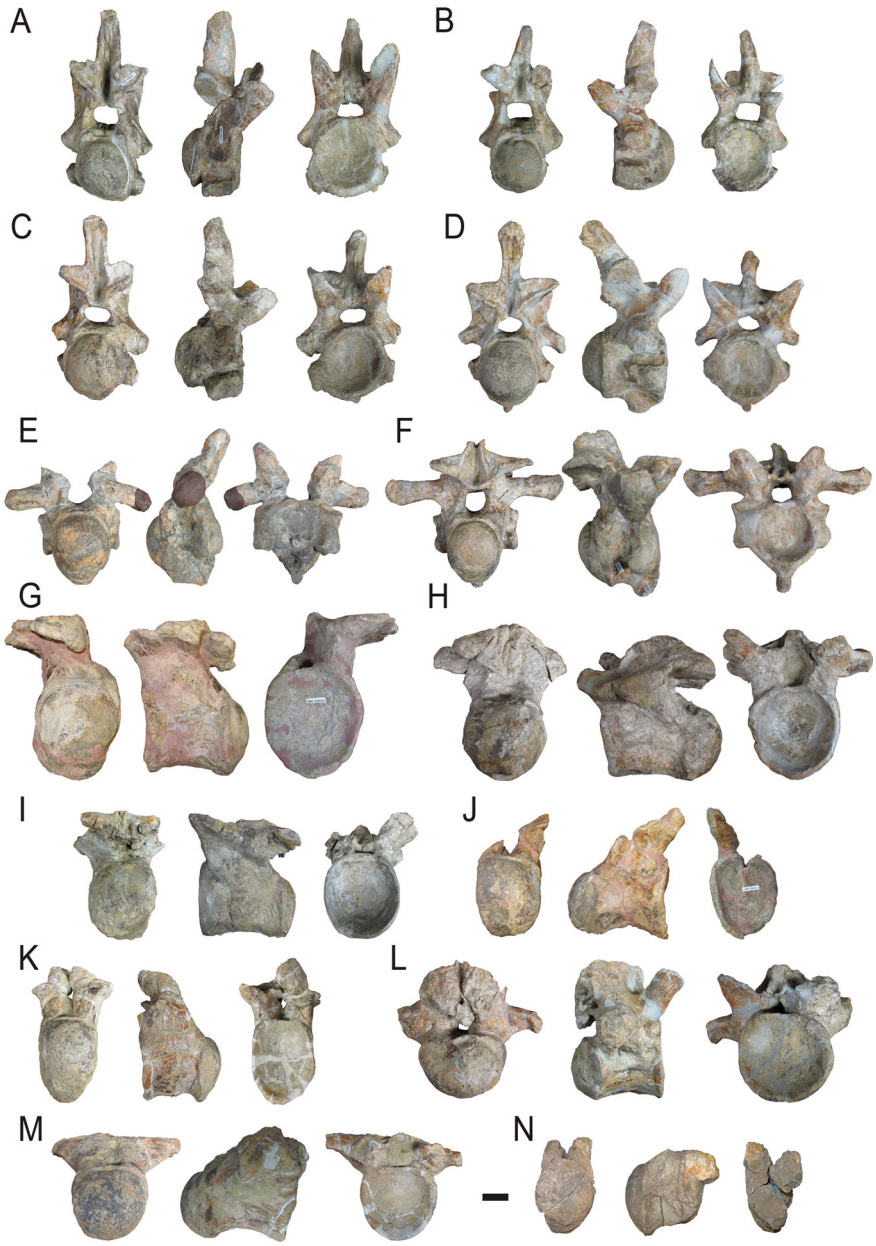

FIGURE 19. *Deinosuchus riograndensis* (TMM 43632-1) selected vertebrae. Single vertebrae arranged clockwise in posterior, lateral, and anterior views. **A**–**D**, cervical vertebra. **E**, **F**, anterior thoracic vertebra. **G**–**K**, thoracic vertebra. **L**, **M**, lumbar vertebra. **N**, dorsal vertebra. Scale bar equals 5 cm.

sutural marks on the articular indicate that the surangular extended to the dorsal tip of the retroarticular process.

Angular—When viewed medially, the angular forms the posterior, ventral, and dorsal margins of the foramen intermandibularis caudalis (Fig. 16). From a lateral aspect, the angulosurangular suture makes broad contact with the external mandibular fenestra along its ventral margin. Laterally, the element sends two processes anterior to the external mandibular fenestra. The dorsal process is short and is exposed along the lateral face of the element. The ventral process is long and continues along the ventral mandible to a point nearly equal to the anterior processes of the surangular. Posteriorly, the angular continues to the dorsal tip of the retroarticular process.

Articular—The glenoid fossa, save the lateral wall, is formed by the articular (Fig. 16). The retroarticular process is relatively short but broad. TMM 43620-1 preserves a depression on the articular posterior to the glenoid fossa that may represent remnants of the foramen aerum—it is inset medially from the lingual margin of the retroarticular process. Unfortunately, no specimens referable to this species preserve structures that may be confidently identified as the articular foramen aerum. Along the point of contact with the medial surangular and angular, there is cracking and matrix present; no other specimens adequately preserve this area, and characters representing this region's morphology were not coded.

Postcrania—Referred specimen TMM 43620-1 preserves portions of the axial skeleton and both limb girdles. Numerous osteoderms are present, some in association (Fig. S5) and all have inflated keels with lumpy, deeply pockmarked ornamentation. No osteoderm bears straight margins when viewed from the dorsal perspective. Many osteoderms are presumably from the midline of the dorsal shield—width greatly exceeds length, and

keels are large, lumpy, and symmetrical when viewed from the posterior or anterior perspective. A few are from the dorsal shield but would have been separated from the midline by one or more osteoderms—width greatly exceeds length, and keels are pronounced, large, and lumpy from the posterior or anterior perspective but are not symmetrical; they demonstrate a lean toward their lateral margin. Comparison with *Alligator* indicates that TMM 43632-1 preserves an osteoderm from the dorsal shield presumably just to the posterior of the hind limbs (Fig. 17I, J). The element is likely from the lateral-most margin and is approximately as wide as it is long. The inflated keel is asymmetrical when viewed from the anterior or posterior—one side of the keel demonstrates a nearly linear slope from the margin to the apex, whereas the other demonstrates a strong concavity.

TMM 43620-1 preserves a second cervical rib; it is approximately 10 cm in length and is missing both rib heads (Fig. 18I). The body of the rib tapers from anterior to posterior and ends in a blunt tip. A large dorsal rib is preserved; portions of the mid-body have been reconstructed using clay. The rib head is missing. The body of the rib is nearly equal in diameter along its length—the site of articulation with the costal cartilage is slightly greater in diameter, and more robust, relative to the mid-body of the element.

TMM 43632-1 preserves a cervical rib and three large thoracic ribs (Fig. 17A–E). The cervical rib is a right anterior cervical rib located no further forward than the third cervical vertebra. Its body is short and tapers anteriorly and posteriorly to a blunt tip. Of the thoracic ribs, the first is from immediately posterior to the forelimb girdle (Fig. 17C). The rib is reconstructed using plaster or clay; only the anterior portion of the rib remains. The dorsal rib head is missing; the ventral is mostly preserved. The second rib is the best preserved of the three and is a thoracic rib from the anterior of the thoracic series (Fig. 17D). The body is robust and nearly equal in diameter throughout. The body gradually expands to accommodate the wider diameter of the posteroventral end of the rib for articulation with the costal cartilages. The ventral rib head is preserved; the dorsal is missing. The third rib is from the posterior of the thoracic series of ribs (Fig. 17E). The ventral rib head is preserved, but the dorsal head is missing.

TMM 43620-1 preserves four vertebrae from the dorsal series. These vertebrae are likely from the lumbar region because the long transverse processes do not bear articular surfaces for rib capitula. The vertebrae were discovered in association, and proportions suggest that they were contiguous in series. When present, dorsal-most neural spines demonstrate a mediolateral swelling for the attachment of epaxial musculature. The dorsal-most extent of this feature is flat. The mediolateral swelling differs among the sample, and some are larger than others.

TMM 43632-1 preserves 14 vertebrae, four cervical and 10 dorsal. Ventral keels are short for the anterior-most cervical vertebrae and increase in length to the posterior of the cervical series. Not all cervical vertebrae are preserved—the four (Fig. 19A–D) here likely represent the anterior-most elements in the cervical series. Two anterior thoracic vertebrae (Fig. 19E, F) are preserved. They bear pronounced ventral keels, have facet attachments for two rib heads, and have dorsally displaced transverse processes that attach high on the neural arch. Five of the dorsal vertebrae are from the thoracic series (Fig. 19G–K). They are too incomplete to determine their position but have vertebral bodies that do not bear articular facets for ribs as well as transverse processes that are located high on the neural arch. Two of the vertebrae likely belong to the lumbar series (Fig. 19L, M). They are robustly built, do not have attachments for ribs, and have their transverse processes located low on the neural arch. One vertebra has an uncertain placement among the vertebral series (Fig. 19N). It preserves the vertebral body and portions of both pedicles. The body does not preserve articular facets for the attachment of rib heads—in life, it was posterior to the cervical series.

TMM 43620-1 preserves forelimb and girdle elements consisting of a coracoid, radius, ulna, humerus, and indeterminate phalanges (Fig. 18). A complete left coracoid preserves the ventral portion of the glenoid fossa (Fig. 18B). A foramen is present immediately anterior to the posterolaterally flaring glenoid fossa, and the blade flares ventrally. The ventrally flaring blade preserves an anteroventral corner bearing a blunt projection that grades dorsally into the blade via a concave angle. A right humerus is preserved (Fig. 18A). The deltopectoral crest is missing; no characters could be coded for this structure. Sutural scars for M. teres major and M. dorsalis scapulae are not clear. Both the proximal and distal articular ends of the bone are incompletely preserved. The anterolateral side of the shaft preserves a strong concave curve, whereas the posteromedial side preserves a strong convex curve. The left radius and ulna are preserved (Fig. 18D). The distal epiphysis of the ulna is complete; the proximal epiphysis is missing. The radius does not preserve either epiphysis. TMM 43620-1 preserves three phalanges. One is missing the distal end (Fig. 18F), one is missing the proximal end, and the third is complete (Fig. 18G). A right proximal radiale is preserved (Fig. 18H).

TMM 43620-1 hind limb girdle elements consist of an ilium and pubis (Fig. 18). The anterodorsal portion of the right ilium is poorly preserved—morphology is enigmatic (Fig. 18E). The left pubis is preserved; its blade flares anteriorly (Fig. 18C). The anteromedial corner ends in a blunt point whose dorsomedial margin gently grades via a concave curve into the dorsal blade. The shaft is broadly curved to the anterior, but cracking is present at the juncture of the blade and shaft; extent of the curvature may be taphonomic. TMM 43632-1 preserves a femur, a calcaneum, and a metatarsal (Fig. 17). A left femur is preserved; a portion of the mid-shaft is not preserved (Fig. 17K). The proximal epiphysis is bulbous and nearly featureless. The lateral condyle of the distal epiphysis is much larger and anteroposteriorly more expansive than the medial counterpart. The fourth trochanter is preserved; it is visible on the posteromedial side of the shaft ventral to the proximal epiphysis. A distal end of a calcaneum is preserved (Fig. 17G, H). TMM 43632-1 preserves a distal metatarsal (Fig. 17F).

SYSTEMATIC PALEONTOLOGY

CROCODYLIA Gmelin, 1789, sensu Benton and Clark, 1988
ALLIGATOROIDEA Gray, 1844
DEINOSUCHUS SCHWIMMERI, sp. nov.
(Figs. 20–27)

Holotype—MMNS VP-256 (Figs. 20–22).

Referable Specimens—TMM 45973-1 consists of an upper jaw and mandible from the lower Campanian Mooreville Formation of Lowndes County, Alabama, U.S.A. (Figs. 23, 24). ALMNH 1002 consists of a postcranial skeleton from the lower Campanian Mooreville Formation of West Greene, Greene County, Alabama, U.S.A. (Fig. 25).

Diagnosis—Deep occlusal marks present on the premaxilla between the first and second alveoli and lingual to the third and fourth alveoli; premaxillary-maxillary notch is lateral to the fifth premaxillary tooth; angular, posterior to external mandibular fenestra, is dorsoventrally expanded so as to form a hump on the dorsal margin; anterior margin of suborbital fenestra blunt and extends no further than the 10th maxillary alveolus from the end of the tooth row; ophthalmic groove trends dorsoventrally.

Occurrence—Middle Campanian, Late Cretaceous, Coffee Sand Formation, along Tulip Creek near Tupelo, Lee County, Mississippi, U.S.A.

Etymology—The specific epithet is named in honor of David R. Schwimmer for his tireless work on the Late Cretaceous paleontology of the Southeast and Eastern Seaboard, U.S.A.

Description

Deinosuchus schwimmeri MMNS VP-256 represents a beautifully preserved posterior skull and partial mandible (Figs. 20–22) from the Coffee Sand Formation of Lee County, Mississippi. The right side of the skull preserves a greater number of complete elements and clearer sutural contacts than the left side.

Nasals—The posterior half of the nasals are preserved (Fig. 20A). Anterior to the prefrontals, their lateral margins are nearly linear. The posterior processes of the nasals bound the anterior projection of the prefrontal; it does not contact the lacrimals. The posterior-most nasals contact the anterior margin of the frontal.

Maxilla—The anterior maxilla, along with the rest of the anterior rostrum, is not preserved (Fig. 20A). Posteriorly, a short acute process of the maxilla extends between the lacrimal and the nasal, and a blunt posterior process extends between the anterior lacrimal and the jugal. A posterolateral process of the maxilla separates the anterolateral jugal from contacting the lateral margin of the snout.

Ventrally, the maxilla preserves spaces for 13 posterior alveoli. Preserved teeth are missing their crowns. Assigning positions from the posterior of the tooth row, teeth are preserved in alveoli 3–6 and 8–13. Tooth diameter increases from posterior to anterior. Preserved portions indicate that enamel and dentin are thick; posterior teeth have very small pulp cavities.

The maxillary foramen for the palatine ramus of cranial nerve V is relatively small and is situated medial to the junction of the 12th and 13th alveoli from the posterior. The maxilla separates the ectopterygoid from the posterior tooth row. The maxilla forms the anterior, anteromedial, and anterolateral margins of the anteroposteriorly expansive suborbital fenestrae. The right suborbital fenestra is better preserved than the left; its posterior margins are missing. Anteriorly, the fenestra ends in a blunt point approximately in line with the junction of the 10th and 11th alveoli from the posterior. The posterior process of the maxilla extends into the lateral palatine along the medial margin of the suborbital fenestra where it extends with the level of the eighth alveolus from the posterior.

Palatine—Ventrally, the anterior portion of the right palatine is preserved (Fig. 20B). The anterior maxillopalatine suture is nearly linear and is mediolaterally oriented; the sutural contact is complex. The lateral portion of the anterior suture is nearly linear and ends as a small, blunt anterior projection. Preserved portions indicate that the palatines contributed to the medial margins of the suborbital fenestrae.

Ectopterygoid—Dorsal portions of the ectopterygoids are preserved; ventral portions along the pterygoid wings have been lost (Fig. 20B). Ventrally, at the juncture of the postorbital bar and the jugal, the ectopterygoid sends a blunt, broadly curved process medially along the ventral base of the bar. The posterodorsal portion of the element in contact with the jugal is separated from the ventrolateral margin of the skull by a short distance. Anteriorly, the maxillary face of the element extends parallel to the posterior maxillary tooth row and ends in an acute point at the anterior margin of the sixth maxillary tooth from the posterior. The ectopterygoid is separated from contacting the posterior tooth row by the maxilla.

Jugal—The jugals are long and broad (Fig. 20A). The maxillojugal suture trends anteromedially from the lateral margin of the posterior snout toward the midline. The anterior extent of the jugal ends in a blunt point where it approaches within 3–4 cm of the anterior margin of the lacrimal. The jugolacrimal suture is nearly linear. The anterior ramus of the jugal is widest and deepest immediately anterior to the orbit. The jugal forms an upturned lateral margin of the orbit.

The ventral portion of the postorbital bar is formed by the jugal; the bar is inset from the lateral jugal surface. The bar is large in diameter and when viewed from an anterior aspect; the bar is 'L'-shaped and at the midpoint of its body bows toward the midline of the skull. When viewed ventrally, the medial jugal foramen cannot be located due to poor preservation, but a small unrelated foramen is present posterior to the confluence of the posttemporal bar and the lower temporal bar. The lower temporal bar is formed by the posterior ramus of the jugal. Posteriorly, the jugal tapers to a point where it meets the quadratojugal at a suture that trends posterolaterally from the posterolateral corner of the infratemporal fenestra to the lateral margin of the skull.

Lacrimal—Both lacrimals are preserved; the right element demonstrates clear sutural contacts (Fig. 20A). The anterior lacrimal ends in a blunt point. Sutural contacts with the jugals, nasals, and prefrontals are broad, nearly linear, and trend anteroposteriorly. The lacrimal extends slightly farther to the anterior and much farther to the anterior than the jugal and the prefrontal, respectively. The posterior lacrimal is somewhat mediolaterally constricted compared with the anterior. A dorsoventrally oriented, 'V'-shaped notch is present along the anterior margin of the orbit, which is formed by the lacrimal.

Prefrontal—Both prefrontals are preserved; the anterior margins end in an acute point bounded anteriorly by the nasals (Fig. 20A). The prefrontals exceed the frontal in their anterior extent. Along much of its length, the prefrontofrontal suture is anteroposteriorly oriented and nearly linear; at the posterior-most extent, the suture forms a nearly right angle and trends mediolaterally to the medial margin of the orbit. The prefrontal forms the upturned anteromedial margin of the orbit. Ventrally, the dorsal prefrontal pillars are preserved; the medial processes are expanded anteroposteriorly. Anterolateral to the pillars lie anteroposteriorly oriented elliptical recesses of the prefrontal.

Frontal—Anteriorly, the frontal ends in a blunt point where it contacts the nasals (Fig. 20A). The lateral edges of the anterior process of the frontal are linear. Posteriorly, the frontal forms the upturned medial margin of the orbit, confluent with the upturned anteromedial margin formed by the prefrontal. The frontal contacts the postorbital anteriorly at the posteromedial corner of the orbit. The frontoparietal suture is concave anteriorly. Posterolaterally, processes of the frontal form part of the anterior margin of the supratemporal fenestrae. When viewed internally, the projection that forms the anterior margin also forms the anterior wall of the fenestra and prevents the parietal from contacting the postorbital.

Orbit—The orbits are 'telescoped' or elevated above the dorsal surface of the rostrum, along the anterior and lateral margins and gently upturned along the medial margin (Figs. 20A, 21C). The prefrontals, lacrimals, and jugals contribute to this morphology. The gently upturned medial margins formed by the frontal are confluent with the 'telescoped' anterior and lateral margins formed by the prefrontal, lacrimal, and jugal. At the anterior-most margin lies a ventrally displaced 'V'-shaped depression (Fig. 21C). The result is that the anterior and medial margins of the orbit are cup-like and are formed in part by contributions of the frontal, prefrontal, lacrimal, and jugal.

Skull Table—The skull table slopes ventromedially toward the sagittal axis, forming a midline furrow contributed to in part by the frontals, parietals, and supraoccipital (Figs. 20A, 21C). The lateral margins of these elements are raised relative to their midline. Elements forming the lateral margins of the skull table, the postorbital, and the squamosal, are on a single plane dorsal to the midline furrow. The result is a skull table the midline of which is ventrally depressed relative to the lateral margins (Fig. 21C).

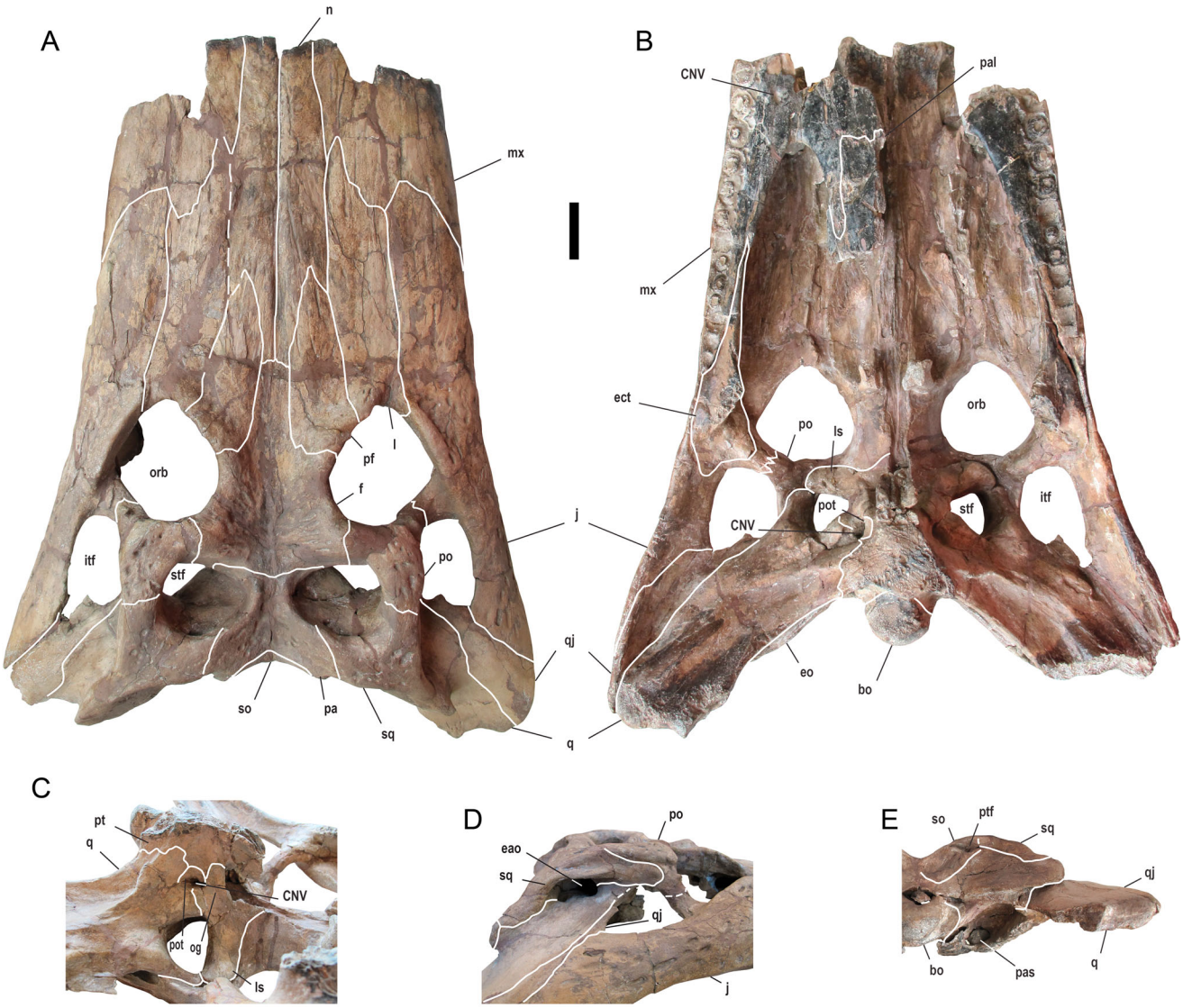

FIGURE 20. *Deinosuchus schwimmeri* (MMNS VP-256) skull. **A**, dorsal view. **B**, ventral view. **C**, lateral view of braincase elements. **D**, lateral view of otic region elements. **E**, posterior view of skull. **Abbreviations**: **bo**, basioccipital; **CNV**, cranial nerve V; **eao**, external auditory opening; **ect**, ectopterygoid; **eo**, exoccipital; **f**, frontal; **itf**, infratemporal fenestra; **j**, jugal; **l**, lacrimal; **ls**, laterosphenoid; **mx**, maxilla; **n**, nasal; **og**, ophthalmic groove; **orb**, orbit; **pa**, parietal; **pal**, palatine; **pas**, paranasal air sinus; **pf**, prefrontal; **po**, postorbital; **pot**, prootic; **pt**, pterygoid; **ptf**, posttemporal fenestra; **q**, quadrate; **qj**, quadratojugal; **so**, supraoccipital; **sq**, squamosal; **stf**, supratemporal fenestra. Scale bar equals 5 cm.

Postorbital—The postorbital forms the posterior margins of the orbits and the anterolateral margins of the large supratemporal fenestrae (Fig. 20A). The postorbitosquamosal suture trends diagonally from the lateral margin of the skull table to the point where it intersects the supratemporal fenestra along the midpoint of its lateral margin. The postorbital contacts the quadrate and the quadratojugal along the dorsal angle of the infratemporal fenestra. The postorbital process is moderately inset from the anterolateral margin of the skull table and extends along the dorsolateral face of the postorbital bar, forming much of the structure. When viewed laterally, the anterodorsal portion of the postorbital bears an anteroposteriorly oriented groove near the suture with the anterior projection of the squamosal. This groove is confluent with a groove on the squamosal and in life formed the attachment site for the muscular ear flap.

Parietal—The parietal is hourglass-shaped in dorsal view (Fig. 20A). Dorsally, the element forms the medial margins of the supratemporal fenestrae and, within the fenestrae, the medial walls. The anterior margin of the parietal enters the supratemporal fenestrae via lateral processes; these processes form the anteromedial walls of the fenestrae. The parietal extends laterally, relative to the supraoccipital, to the posterior margin of the skull table. Sutural contact with the squamosal is nearly linear and trends posterolaterally from the posterior margin of the supratemporal fenestrae to the posterior skull table. Along the posterior wall of the supratemporal fenestrae, the parietosquamosal suture makes a lateral excursion where it intersects the medial margin of the anterior opening of the temporal canal. When viewed from a posterior aspect, the parietal-squamosal suture intersects the posttemporal fenestrae midway along the dorsal margin. The parietal comprises the dorsomedial margins of the posttemporal fenestrae.

Squamosal—The squamosal forms the posterolateral corner of the skull table (Fig. 20A). The posterolateral margins of the

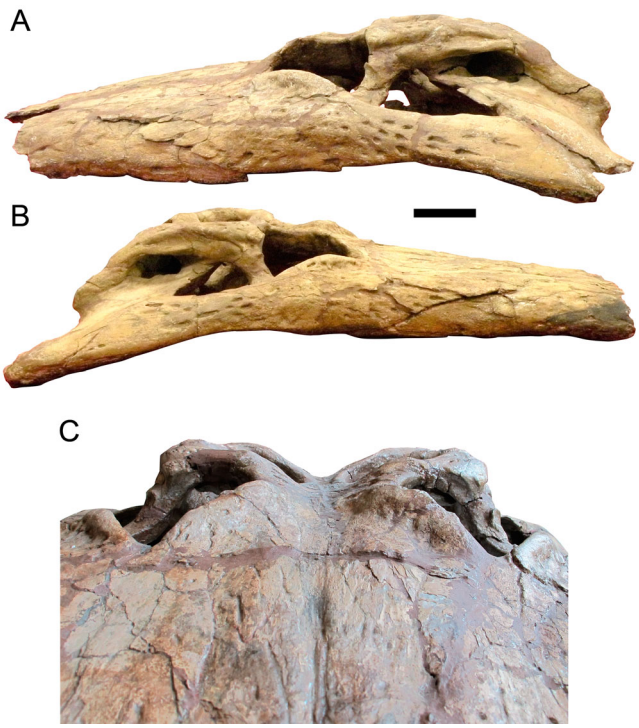

FIGURE 21. *Deinosuchus schwimmeri* (MMNS VP-256) skull. **A**, left lateral view. **B**, right lateral view. **C**, anterodorsal view demonstrating the unique orbital morphology and midline furrow of the skull table. Scale bar equals 5 cm.

supratemporal fenestrae are formed by the element. Within the fenestra, the squamosal forms the posterolateral wall. All margins, save the medial, of the anterior opening of the temporal canal are formed by the squamosal. Laterally, the squamosal forms the roof of the otic aperture, the posterior margin of the external auditory meatus, and the dorsal-most margin of the infratemporal fenestra. The huge squamosal groove, for attachment of the external ear valve musculature, is dorsoventrally expansive (Fig. 20D). The dorsal and ventral rims of the groove flare anteriorly then slightly contract at their anterior-most extent. The posterolateral ramus of the squamosal is relatively short. The ventral portion of the ramus contacts the lateral extent of the paroccipital process of the exoccipital. When viewed from a posterior aspect, the squamosal forms much of the dorsal margin of the posttemporal fenestra.

Supraoccipital—The supraoccipital is crescent-shaped; the mediolateral breadth of the element exposed on the dorsal skull table greatly exceeds the length (Fig. 20A). A blunt point is present at its anterior extent. When viewed posteriorly, the supraoccipital is shaped like a cut gemstone the dorsal margin of which is ventrally indented. Posteriorly, the medial margins of the posttemporal fenestrae are formed by the dorsolateral margins of the element. The posterior body of the supraoccipital bears mediolaterally trending indentations separated by a medial ridge that extends from the dorsal skull table to the ventral margin of the element.

Exoccipital—The exoccipitals are complete (Fig. 20D) and form the ventral margins and floor of the posttemporal fenestra; the floor of the fenestra is visible when the skull is viewed dorsally (Fig. 20A). Anteriorly, very little of the exoccipital is preserved on the lateral braincase; ventral portions are missing. The paroccipital process is wide and makes extensive contact with the quadrate. The element extends further laterally than the posterior squamosal prong that contacts the paroccipital process of the exoccipital posteriorly. Ventrally, and somewhat medial to the lateral-most extent of the paroccipital process, the exoccipital forms the roof of the cranioquadrate recess; the floor of the recess is formed by the quadrate. The dorsal and lateral margins of the foramen magnum are formed by the exoccipitals. Lateral to the occipital condyle, the element preserves openings for cranial nerves and blood vessels. These features are clearest on the left side. Three openings are preserved; they are separated by slight ridges. The dorsal and ventral foramina are roughly the same size and are deeper than the opening in the middle position. The dorsal foramen, presumably for the passage of cranial nerve XII, is lateral to the dorsal-most extent of the occipital condyle and bears foramina within its margins. The middle depression is presumably for the passage of cranial nerves IX-XI and the jugular vein while the ventral depression is presumably for the passage of the carotid artery. Neither depression bears obvious foramina within their margins.

Basioccipital—The dorsal basioccipital remains, but ventral portions have been lost (Fig. 20E). The floor of the foramen magnum is formed by the element. The occipital condyle is formed by the basioccipital; some breakage is present on the right ventral margin of the condyle. When viewed laterally, the dorsal margin of the occipital condyle slopes slightly ventrally from anterior to posterior.

Laterosphenoid—Much of the anterior and ventral laterosphenoids are missing (Fig. 20B, C). Sutures separating braincase elements are difficult to discern. The anterior margin of the trigeminal foramen is formed by the element. Laterally, the capitate process is oriented anteroposteriorly toward the midline. The laterosphenoid makes a robust contact with the quadrate ventral to the postorbital. The element preserves the ophthalmic groove, which trends dorsally as it moves from the trigeminal foramen to the anterior.

Quadratojugal—Both quadratojugals are preserved; the right side is complete (Fig. 20A, B). The posterior margin of the infratemporal fenestra is formed by the element. The jugoquadratojugal suture is linear and intersects the posterior angle of the infratemporal fenestra anteriorly. The element preserves a quadratojugal spine that projects into the infratemporal fenestra along the posterior wall between the posterior and superior angles. A dorsal process of the element reaches the dorsal corner of the infratemporal fenestra where it contacts the squamosal.

Quadrate—Both quadrates are preserved; the right side is complete (Fig. 20A, B). Dorsally, the element forms the floor of the otic aperture. The anterior and ventral walls of the external auditory meatus are formed by the quadrate. The squamosal-quadrate suture extends to the posterodorsal corner of the external auditory meatus. Posteroventrally, modest crests for the attachment of the posterior m. adductor mandibulae are present; they are oriented anteroposteriorly along the posterior ramus. The anterodorsal-most extent of the quadrate, ventral to the supratemporal fenestra, contacts the capitate process of the laterosphenoid. The ventral process of the quadrate is significant and forms much of the lateral braincase wall. The posterior half of the trigeminal foramen is formed by the quadrate. The floor of the cranioquadrate recess is formed by the quadrate. The medial hemicondyle is incompletely preserved; it is unknown which hemicondyle was larger in the species. The quadrate foramen aerum could not be located.

Mandible—A partial mandible is preserved (Fig. 22). Portions of the left dentary, splenial, surangular, angular, and articular are preserved, along with a more complete right articular and right coronoid. The splenial is very fragmentary; no characters were coded for the element. The posterior-most dentary maintains the anterior, anterodorsal, and anteroventral margins of the external mandibular fenestra. All margins of the fenestra are chipped, but proportions and contribution of elements are

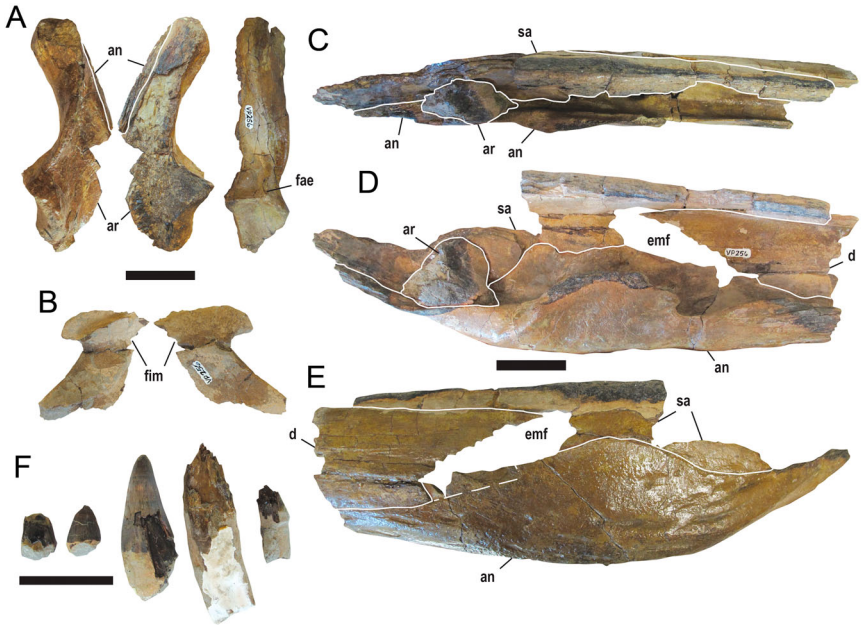

FIGURE 22. *Deinosuchus schwimmeri* (MMNS VP-256) left mandibular elements and loose teeth. **A**, left retroarticular process in medial, lateral, and dorsal views. **B**, left coronoid in medial and lateral views. **C**, left posterior mandible in dorsal view. **D**, left posterior mandible in medial view. **E**, left posterior mandible in lateral view. **F**, loose teeth in medial and lateral views. **Abbreviations**: **an**, angular; **ar**, articular; **d**, dentary; **emf**, external mandibular fenestra; **fae**, foramen aerum; **fim**, foramen intermandibularis medius; **sa**, surangular. Scale bars equal 5 cm.

clear. Posteroventrally, the dentary stops anterior to the external mandibular fenestra, but possible sutural marks on the angular may attest to the dentary extending along the ventral margin of the external mandibular fenestra.

Surangular—The surangular is poorly preserved anteriorly, medially, and posterodorsally, making description difficult (Fig. 22C–E). The posterior and posterodorsal margins of the external mandibular fenestra are formed by the surangular. The

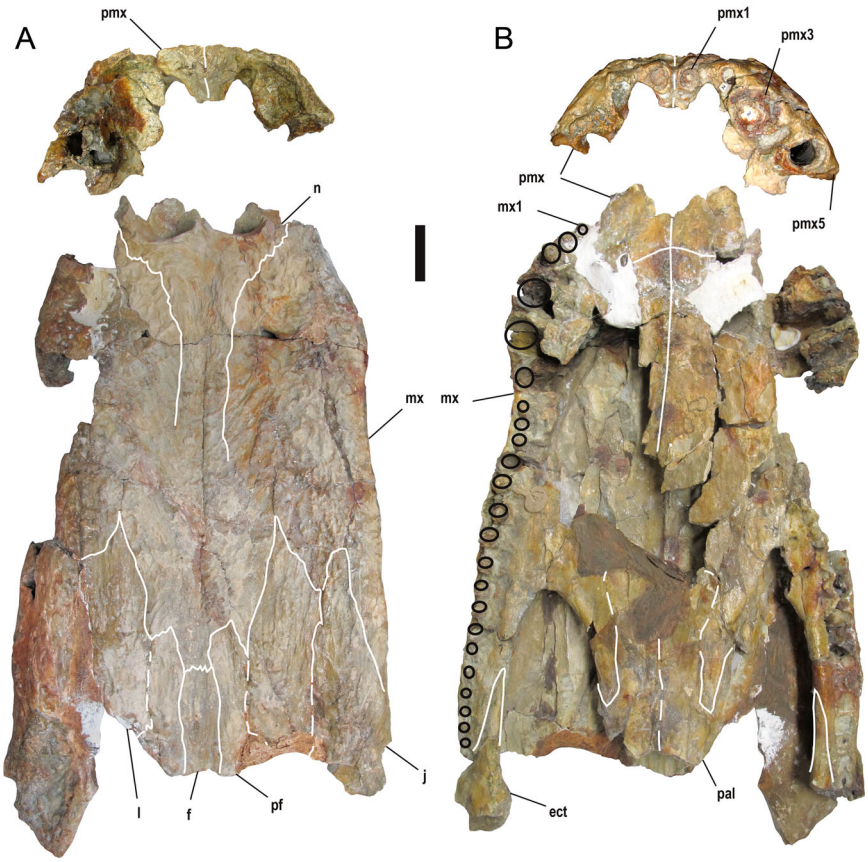

FIGURE 23. *Deinosuchus schwimmeri* (TMM 45973-1) upper jaw. **A**, dorsal view. **B**, ventral view. **Abbreviations**: **ect**, ectopterygoid; **f**, frontal; **j**, jugal; **l**, lacrimal; **mx**, maxilla; **mx1**, maxillary alveolus 1; **n**, nasal; **pal**, palatine; **pf**, prefrontal; **pmx**, premaxilla; **pmx1**, premaxillary alveolus 1; **pmx3**, premaxillary alveolus 3; **pmx5**, premaxillary alveolus 5. Scale bar equals 5 cm.

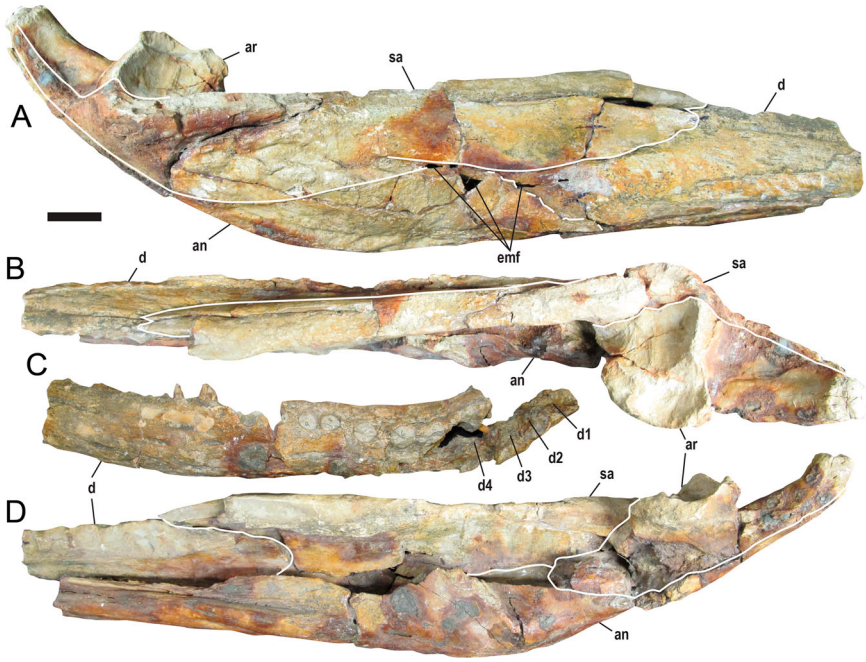

FIGURE 24. *Deinosuchus schwimmeri* (TMM 45973-1) right mandible. **A**, posterior elements in lateral view. **B**, posterior elements in dorsal view. **C**, anterior elements in dorsal view. **D**, posterior elements in medial view. **Abbreviations**: **an**, angular; **ar**, articular; **d**, dentary; **emf**, external mandibular fenestra; **d1**, dentary alveolus 1; **d2**, dentary alveolus 2; **d3**, dentary alveolus 3; **d4**, dentary alveolus 4; **sa**, surangular. Scale bar equals 5 cm.

suranguloangular suture contacts the external mandibular fenestra along its ventral margin. Sutural marks on the right articular suggests that the surangular formed the lateral margin of the glenoid fossa. Characters near the juncture of the surangular, angular, and articular were not coded due to poor preservation. Sutural marks on the retroarticular process suggest that the surangular reached the dorsal tip of the articular.

Angular—The angular is incompletely preserved; the anterior and posterior-most margins are missing (Fig. 22C–E). The element forms the posteroventral margin of the external mandibular fenestra. Posterior to the fenestra, the element expands dorsoventrally such that the dorsal margin has a pronounced hump when in lateral view. Sutural marks on the articular suggest that the posterior margin of the angular extended to the dorsal tip of the retroarticular process. Although incompletely preserved, the angular forms the posterior and ventral margins of the foramen intermandibularis caudalis. An anterior process of the angular possibly formed part of the dorsal margin as well. Posterior to the foramen, the angular becomes dorsoventrally more expansive, resulting in a hump-like morphology of the dorsal margin on the medial side of the element.

Coronoid—A right coronoid is preserved; the anterior margin is damaged in places (Fig. 22B). The element appears to form the posterior margin of the foramen intermandibularis medius. Because it is disassociated from the mandible, the extent of its contribution to the margins of the foramen intermandibularis caudalis is unknown. Although disassociated, the superior margin of the element appears to slope anteriorly; this character was left uncoded in the matrix.

Articular—The left hemimandible portion preserves a fragment of the ventral articular (Fig. 22C, D). A right articular is present but is disassociated from other mandibular elements. The left fragment does not preserve any codable morphology. The right fragment preserves the glenoid fossa and the retroarticular process (Fig. 22A). A depression likely representing the foramen aerum of the articular is inset from the lingual margin of the posterodorsally projecting retroarticular process.

Teeth—Five partial loose teeth are associated with MMNS VP-256 (Fig. 22F). Enamel is thick and in the best-preserved teeth demonstrate apicobasal striations. Three are small posterior teeth, one of which preserves a complete crown that is roughly conical; the crown is short. Two are larger anterior dentary or maxillary teeth; one preserves a tall conical crown. The largest and most complete of the crowns demonstrates a slight carina on the mesial and distal sides.

TMM 45973-1

This specimen consists of a complete snout and mandible (Figs. 23, 24) from the lower Campanian Mooreville Formation of Lowndes County, Alabama, U.S.A. It is approximately the same size as the *D. schwimmeri* holotype. The specimen was found on the west bank of the Alabama River approximately 200 m upstream from the Army Corps of Engineers Lock and Dam.

Surficial bone is deteriorating from moisture-induced destruction via geochemical processes or 'pyrite disease'; a gray powdery substance has replaced fossilized bone in affected areas. The bone has two textures: one is powdery, light tan in color, and feels slightly rough to the touch; the other texture is dark tan in color and smooth to the touch. Powdery tan areas obscure sutures, likely as a result of 'pyrite disease.' The posterior of the snout near the right orbit and along the posterolateral margin of the left side has been reconstructed with a dark tan clay.

The skull has experienced dorsoventral crushing. Reconstruction efforts were made to separate the palatal portions from the roof of the snout, but palatal elements are largely in a single plane. Some of the three-dimensional morphology is obscured, but spatial relationships are maintained. The anterior portion of the snout bearing the premaxillae is in a poor state of preservation. The anteroventral portion bearing the premaxillary alveoli suggests that the anterior snout was moderately deep; it is not likely that the depth equaled that of *D. riograndensis*.

Premaxilla—The premaxilla is preserved, but the anterior portion is disassociated from the rest of the skull; dorsal margins are largely destroyed (Fig. 23A, B). The premaxilla has five alveoli per side. The left side preserves five alveoli with five broken teeth. The right side of the element preserves the first and second alveolar positions and the anterior margin of position

FIGURE 25. *Deinosuchus schwimmeri* (ALMNH 1002). **A**, vertebrae in right lateral view; sacral vertebrae in dorsal view. **B**, left ilium, ischium, and pubis (clockwise) in lateral view. **C**, right femur in medial view. **D**, left tibia in medial view. **E**, left fibula in medial view. **F**, metatarsals in anterodorsal view. **G**, calcaneum, astragalus, and tarsals (clockwise) in various views. **H**, chevron in anterior view. **I**, phalanges in anterodorsal view. **J**, osteoderms in dorsal and anterior views. Scale bars equal 5 cm.

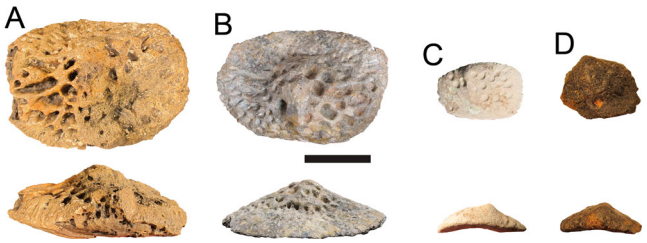

FIGURE 26. Comparison of dorsal osteoderms in dorsal and anterior views. **A**, *Deinosuchus hatcheri*, CM 963. **B**, *Deinosuchus riograndensis*, TMM 43620-1. **C**, *Deinosuchus schwimmeri*, ALMNH 1002. **D**, *Deinosuchus schwimmeri*, MMNS VP-5997. Scale bar equals 5 cm.

the fourth; the first position bears a broken tooth. Where the third alveolus is predicted to be, there is either bone overgrowth or the products of 'pyrite disease.' Proportions of the teeth can be determined from the left side. Teeth in positions 1 and 2 are small; teeth in positions 3 and 4 are large; the fifth tooth is small. Among the premaxillary teeth, the third tooth is the largest and the fifth is the smallest.

Posterior to the space between the first and second teeth, there is a groove produced by the occlusion of the first dentary tooth with the premaxilla. A second groove is present between the third and fourth premaxillary teeth. This groove was likely produced by occlusion with the second dentary tooth. Posterior to the fourth alveolus and posteromedial to the fifth is a large groove for receiving the third and fourth dentary teeth. When viewed from the anterior, the mesial-most and distal-most premaxillary tooth row is dorsally displaced relative to the third and fourth premaxillary teeth. The effect is a ventral bulge of the premaxilla at the point of the third and fourth alveoli. Posteroventral margins of the element are preserved. Sutures with the maxilla are mediolaterally oriented and trend anteriorly toward the midline. Anteroventrally, the element may bear remnants of the incisive foramen.

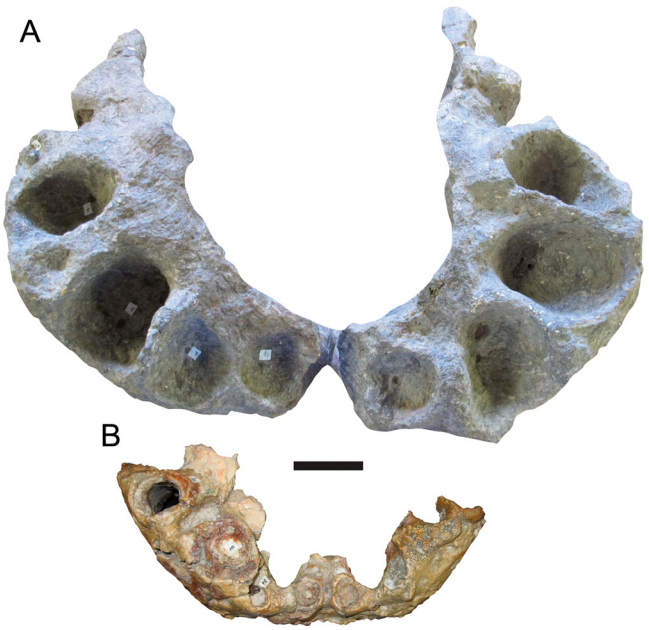

FIGURE 27. Comparison of premaxillae in occlusal view. **A**, *Deinosuchus riograndensis*, AMNH 3073. **B**, *Deinosuchus schwimmeri*, TMM 45973-1. Scale bar equals 5 cm.

Nasal—The sutural contacts between the nasals and other elements are clearest in the anterior snout (Fig. 23A). The anterior nasals are laterally expanded and form the posterior margin of the bony narial aperture. Along the midline, the nasals project into the aperture at the midline. There is evidence of broken bone; in life, the projection may have extended further forward, but proportions suggest that it would not have extended far enough to bisect the large bony narial aperture. Preserved margins suggest that the aperture was very wide.

Posterior to the bony narial aperture, sutures with the maxilla are mediolaterally oriented and trend anteriorly toward the midline where the nasals proceed posteriorly and whose margins are nearly parallel. At midsnout, anterior to the frontals and prefrontals, the sutures are obscured due to the effects of 'pyrite disease.'

Maxilla—The maxillae are preserved; the right side is nearly complete save its ventral surface (Fig. 23A, B). Due to 'pyrite disease' and the powdery texture of surficial bone, sutures on the dorsal side of the snout are very difficult to determine. The element's contribution to the bony narial aperture is unknown. However, the maxillary tooth row appears to be complete on the right side, suggesting that the anterior maxilla is known and was excluded from the posterior and posterolateral apertures.

There are 28 teeth in the upper jaw: 23 maxillary, five premaxillary (Fig. 23B). The right side has the best preservation of the tooth row, and comparison with MMNS VP-256 suggests that the posterior-most alveoli are preserved. The animal had an overbite, as suggested by occlusal marks lingual to the maxillary tooth row.

Two mediolateral expansions are present along the maxillary tooth row. The anterior expansion occurs in the area between the first and seventh alveoli, and the posterior expansion corresponds to the area between the 10th and 14th alveoli. The former expansion is pronounced, and the latter is minimal. The diameter of the teeth increases from the anterior-most alveolus to the alveoli at the midpoint of the anterior expansion and then gets progressively smaller toward the posterior—the fourth maxillary alveolus is the largest; the fifth appears to have been nearly as large.

Posterodorsally, the posterior process of the maxilla extends between the anterior processes of the lacrimal and jugal. Additional processes separating posterior snout elements are impossible to determine due to 'pyrite disease.'

The suborbital fenestrae are large. Their posterior margins are missing; the anterior margin is best preserved on the right side. The anterior margin ends in a blunt point at the ninth alveolus from the end of the maxillary tooth row. The maxilla forms the anterior margin and much of the medial and lateral margins. The posterior process of the maxilla separates the palatines from the anteromedial margin of the fenestra.

Palatine—The sutures uniting the left and right palatines are present between the suborbital fenestrae (Fig. 23B). The skull is dorsoventrally compressed in this area, and the posterior-most margins of the element are missing. Much of the anterior palatines are obscured or missing. The palatines make up part of the medial margins of the suborbital fenestrae.

Lacrimal and Jugal—The dorsal side of the posterior snout is poorly preserved; bone is missing, and remaining bone is affected by 'pyrite disease' (Fig. 23A). Some regions are reconstructed from clay. The sutural contacts between the lacrimals and the maxillae are clearest on the right side. The lacrimals are long and wide. Their anterior extent ends in an acute point beyond the anterior-most extent of the jugal. The sutural contact with the broad jugal is nearly linear. The jugal is best preserved on the right side and ends in a blunt point.

Ectopterygoid—The ectopterygoids are preserved; the right element is more complete (Fig. 23B). The maxillary face of the ectopterygoid extends along the maxilla to an acute point

medial to the anterior margin of the fifth alveolus from the posterior. The maxillary face is broadly separated from the posterior tooth row by the maxilla. Posterior to the maxillary face, a fraction of the jugal face of the ectopterygoid is preserved. Ventralmost portions of the element are missing.

Mandible—A complete right mandible is preserved (Fig. 24); the mandible has been twisted during burial, and elements have been offset. Along the lingual margin of the mandible, 'pyrite disease' has replaced fossilized bone with iron sulfide minerals. The number of teeth in the mandible is unknown; the posterior tooth row is very fragmentary.

Dentary—The dentary is nearly complete (Fig. 24). Anteriorly, the mandibular symphysis is missing along its medial margin; the lingual margins of some anterior teeth are preserved. It is impossible to determine whether the third and fourth dentary alveoli were confluent. Dorsoventral crushing is present at the point of the external mandibular fenestra; it is likely that the dentary contributed to the anterior and dorsal margins of the fenestra.

Splenial—A disassociated, partial splenial is present. The medial side of the element preserves the Meckelian groove. No characters were coded for the element.

Surangular—The surangular is preserved (Fig. 24A, B, D). The anterior processes of the surangular are subequal. A process of the surangular extends anteriorly along the medial margin of the final alveolus; the anterior-most tip of the process is missing. The suranguloangular suture appears to pass broadly along the ventral margin of the dorsoventrally crushed external mandibular fenestra. It appears that the surangular forms the posterodorsal margin of the external mandibular fenestra. The lateral margin of the glenoid fossa is composed of the surangular; the articular forms the remaining margins of the fossa. Characters near the juncture of the surangular, angular, and articular were not coded due to poor preservation. Sutural marks on the retroarticular process of the articular suggest that the surangular and angular reached the tip of the retroarticular process.

Angular—The angular is preserved, but some crushing is present anteriorly (Fig. 24A, B, D). The element likely forms the posteroventral margin of the external mandibular fenestra. Posterior to the fenestra, the element expands dorsoventrally; the dorsal margin has a pronounced hump in lateral view. The posterior margin of the angular extended to the dorsal tip of the retroarticular process, as evidenced from sutures on the articular. The entire ventral margin and part of the posterior margin of the foramen intermandibularis caudalis are preserved; they are formed by the angular. Posterior to the foramen, the medial side of the angular becomes dorsoventrally expansive.

Articular—A nearly complete articular is preserved (Fig. 24A, B, D). The element preserves the glenoid fossa and the retroarticular process. The foramen aerum of the articular cannot be located. Poor preservation and 'pyrite disease' make morphology of the medial mandible, where the articular, surangular, and angular meet, impossible to interpret; morphology in this region was not included in the phylogenetic analysis.

ALMNH 1002

This specimen is tentatively assigned to *D. schwimmeri* and represents the most complete postcranial skeleton attributable to the species (Fig. 25). The specimen represents a small, immature individual from the lower Campanian Mooreville Formation near West Greene, Greene County, Alabama, U.S.A. Hind limbs, vertebrae, chevrons, and numerous osteoderms are preserved.

Limbs and Limb Girdles—Hind limbs and limb girdles are mostly complete. Left and right ilia are present (Fig. 25B). The iliac anterior process is virtually absent, and the dorsal margin of the iliac blade is rounded with modest dorsal indentation. The supraacetabular crest is narrow. Fragmentary pubes are present; blades flare anteriorly (Fig. 25B). Shafts are short and curve to the anterior. Ischia are complete (Fig. 25B). The limbs are represented by both femora (Fig. 25C), a complete left tibia and fibula (Fig. 25D, E), and a distal right tibia and fibula. A left astragalus and calcaneum (Fig. 25G) and two tarsals of unknown identity are present (Fig. 25G). Metatarsals I–III and V are present on the right side; the left side preserves metatarsals I–IV (Fig. 25F). Seven phalanges are preserved and likely represent hind limb elements (Fig. 25I).

Vertebrae—Twenty-nine vertebrae are preserved from the dorsal through caudal series (Fig. 25A). Some neural arches are fully coossified with the vertebral centra, indicating that this specimen represents a nearly mature individual. Ten dorsal vertebrae, both sacral vertebrae, and 17 caudal vertebrae are preserved. Dorsal vertebrae possess mediolaterally broad terminal neural spines and transverse processes that are nearly on the same plane as the postzygapophyses. The anterior sacral rib capitulum projects anteriorly of the tuberculum and is visible in dorsal view.

Osteoderms—Numerous osteoderms are preserved, representing most parts of the dorsal and nuchal shields (Fig. 25J). Dorsal surfaces are deeply pitted. Smaller osteoderms, presumably from the nuchal shield, are oval in shape and bear inflated keels. Larger osteoderms, likely from the dorsal shield, are rectangular in shape. Some are nearly flat in anterior or posterior view with small keels. Others bear inflated keels.

Referral of Material to *Deinosuchus schwimmeri*

TMM 45973-1 was found in a similar geological context to the holotype specimen from the Coffee Sand Formation of Lee County, Mississippi, U.S.A. The Mooreville Formation is a facies equivalent of the Coffee Sand Formation (Cushing et al., 1964). In addition to their similarity in proportions, size, and geological context, TMM 45973-1 may be referred to *D. schwimmeri* based on a similar angular morphology. Like the holotype, the angular of TMM 45973-1, posterior to the external mandibular fenestra, is dorsoventrally expanded so as to form a hump on the dorsal margin. Additionally, the anterior margin of the suborbital fenestra is blunt in both the holotype specimen and TMM 45973-1; it extends no further than the 10th maxillary alveolus from the end of the tooth row.

ALMNH 1002 does not share elements with the holotype and thus cannot be definitively referred to *D. schwimmeri*. This specimen has been tentatively referred to the species based on possession of mediolaterally broad terminal neural spines, transverse processes are nearly on the same plane as the postzygapophyses, and some osteoderms have moderately inflated keels. Additionally, its large size is shared with the holotype and TMM 45973-1. Geological context also unites both ALMNH 1002 and the most complete skull and lower jaw referable to *D. schwimmeri* (TMM 43973-1). They are both from the Mooreville Formation, which underlies the Coffee Sand Formation in Mississippi (Dockery and Jennings, 1988), which preserves the *D. schwimmeri* holotype (MMNS VP-256).

COMPARISONS

Opening of Bony Narial Aperture

The direction in which the bony narial aperture opens was left uncoded for *D. schwimmeri*. No complete anterior snout is known for *D. schwimmeri* specimens, but a posterior bony narial aperture is known for TMM 45973-1.

Orienting the premaxilla and maxilla attributed to *D. riograndensis* (AMNH 3073) suggests that the bony narial aperture opened posterodorsally. However, this is based on the assumption that the elements, which are not articulated or contiguous, are oriented as they would be in life. The anterior snout of

D. riograndensis (TMM 43620-1), the most complete skull from the *D. riograndensis* type locality, has been dorsoventrally crushed, but overall proportions suggest that the bony narial aperture projected posterodorsally.

Among other large-bodied alligatoroids (e.g., *Mourasuchus* and *Purussaurus*), large bony narial apertures are common. The large aperture found in species of *Deinosuchus* is shared with most species of *Purussaurus* and *Mourasuchus amazonensis* but is achieved in different ways. Species such as *Purussaurus mirandai* Aguilera, Riff, and Bocquentin-Villaneuva, 2006, and *Purussaurus brasiliensis* Barbosa-Rodrigues, 1892, have external nares that are much longer than they are wide, such that the posterior extent of the bony narial aperture approaches the orbits.

The bony narial aperture in species of *Deinosuchus* is wider than it is long and resembles that in *Mourasuchus amazonensis* Price, 1964, in its proportions. Unlike in *M. amazonensis*, where the premaxilla forms the entirety of the bony narial aperture, the nasals contribute to the posterior margin of the aperture in species of *Deinosuchus*. Additionally, considerably more bone separates the bony narial aperture from the margins of the snout, producing the more robust morphology found in species of *Deinosuchus*.

Occlusal Marks on the Premaxilla

On the left premaxilla of the *D. riograndensis* holotype (AMNH 3073), lingual to the space separating the third and fourth alveoli, is a small depression created by the occlusion of the second dentary tooth. TMM 43620-1, a *D. riograndensis* specimen of similar size to the holotype, shows the development of a similarly shallow depression. A *D. schwimmeri* specimen from Alabama (TMM 45973-1) demonstrates an occlusal mark in the form of a deep groove (Fig. 27).

The development of a deep groove would be predicted for the large *D. riograndensis* specimens if due to wear through ontogeny. However, *D. schwimmeri* TMM 45973-1 represents a smaller individual relative to the *D. riograndensis* specimens from Texas. The very deep occlusal mark in this specimen is not likely the endmember of a transformational process such as is found in mature *Caiman crocodilus* where repeated occlusion of the fourth dentary tooth on the maxilla initially forms a pit and over time transitions to a groove.

There are additional differences in occlusal patterns between the species in the form of the pits present posterior to the juncture of the first and second premaxillary teeth. There are shallow occlusal marks between the first and second teeth in AMNH 3073 and TMM 43620-1, two *D. riograndensis* specimens of similar size from Texas. TMM 45973-1, a *D. schwimmeri specimen* from Alabama, demonstrates very deep occlusal marks posterior to the space between the second and third alveoli. Ontogeny cannot account for the differences in occlusal morphology in this taxon.

Premaxilla-Maxilla Notch

The position of the fifth premaxillary tooth relative to the premaxilla-maxilla notch differs between *D. riograndensis* and *D. schwimmeri*. The notch is posteromedial to the fifth premaxillary tooth in *D. riograndensis*. Only the anterior margin of the notch is preserved for *D. schwimmeri*, but differences in morphology are evident; the anterior margin of the notch is lateral to the fifth premaxillary tooth.

The premaxilla-maxilla notch found in species of *Deinosuchus* is not likely to be due to wear from prolonged occlusion. The notch is more like that of *Leidyosuchus canadensis* or species of *Diplocynodon*. In these species, the notch is present throughout ontogeny. This condition is in opposition to a similar but unrelated morphology found in *Caiman crocodilus* in which the fourth dentary tooth occludes with the ventral surface of the maxilla. This prolonged wear produces a pit on the upper jaw early in ontogeny and transitions to an open notch later in ontogeny.

Premaxillary Fenestrae

The premaxillary fenestrae (Fig. 13) may be autapomorphic for *D. riograndensis* and are completely preserved in the holotype (AMNH 3073) and the most complete specimen known for the species (TMM 43620-1). Complete premaxillae are known for *D. riograndensis* but not *D. schwimmeri*. Portions of the ventral and ventrolateral margins of the fenestra may be preserved by additional *D. riograndensis* specimens, TMM 40571-1 and TMM 43632-1, respectively. When complete, the anterior premaxillae in these specimens bear large fenestrae that are wider than they are tall.

The holotype of *D. riograndensis*, AMNH 3073, possesses premaxilla material that is very bulbous. The premaxillae belonging to *D. riograndensis* TMM 43620-1, an animal approaching the size of the holotype specimen, are dorsoventrally compressed due to burial. The amount of compressed bone in the region suggests that its proportions were nearly as bulbous as the holotype material.

Mourasuchus amazonensis also has large fenestrae present on the premaxilla; they are wider than they are long and are slightly inset from the premaxillary tooth row. The fenestrae are approximately the diameter of an anterior dentary tooth in the species. Although the fenestrae are situated somewhat dorsally on the premaxilla, the anterior snout is not particularly deep. They were likely formed by the occlusion of the dentary teeth on the roof of the premaxilla. Other species of *Mourasuchus* are known to have one or more foramina per side of the premaxilla for receiving the anterior dentary teeth (Cidade et al., 2017).

The function of the very large premaxillary fenestrae in *D. riograndensis* is unknown. It is unlikely that they are for receiving enlarged dentary teeth; the anterior dentary teeth would have to reach unprecedented lengths and diameters for a crocodylian to form these fenestrae.

Using extant relatives of *Deinosuchus* as models for their formation and function is inadequate. The formation of the fenestrae in modern species is due to continued occlusion against the premaxillary surface over ontogeny—they are approximately the same diameter as the occluding teeth and transition into a notch late in ontogeny. In species of *D. riograndensis*, the fenestrae are many times the diameter of the anterior dentary teeth and are situated far more dorsally than any known species. The hypothesis that they were formed by occlusion must be discounted, and an alternative hypothesis must be presented.

The fenestrae could have functioned as a means to lighten the anterior snout. The mass of the bone forming the deep anterior snout is considerable. Large fenestrae could be an adaptation to the increased mass in this area. However, the anterior snout functions as a means by which to capture prey, and the prey consumed by *Deinosuchus* was presumably very large. It would seem that large fenestrae at the tip of the snout would be selected against if they dramatically weakened the anterior snout. Yet the effect of this morphology does not seem to hinder the geographic and geologically widespread occurrence of species of the taxa.

An additional hypothesis is that the fenestrae were for supporting soft tissues. However, there is no evidence in the form of accessory growths of bone or neurovascular foramina in the area around the fenestral margins on the external surface of the snout. But the *D. riograndensis* holotype (AMNH 3073) preserves a dorsoventrally oriented osteological projection along the anterior margin of the internal premaxillary surface. This feature is presumed to have extended further to the posterior, forming a wall of bone separating the paranasal air sinus from

the nasal passage, and indicates that the fenestrae would have been indirectly associated with the respiratory system. Soft tissues in this area could have been used as a means of thermoregulation, generation of vocalizations, or otherwise. In addition to an association with the respiratory system, the pneumatization of the anterior snout would have been comparatively lighter relative to a solid structure.

Mediolateral Expansion of Maxilla

The mediolateral expansion of the lateral margin of the maxilla varies between specimens of *D. riograndensis* and *D. schwimmeri* in two ways: first, the posterior expansion of the maxilla is less pronounced in *D. schwimmeri*; second, the diameter of the teeth in the second region of expansion show less variability for *D. schwimmeri* relative to *D. riograndensis.*

Complete maxillary tooth rows are known for both *D. riograndensis* and *D. schwimmeri* (TMM 43620-1 and TMM 45973-1, respectively). Additional specimens of *D. schwimmeri* (MMNS VP-256) and *D. riograndensis* (TMM 40571-1) possess the posterior-most 14 alveoli and first 15 maxillary alveoli, respectively. Comparison with *D. schwimmeri* from Alabama (TMM 45973-1) indicates that approximately 60% of the maxillary tooth row is preserved in MMNS VP-256 with no deformation.

Deinosuchus schwimmeri and *D. riograndensis* specimens preserving the entire maxillary tooth row have a mediolaterally oriented anterior expansion of the maxilla between the first and seventh alveoli and a posterior expansion between the 10th and 14th alveoli. The species differ in the posterior expansion—it is less pronounced in specimens referable to *D. schwimmeri*. In the expanded regions of specimens referable to *D. riograndensis*, the diameters of the teeth increase from the anterior-most alveolus to the alveoli at the midpoint of the swelling and then decrease progressively toward the posterior. This is only true for the anterior expansion in specimens referable to *D. schwimmeri*; the posterior expansion does not show obvious differences in tooth diameter. The *D. schwimmeri* holotype specimen, although missing the first alveolus of the swelling, agrees with the *D. schwimmeri* specimen from Alabama (TMM 45973-1); teeth of this region are of a proportionally similar diameter relative to specimens referable to *D. riograndensis.*

Species of *Deinosuchus* and *L. canadensis* share swellings of the lateral margins of the anterior maxilla. Many eusuchians bear these swellings, but the morphology is pronounced in species of *Deinosuchus* and *L. canadensis.* In *L. canadensis*, the swellings are in the region of the first to seventh maxillary alveoli, with a constriction at the juncture of the seventh and eighth maxillary alveoli. Species of *Deinosuchus* bear swellings from the first to the sixth maxillary alveoli, with a constriction at the juncture of the sixth and seventh alveoli. Additionally, the anterior-most portion of the swelling is more pronounced in *L. canadensis* owing to the extreme constriction of the snout at the premaxilla-maxilla notch.

Suborbital Fenestrae

Comparison with more complete fossil samples recovered from a single locality such as the tens of skulls belonging to *Borealosuchus formidabilis* Erickson, 1976, indicates that intraspecific variability in the shape and extent of the suborbital fenestrae is limited (A.P.C., pers. observ., 2019). Ontogenetic scaling does not affect the anterior extent of the fenestrae in this species. Anteriorly, the suborbital fenestra consistently extends to the same alveolus from the posterior tooth row. In light of this observation, the interspecific variability present between *D. riograndensis* and *D. schwimmeri* is used as a means to differentiate the species.

Colbert and Bird (1954) suggest an extreme anterior extent of the suborbital fenestra in the *D. riograndensis* holotype (AMNH 3073). The authors identify this feature as part of a maxillary sinus and suggest that this specimen does not preserve the suborbital fenestra. TMM 43620-1 is the only *D. riograndensis* specimen to adequately preserve the suborbital fenestrae. The anterior margin is acute and extends to the posterior margin of the 12th maxillary alveolus numbered from the end of the tooth row. As reconstructed, an additional *D. riograndensis* specimen from Texas (TMM 43632-1) preserves a blunt anterior margin of the fenestra. The specimen is extensively cracked and has been subject to considerable preparation and reconstruction. It is unknown to which alveolus the structure extended to in this specimen.

The *D. schwimmeri* holotype (MMNS VP-256) preserves a suborbital fenestra of which the anterior margin is blunt and extends to the 10th alveolus from the posterior tooth row. Additionally, *D. schwimmeri* TMM 45973-1 preserves a relatively complete right suborbital fenestra; the anterior margin is blunt and extends to the juncture of the 9th and 10th alveoli from the end of the maxillary tooth row.

Skull Table

The skull table of *Deinosuchus* is reminiscent of gavialoids, *Bernissartia fagesii*, *Leidyosuchus canadensis*, and species of *Borealosuchus.* However, species of *Deinosuchus* preserve a combination of character states absent in these taxa.

In species of *Deinosuchus*, the lateral margins of the skull table are nearly parallel from the dorsal perspective and preserve mediolateral constrictions anterior to the squamosal rami. Additionally, the anterolateral corners of the skull table are angular in dorsal outline. Unique among alligatoroids, the skull tables of specimens referred to *Deinosuchus* have lateral margins that are elevated relative to the midline such that a deep furrow is formed along the sagittal axis.

Supratemporal Fenestrae

The supratemporal fenestrae of *Deinosuchus* are large relative to extant alligatorids and occupy much of the skull table. Large supratemporal fenestrae appear to be common among basal taxa and are found in fossil taxa such as *Leidyosuchus canadensis*, species of *Borealosuchus*, *Bernissartia fagesii*, and gavialoids.

Enlarged supratemporal fenestrae are associated with longirostrine species, where the snout anterior to the orbits accounts for 70% or more of total skull length (Busbey, 1995), in both the modern and fossil records. Most taxa with large supratemporal fenestrae generally achieve this morphology through decreased skeletal robusticity surrounding the structure. When viewed from the dorsal perspective, the elements surrounding the supratemporal fenestrae are relatively thicker in outline for species of *Deinosuchus.*

Ophthalmic Groove

The orientation of the ophthalmic groove varies between those specimens preserving the area. In TMM 43620-1 and TMM 43632-1, specimens referred to *D. riograndensis*, the groove is oriented more anteroposteriorly relative to the *D. schwimmeri* holotype (MMNS VP-256). The functional significance of this variation is unknown.

Exoccipital Foramina for Cranial Nerves

Specimens preserving ventral portions of the exoccipitals bear foramina or depressions lateral to the occipital condyle, although proportions vary between specimens referable to

D. riograndensis and *D. schwimmeri*. *Deinosuchus riograndensis* TMM 43632-1 has dorsal foramina lateral to the foramen magnum and separated from the other depressions by a short distance that are not found in *D. schwimmeri* MMNS VP-256. This is likely due to differential preservation in the region and is not a product of divergent evolution between the forms. Via comparison with modern species the dorsal-most foramen in *D. riograndensis*, TMM 43632-1 is likely for the passage of cranial nerve XII.

In both *D. riograndensis* and *D. schwimmeri*, lateral to the occipital condyle, lie three depressions separated by a series of ridges for the conveyance of cranial nerves and blood vessels. The deepest depression in TMM 43632-1 (*D. riograndensis*) and MMNS VP-256 (*D. schwimmeri*) is the dorsal-most of the three. It is roughly triangular in shape in *D. riograndensis* but is more oval in *D. schwimmeri*. In both species, this depression bears foramina within its margins, presumably for the passage of cranial nerve XII. In *D. riograndensis*, the middle foramen is much smaller than the dorsal and ventral foramina, is trough-like and elongate, and has roughly parallel sides. In *D. schwimmeri*, the middle foramen is only slightly smaller than the other foramina, is oval in shape, and is separated from the other two by slight ridges. The middle foramen is likely for the passage of cranial nerves IX–XI and the jugular nerve. In both species, the ventral-most opening is nearly the same size as the dorsal-most opening but is very shallow. No obvious foramina are present within its borders. This structure probably allowed passage of the carotid artery.

The morphology of the three depressions lateral to the occipital condyle is unique to species of *Deinosuchus*. As evidenced by the foramina within its borders, the dorsal-most depression is for the passage of cranial nerves and blood vessels, but the functions of the depressions ventral to it are unknown. The prominence of the ridges separating the depressions, a lack of foramina within the borders of the middle and ventral structures, and shallow depth of the depressions indicate that their likely function may not have been for the conveyance of cranial nerves and blood vessels but rather for the attachment of epaxial muscles.

Confluence of Third and Fourth Dentary Teeth within Alveoli

Species of *Deinosuchus* bear confluent third and fourth dentary alveoli. This feature is shared with the basal alligatoroids *Leidyosuchus canadensis* and species of *Diplocynodon*.

The *D. riograndensis* holotype (AMNH 3073) shows individual variability in the degree of the placement of the third and fourth dentary teeth within the confluent alveoli. A wide space is present between the third and fourth dentary teeth of the left side, but their counterparts on the right abut one another; no signs of pathology are present. TMM 43620-1, a specimen referable to *D. riograndensis*, preserves both anterior dentaries; the third and fourth dentary teeth do not have a space between them.

Teeth

Deinosuchus rugosus is diagnosed in part by thick enamel (Emmons, 1858). However, this character state is shared with other species of *Deinosuchus* and is therefore undiagnostic. The *D. riograndensis* holotype (AMNH 3073) bears teeth that demonstrate enamel exceeding the thickness of that of the *D. rugosus* holotype (USNM PAL 535447). The enamel of a small, low-crowned tooth from TMM 43620-1 matches the thickness of *D. rugosus*. The *D. schwimmeri* holotype bears five loose teeth that demonstrate thick enamel.

Additional diagnostic characters for *D. rugosus* include teeth with wrinkled enamel surfaces. Specimens attributed to species of *Deinosuchus* also share this morphology. A tooth, likely from the posterior to mid-jaw tooth row, is preserved for the *D. riograndensis* holotype (AMNH 3073); it demonstrates wrinkling of the enamel that closely matches the condition of the *D. rugosus* holotype. The *D. schwimmeri* holotype (MMNS VP-256) also has an associated posterior to mid-jaw tooth that demonstrates pronounced wrinkling of the enamel.

External Mandibular Fenestra

Deinosuchus riograndensis TMM 43620-1 and *D. schwimmeri* MMNS VP-256 are the only specimens to preserve relatively complete external mandibular fenestrae. Although some breakage is present along the anterior margin of the fenestra, the structure appears to be relatively larger in the MMNS specimen compared with the TMM specimen. The difference in size is pronounced in light of the TMM specimen being from a much larger individual. It would appear that *D. riograndensis* has proportionally smaller external mandibular fenestrae. Whether this difference in size is found in all ontogenetic stages is unknown. Alternatively, as the animal grew, bone overgrowth could diminish the size of the external mandibular fenestrae through ontogeny.

The contribution of the dentary to the margin of the external mandibular fenestra may differ between MMNS VP-256 and TMM 43620-1. In MMNS VP-256, the posterior dentary may have extended further to the posterior relative to that of TMM 43620-1. In the MMNS specimen, the dentary may stop anterior to the external mandibular fenestra. However, possible sutural marks on the angular would suggest that the dentary extended along the ventral margin of the fenestra. This would differ from TMM 43620-1 in which the angular forms the anteroventral margin of the fenestra. Should the interpretation of sutural marks on the angular in the region of the anteroventral margin of the external mandibular fenestra prove to be false, then the MMNS and TMM specimens would share similar morphologies.

Dorsal Margin of the Angular

The dorsal margin of the angular has a pronounced hump posterior to the external mandibular fenestra in *D. schwimmeri*. In TMM 43620-1, the only *D. riograndensis* specimen with an intact posterior mandible, preserved morphology suggests that the dorsal margin of the angular, posterior to the external mandibular fenestra, was moderately inflated but not to the same degree as in *D. schwimmeri*.

Vertebrae

Holland (1909) includes characters derived from vertebrae in his diagnosis of *D. hatcheri*. It is stated that the species is differentiated from other crocodylians by an expansion of the terminal neural spines of the dorsal vertebrae and postzygapophyses residing nearly on the same plane as the transverse processes.

Some archosaurian and crocodyliform taxa demonstrate anteroposteriorly oriented expansions ('spine tables') of the terminal neural spine (Clark, 2011; Nesbitt, 2011), but this morphology is unlike that of species of *Deinosuchus*. The Early Cretaceous (Aptian–Albian) crocodyliform *Sarcosuchus imperator* de Broin and Taquet, 1966, demonstrates dorsal vertebrae with mediolaterally broad terminal neural spines (Sereno et al., 2001). The spines are short and stout, with a terminal end that is moderately wider than the body of the spine and grades gently into the base of the spine when viewed from the anterior or posterior perspective. Late Cretaceous crocodylians such as *L. canadensis* Lambe, 1907, *Bottosaurus harlani* Meyer, 1832, species of *Brachychampsa* Gilmore, 1911, *Borealosuchus threeensis* Brochu et al., 2012, and *Eothoracosaurus mississippiensis* Brochu, 2004, do not bear expansions of their terminal neural spines.

Known species of crocodyliformes demonstrate expansions of the terminal neural spine that are morphologically distinct from species of *Deinosuchus*. Comparison with allied taxa indicates that mediolaterally expanded but dorsoventrally abbreviated terminal neural spines are unique to species of *Deinosuchus* among Crocodylia and more broadly Crocodyliformes.

Specimens referable to both *D. riograndensis* (TMM 43632-1, TMM 43620-1) and tentatively to *D. schwimmeri* (ALMNH 1002) bear vertebral morphology similar to that described by Holland (1909) as diagnostic for *D. hatcheri* (Fig. 5). A specimen of *D. riograndensis* (TMM 43632-1) maintains a dorsal vertebra that preserves a left postzygapophysis and a partial left transverse process; they are nearly in the same plane. An additional specimen of *D. riograndensis* (TMM 43620-1) preserves a mostly complete dorsal vertebra the postzygapophysis and transverse process of which are nearly in the same plane. This specimen also bears a transversely broad terminal dorsal spine. When viewed from a posterior aspect, the specimen looks nearly identical to figure 3 of Holland (1909). Additionally, ALMNH 1002 preserves a dorsal vertebra whose postzygapophyses are nearly in the same plane as the transverse processes and which bears a dorsal spine whose terminal end is transversely expanded.

Colbert and Bird (1954) compared the vertebrae associated with the *D. riograndensis* and *D. hatcheri* holotypes. The vertebrae are comparable in size, shape of the articular surfaces, and centra, and both possess relatively high neural arches. They stated that enough similarities are present to conclude that the holotype specimens are at least members of the same genus.

Osteoderms

Deinosuchus hatcheri preserves osteoderms that are very lumpy, bear irregular, deeply pitted surfaces, and have inflated keels (Fig. 26A). *Deinosuchus riograndensis* bears osteoderms that are irregular, lumpy, and have inflated keels (Fig. 26B), but not to the degree seen in *D. hatcheri*. In opposition to this condition, *D. schwimmeri* osteoderms preserve inflated keels but are often thinner and more regular in shape (Fig. 26C, D). Dorsal surfaces are pitted in all species. Within a species, depth and irregularity of pitting tends to be size dependent. Comparison between *D. riograndensis* TMM 43620-1 and the larger *D. riograndensis* TMM 43632-1 demonstrates deeper pitting and increased irregularity with increasing size.

Deinosuchus hatcheri is diagnosed in part by indentations along the edge of some osteoderms. These osteoderms are tentatively identified as belonging to the lateral margin of the dorsal shield. This character state is not found in either *D. riograndensis* or *D. schwimmeri*. Further, the osteoderms of *D. riograndensis* and *D. schwimmeri* do not preserve diagnostic characters allowing for differentiation using morphology.

Schwimmer (2002) makes an argument for the differences between eastern and western specimens being due to allometric changes in morphology. To reduce the effects of allometry, Schwimmer compared what he believed to be the largest eastern osteoderms with small western osteoderms and found little difference between the taxa. However compelling, it cannot be known whether the osteoderms under comparison were from the same region of the body.

Perceived similarities, or differences, in morphology could be due to the position in which the osteoderm resided or due to allometry; positive allometry is expected for an element forming a functional part of the dorsal musculature. It should be noted that variability in osteoderm shape, size, and pronouncement of the keel is only found in eastern specimens. *Deinosuchus riograndensis* osteoderms are invariably lumpy, thick, and bear inflated keels no matter the size or placement within the dermis.

A *D. schwimmeri* specimen attributed to a young adult (ALMNH 1002) preserves dorsal osteoderms that approach the size of the large eastern osteoderm used in Schwimmer's figure. This specimen's osteoderms are thin, moderately pitted, and preserve a pronounced keel. Dorsal osteoderms matching this description are unknown for western specimens. Additional osteoderms from this specimen bear irregular margins, moderate pits, and moderately inflated keels. Their morphology is similar to that in *D. hatcheri* and *D. riograndensis*, but they are relatively thinner when viewed from the anterior or posterior perspective.

The authors sought to reduce the effects of size when comparing osteoderms. To do so, dorsal osteoderms of nearly the same size were compared. NCSM 14952, a dorsal osteoderm from the *D. rugosus* type locality in North Carolina, measures approximately 13 cm wide. When compared with TMM 43620-1, a specimen from the type locality of *D. riograndensis* and possessing similarly sized osteoderms to the North Carolina specimen, it is clear that the osteoderms of Texas *Deinosuchus* are considerably lumpier in appearance and bear keels that are inflated to a greater degree.

PHYLOGENETIC ANALYSIS

Matrix

The matrix used in this analysis follows Brochu (2011) and Cossette and Brochu (2018). Changes have been made to the matrix, including the addition of *Deinosuchus riograndensis* and *Deinosuchus schwimmeri* as well as the addition of new character states. Invariable characters among ingroup taxa are excluded from this analysis. The matrix contains 163 morphological characters and 82 ingroup taxa. *Bernissartia fagesii* is used as an outgroup to root the trees. Codings are presented in Appendix S1 of Supplemental Data 1.

New characters and character states added to this matrix are the following: 47(5), splenial reaches mandibular symphysis but does not touch other splenial; 72(2), naris projects posterodorsally; 117(3), anterior margins of orbit telescoped; 135(2), skull table surface slopes ventrally toward sagittal axis at maturity, lateral elements planar; 160, dorsal shield osteoderms planar, exclusive of keel (0) or osteoderms robust, keel inflated (1); 161, lateral-most dorsal shield osteoderms with smooth margins (0) or bear indentation (1); and 162, floor of posttemporal fenestrae not visible in dorsal view (0) or visible in dorsal view (1) at maturity; 163, mid-maxillary constriction not present (0) or present between maxillary teeth 5 and 6 (1), 6 and 7 (2), 7 and 8 (3), 8 and 9 (4), or 10 and 11 (5).

Methods

A maximum parsimony analysis using TNT 1.5 was conducted (Goloboff et al., 2008). Matrices were managed in Mesquite 3.04 (Maddison and Maddison, 2015). Traditional heuristic searches performing 1,000 replicates of Wagner trees (using random addition sequences) were conducted and followed by the tree bisection reconnection swapping algorithm (holding 10 trees per replicate). Collapsing rules and character weighting were not applied for the reconstructions. Multistate characters were treated as unordered.

Character support of the nodes present in the most parsimonious trees was calculated using two different methods. The first method is bootstrapping applied to character resampling (100,000 pseudoreplicates of the bootstrapping procedure were performed) (Efron, 1979; Felsenstein, 1985). The second method is Bremer support (Bremer, 1988, 1994). TNT 1.5 was used to calculate bootstrapping and Bremer supports (Goloboff et al., 2008). Absolute frequencies were used to summarize the topologies obtained during the bootstrap replicates (Goloboff et al., 2003).

Results

Multiple analyses were completed. Maximum parsimony analysis of the full taxon matrix recovers 2,870 shortest trees (tree length = 584, consistency index with uninformative characters removed = 0.38, retention index = 0.82). *Deinosuchus riograndensis* and *Deinosuchus schwimmeri* are recovered as sister taxa (Fig. 28). The *Deinosuchus* clade is included in a basal polytomy with *Leidyosuchus canadensis*, a taxon commonly recovered as the basal-most alligatoroid (Brochu, 2010, 2011; Martin et al., 2014; Hastings et al., 2016), Diplocynodontinae, and a clade including Cretaceous globidontans and Alligatoridae.

In this analysis, crown alligatorids form two primary lineages, one including *Alligator* and its North American and Eurasian relatives and the other including the living caimans and their North American and neotropical relatives.

Strict consensus trees recover a monophyletic Globidonta. In this analysis, Cretaceous globidontans (*Stangerochampsa*, *Albertochampsa*, and *Brachychampsa*) are the sister group to Caimaninae. Tree length increases by one step if Cretaceous globidontans are moved outside of crown Alligatoridae. Cretaceous globidontans are united with Caimaninae due to the angular not extending dorsally beyond the anterior end of the foramen intermandibularis caudalis; the anterior tip of the angular is very blunt.

This analysis diagnoses Alligatoroidea with the following character states: 54(1), anterior processes of the surangular are equal to subequal; 63(1), foramen aerum of articular set in from margin of retroarticular process; 82(0), all dentary teeth occlude lingual to maxillary teeth; 102(1), the quadratojugal spine is high, between posterior and superior angles of infratemporal fenestra; 112(1), anterior tip of frontal forms broad, complex sutural contact with the nasals; 121(1), quadratojugal spine high, between posterior and superior angles of infratemporal fenestra; and 153(1), quadrate foramen aerum on dorsal surface.

The *Deinosuchus* clade is unambiguously diagnosed by 12 character states: 42(0), dentary symphysis extends to fourth or fifth alveolus; 47(5), splenial reaches mandibular symphysis but does not touch its counterpart; 53(1), angular-surangular suture passes broadly along ventral margin of external mandibular fenestra late in ontogeny; 56(1), external mandibular fenestra present as narrow slit, no discrete fenestral concavity on angular dorsal margin; 114(0), postorbital bar massive; 117(3), anterior margin of orbit telescoped; 122(2), quadratojugal-jugal suture lies at posterior angle of infratemporal fenestra; 124(1), quadratojugal bears modest process, or none at all, along lower temporal bar; 126(0), postorbital-squamosal suture oriented ventrally; 127(1), squamosal groove flares anteriorly; 135(2), skull table surface slopes ventrally toward sagittal axis at maturity; and 160(1), dorsal osteoderms robust, keel inflated. Four of the states are autapomorphic for the clade: 47(5), 117(3), 135(2), and 160(1).

Many character states that diagnose the *Deinosuchus* clade are shared with other species. Character state 42(0), dentary symphysis extends to fourth or fifth alveolus, is shared with alligatoroids and crocodyloids alike. Within Alligatoroidea, all species of *Diplocynodon*, save *D. deponiae*, and large clades within Alligatorinae and Caimaninae share the character state with species of *Deinosuchus*. Within Crocodyloidea, species of *Osteolaemus* and *Crocodylus* share the state with species of *Deinosuchus*. Character state 53(1), angular-surangular suture passes broadly along ventral margin of external mandibular fenestra late in ontogeny, is shared with Crocodylinae, *Eogavialis africanus*, and Caimaninae, save the basal-most member, *Culebrasuchus mesoamericanus*. Character state 56(1), external mandibular fenestra present as narrow slit, no discrete fenestral concavity on angular dorsal margin, is shared with *Borealosuchus threeensis*, *Borealosuchus wilsoni*, *Thoracosaurus neocesariensis*, and *Thoracosaurus macrorhynchus*. Character state 114(0), postorbital bar massive, is shared with Gavialoidea. Character state 124(1), quadratojugal bears modest process, or none at all, along lower temporal bar, is shared with Crocodylidae and *Centenariosuchus gilmorei*. Character state 126(0), postorbital-squamosal suture oriented ventrally to skull table, is shared with *Diplocynodon tormis*, *Diplocynodon remensis*, *Euthecodon brumpti*, *Euthecodon arambourgii*, and *Gavialis gangeticus*. Character state 127(1), dorsal and ventral rims of squamosal groove for external ear valve musculature flares anteriorly, is shared with Gavialoidea. These characters are largely variable within and among the major clades of Crocodylia and may be products of functional constraints, ecology, or otherwise, rather than phylogenetic history.

A sister-group relationship for *D. riograndensis* and *D. schwimmeri* is robustly supported by bootstrap and Bremer supports alike (bootstrap = 99% of replicates, decay index = 6). Traditionally, Alligatoroidea is also robustly supported (Brochu, 1999), but this analysis found that only 12% of bootstrap replicates support the clade (decay index = 2).

Removal of *D. riograndensis* and *D. schwimmeri* from the analysis decreases tree length but increases the number of most parsimonious trees (4,640 shortest trees, tree length = 512, consistency index with uninformative characters removed = 0.41, retention index = 0.84). Topologically, the tree resembles most published analyses of Alligatoroidea that do not include species of *Deinosuchus* (e.g., Brochu, 1999; Martin, 2010). *Leidyosuchus canadensis* is recovered as the basal-most alligatoroid and one node crownward Diplocynodontinae forms a sister-group relationship with Cretaceous globidontans and Alligatoridae.

Additionally, the removal of *D. riograndensis* and *D. schwimmeri* increases bootstrap support of Alligatoroidea to 17% but has no effect on Bremer supports. Likewise, support increases for basal nodes within the clade, but more nested nodes are largely unaffected. Removal of species of *Deinosuchus* likely removes conflicts arising from homoplasy and explains the increased support for basal nodes.

Deinosuchus hatcheri was added to a second analysis (4,770 shortest trees, tree length = 583, consistency index with uninformative characters removed = 39, retention index = 83). With the inclusion of *D. hatcheri*, the *Deinosuchus* clade is drawn to the base of Alligatoroidea—in opposition to most published studies, *L. canadensis* is no longer the basal-most alligatoroid. Polytomies among basal clades are absent relative to the analysis excluding *D. hatcheri*, and relationships among more derived alligatoroids are unchanged. Bootstrap and Bremer nodal support metrics are lower.

Only 7 characters could be coded for the highly incomplete *D. hatcheri* (versus 81 for *D. riograndensis* and 74 for *D. schwimmeri*). The taxon is labile among the clade, resulting in a polytomy—primarily as a result of the few coded characters in the highly incomplete holotype specimen. Character 161(1), lateral-most dorsal shield osteoderms bear an indentation along their margins, differentiates *D. hatcheri* from specimens of *D. riograndensis* and *D. schwimmeri*.

In the second analysis, the *Deinosuchus* clade is unambiguously diagnosed by 11 character states: 42(0), 47(5), 53(1), 56(1), 114 (0), 117(3), 122(2), 124(1), 127(1), 135(2), and 160(1). Five of the states are autapomorphic for the clade: 47(5), 117(3), 122 (2), 135(2), and 160(1). *Deinosuchus hatcheri* is not coded for any of these characters.

DISCUSSION

Species of *Deinosuchus* bear highly derived, often divergent morphologies in a geologically old member of Alligatoroidea. In addition to a number of autapomorphies for species of *Deinosuchus*, convergent evolution with long-snouted forms is evident.

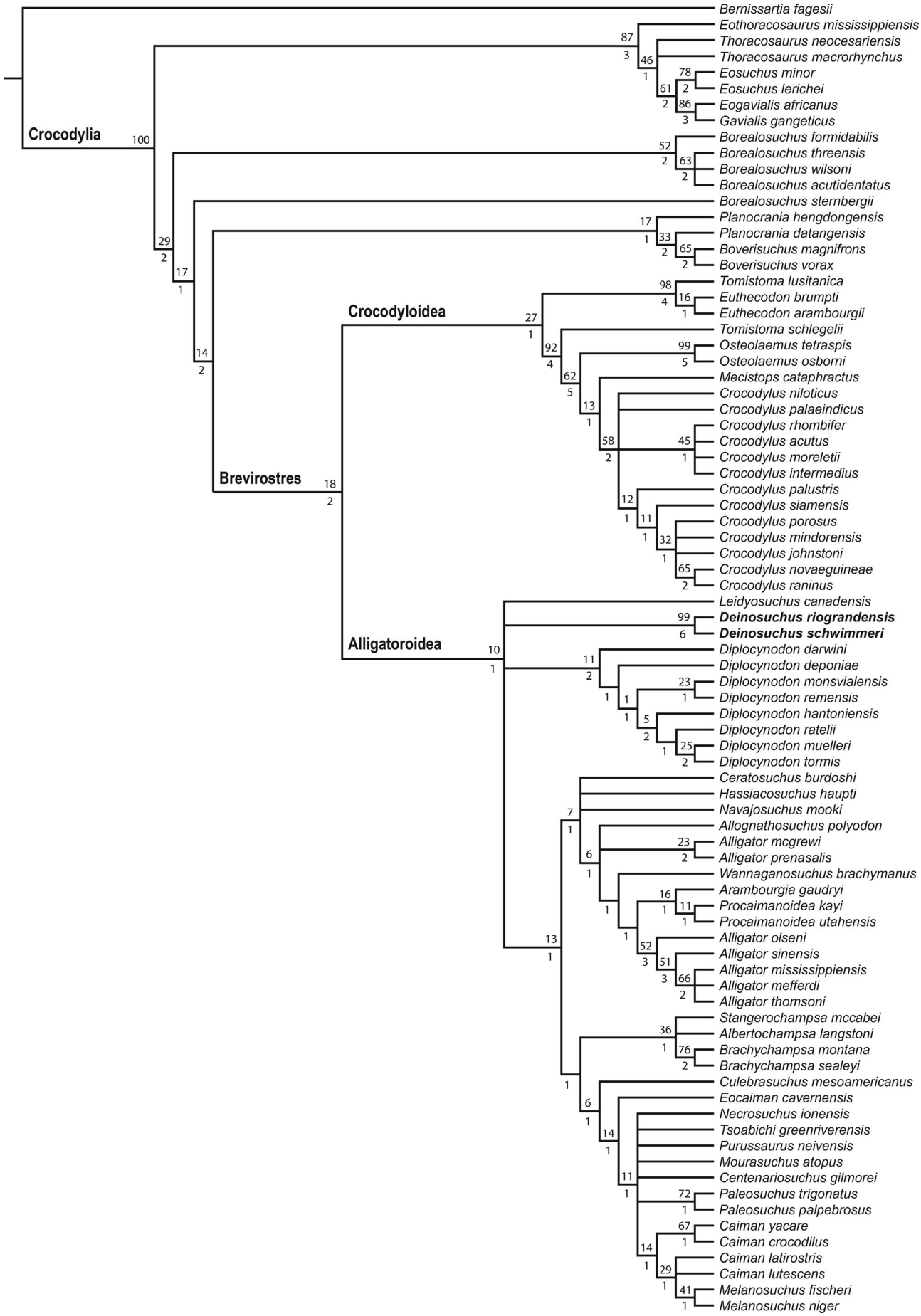

FIGURE 28. Strict consensus tree showing the placement of *Deinosuchus riograndensis* and *Deinosuchus schwimmeri*. Numbers above nodes indicate bootstrap GC values; numbers below nodes indicate Bremer support values.

As such, *Deinosuchus* introduces homoplasy into the data set and resolution at the base of Alligatoroidea is reduced.

Interestingly, five homoplastic character states, 53(1), 56(1), 114(0) 126(0), and 127(1), are shared with gavialoids and one, 126(0), is shared with species of the osteolaemine *Euthecodon*. These taxa, along with species of *Deinosuchus*, are longirostrine. Character states shared among the taxa are located on the skull table and otic area; these regions are known to be functionally constrained by the demands of longirostry (Iordansky, 1973; Langston, 1973; Busbey, 1995).

The addition of *D. hatcheri* results in a polytomy among species of *Deinosuchus* and draws the clade to the base of Alligatoroidea (Fig. S6) as a result of potential optimizations of the highly incomplete *D. hatcheri* holotype specimen. It is clear that *D. hatcheri* is distinct from *D. riograndensis* and *D. schwimmeri*—the lateral-most dorsal shield osteoderms bear an indentation along their margins, character 161(1). However, the highly incomplete nature of the species results in equally parsimonious placements as sister to *D. riograndensis* or *D. schwimmeri*. The matrix, although extensive, does not sample all of the morphological variation among the species of *Deinosuchus*. Many conceivable characters potentially used to differentiate the species such as the extent of the suborbital fenestrae are highly variable among taxa. They are inappropriate for use in a large analysis with diverse taxa and would introduce unacceptable levels of homoplasy.

The phylogenetic analysis, although inconclusive regarding the relationships among the species of *Deinosuchus*, does not solve the underlying systematic issue regarding the poorly known *D. hatcheri*. The three species, which are otherwise differentiated from one another, cannot be separated as a result of the highly incomplete *D. hatcheri* holotype.

Removal of all species of *Borealosuchus* leads to better resolution at the base of Alligatoroidea relative to the full analysis but causes species of *Deinosuchus* and *Diplocynodon* to form a polytomy with Alligatoridae + basal globidontans. Increased resolution in the restricted analysis is due to the removal of homoplasy. Much of the homoplasy results from retained ancestral character states concentrated in the skull table and otic regions in species of *Borealosuchus* and *Deinosuchus*.

In addition to the shared ancestral character states, this analysis recovers convergent morphological features between the roughly contemporaneous species of *Borealosuchus* and *Deinosuchus*. Shared derived character states are concentrated in the mandible. Character state 42(0), dentary symphysis extends to fourth or fifth alveolus, is shared with *B. threeensis*, *B. acutidentatus*, and *B. wilsoni*. Character state 53(1), angular-surangular suture passes broadly along ventral margin of external mandibular fenestra late in ontogeny, is shared with *B. threeensis*. Character state 56(1), external mandibular fenestra present as narrow slit, no discrete fenestral concavity on angular dorsal margin, is shared with *B. threeensis*, *B. acutidentatus*, and *B. wilsoni*. Character state 64 (0), surangular extends to posterior end of retroarticular process, is shared with all species of *Borealosuchus* in this analysis.

Interestingly, *B. sternbergii* does not group with the rest of the *Borealosuchus* clade. It is found one node crownward, forming a sister-group relationship with Planocraniidae and Brevirostres (*B. sternbergii* (Planocraniidae (Brevirostres))). Additionally, *B. sternbergii* has a stronger effect on the topology at the base of Alligatoroidea relative to other species of *Borealosuchus*. Exclusion of the taxon leads to decreased resolution. However, additional complications arise with the addition of more species of *Borealosuchus*—resolution at the base of Alligatoroidea is greatly decreased as a result of homoplasy.

Functional Morphology of the Premaxillary Fenestrae

The functional significance of the premaxillary fenestrae in *D. riograndensis* is unknown. It is possible that they were a means by which to lighten the long, wide, robust snout. However, an additional hole placed at the extreme tip of the snout would presumably form a weaker architecture than otherwise—but no specimens preserve evidence of breakage and healing in this region. Alternatively, in crocodylians demonstrating fenestrae in this region, they are for receiving the anterior dentary teeth. This hypothesis must be discounted because the anterior dentary teeth in *D. riograndensis* are not long enough to project through the fenestrae, nor wide enough to form such expansive fenestration due to progressive wear.

In the *D. riograndensis* holotype specimen, the anterior wall of the premaxilla bears a dorsoventrally oriented structure extending from the roof of the element to the middle of the anterior wall. A 3-cm shelf-like projection extends posteriorly into the hollow of the premaxilla. This bony structure may have extended to the posterior, effectively walling off the nasal cavity from the paranasal air sinus. This suggests that the fenestra opened into the sinus and would have been connected to the respiratory system. The functional significance of this association is unknown.

Gigantism and Thermoregulation

On average, specimens of *D. riograndensis* are much larger than specimens of *D. schwimmeri*. The differences in size between the species of *Deinosuchus* may be due to nontaxomonic reasons. It is possible that better environmental conditions and more abundant prey existed in the west and led to larger body sizes in *D. riograndensis*. Large-scale studies of the stratigraphic and paleontological records could provide evidence in support of this hypothesis. Conversely, *D. riograndensis* may have lived longer relative to *D. schwimmeri*, allowing for continued growth (see Erickson and Brochu, 1999). A study involving the sectioning of osteological elements and counting lines of arrested growth (e.g., Erickson and Brochu, 1999) among both species may provide an answer.

The large bony narial aperture of *D. riograndensis* and *D. schwimmeri* is shared with other very large alligatoroid taxa such as *Purussaurus brasiliensis*, *Purussaurus mirandai*, and *Mourasuchus amazonensis*. The expanded bony narial apertures in these taxa has been hypothesized as a thermoregulatory adaptation because gigantism in crocodylians suggests higher, more stable body temperatures and an increased risk of overheating (Moreno-Bernal, 2007). Additionally, the large bony narial aperture may have been implicated in stress dissipation associated with the presumably immense bite forces produced by these large-bodied taxa (Aureliano et al., 2015).

The large bony narial aperture may have worked in coordination with the premaxillary fenestrae to control body temperature. In life, the premaxillary fenestrae would have connected with the respiratory system via the paranasal air sinus. Air flowing over any associated vascularized soft tissues of the premaxillary fenestrae and bony narial aperture would have exchanged heat between the animal and the environment.

Enlarged supratemporal fenestrae have also been hypothesized as being adaptations to help regulate body temperature in large-bodied alligatoroids. The tissues surrounding the supratemporal fenestrae are highly vascularized. Enlargement of these structures, as suggested for *Aegisuchus witmeri* and *Mourasuchus* (Holliday and Gardner, 2012; Bona et al., 2013), may indicate enhanced vascularization and heat dissipating function.

Adaptations for Longirostry

Species of *Deinosuchus* share a number of homoplastic character states, 53(1), 126(0), and 127(1), with gavialoids and one, 126 (0), with species of *Euthecodon*, taxa commonly reconstructed as specialized piscivores. These taxa, along with *D. riograndensis* and *D. schwimmeri*, possess the longirostrine snout condition.

The character states shared between these taxa are on the skull table and otic area, regions that are known to be functionally constrained by the demands of longirostry (Iordansky, 1973; Langston, 1973; Busby, 1995; Holliday and Witmer, 2007). Additionally, convergent evolution is suggested by similar shapes and proportions of osteological elements and sutural contacts of the skull table and otic regions. Although these taxa are distantly related, their ecologies seem to have produced similar functional morphologies related to their longirostry.

It is of note that these taxa, relative to *D. riograndensis* and *D. schwimmeri*, are markedly different in the width and depth of the snout and that species of *Deinosuchus* are reconstructed as generalist predators capable of taking down, and consuming, very large tetrapod prey (Schwimmer, 2002; Rivera-Sylva et al., 2009). Evidence of predation is preserved on the vertebra of a hadrosaurid dinosaur from the Late Cretaceous (Campanian) of Coahuila, Mexico. It would seem that the most important factor leading to the convergent morphologies of the skull table and otic area is not the prey type, depth, or width of the snout but rather the length because it is the only morphology common among the taxa here.

Enlarged supratemporal fenestrae have also been considered adaptations for seizing fast-moving, active prey (Langston, 1973). Musculus adductor mandibulae externus profundus inserts on the supratemporal fenestrae of extant crocodylians (Iordansky, 1973; Holliday and Witmer, 2007). The relatively larger supratemporal fenestrae of longirostrine crocodylians are related to the enlargement of the muscle in these taxa (Holliday and Witmer, 2007). The enlargement of the supratemporal fenestrae in *D. riograndensis* and *D. schwimmeri*, which possess broad, longirostrine snouts, may be related to the enlargement of M. adductor mandibulae externus profundus. The result would be increased speed and strength of jaw closure.

Geologic Ages of *Deinosuchus*

Deinosuchus specimens are widely distributed in Campanian strata of the United States and northern Mexico. Ages for eastern and western species differ (for a thorough discussion of locality ages, see Schwimmer, 2002). The Judith River Formation has been constrained to ~79.5–75.2 million years via numerical dating and suggests a likely range of ages for *D. hatcheri* (Rogers et al., 2016). Many beds containing *Deinosuchus* fossils have not been subject to radiometric dating, but several units that are both geographically and stratigraphically close have been (Schwimmer, 2002). The oldest occurrence is represented by '*D. rugosus*' in the Blufftown Formation along the Georgia-Alabama border. This unit has been correlated to units dated at approximately 82 million years (Schwimmer, 2002). The type locality of *D. riograndensis* (the Big Bend region of western Texas) has been suggested via correlation to be younger than the oldest '*D. rugosus*' occurrence, but with considerable overlap with younger eastern specimens now attributed to *D. schwimmeri*.

Deinosuchus riograndensis and *D. schwimmeri* were separated by lengthy expanses of marine water. During the Campanian, the Western Interior Seaway bisected North America into two landmasses. Minimum distances of hundreds of kilometers between the eastern and western shores have been predicted for this interval (Lillegraven and Ostresh, 1990; Schwimmer, 2002). Because extant alligatoroids cannot tolerate prolonged exposure to saline waters (Mazzoti and Dunson, 1984; Taplin, 1988), it is possible that their extinct relatives could not effectively osmoregulate in saline waters either (Taplin and Grigg, 1989). As such, dispersal via marine routes is impossible.

Unlike extant alligatoroids, limited evidence has been produced suggesting that specimens referable to *Deinosuchus* may have been able to tolerate some exposure to saline waters. In this case, dispersal via marine routes as is found in extant crocodyloids and gavialoids, and suggested for their extinct relatives, would be possible.

Through stable isotope analysis of carbon and oxygen from tooth enamel, Wheatley (2010) explored marine and freshwater habitat use in a number of fossil crocodylians, including specimens historically referred to as *Deinosuchus* from New Jersey and North Carolina. Because *D. schwimmeri* remains are sometimes found in marine depositional environments, they may have ingested marine resources (i.e., prey and water) (Wheatley, 2010). Wheatley's results suggest that the taxon consumed large amounts of seawater, but these results do not necessarily suggest crossing of marine barriers or saltwater tolerance. Should the taxa be able to osmoregulate in saline environments, an argument can be made that other early alligatoroids were saltwater tolerant and that the physiological adaptation was lost in the ancestor of extant alligatorids. However, because species of *Deinosuchus* were some of the largest crocodylians to have lived, it is possible that they could withstand relatively larger volumes of seawater without possessing anatomical adaptations such as lingual glands for the excretion of salt (Wheatley, 2010). Nonetheless, consumption of saltwater in an organism with no means of processing the excess salt found in seawater is unexpected behavior.

Few specimens attributed to either species have been found in sediments representing deep-water environments. This is not likely due to limited preservation because deep continental shelf deposits of the Late Cretaceous are typically chalk (Schwimmer, 2002). These deep-water deposits are less likely to be disturbed because they are beneath wave base. Preservation potential is high in these environments, yet occurrences of species of *Deinosuchus* in deeper marine deposits are rare. It is possible that the taxa did not, or did not regularly, venture into open waters and those specimens recovered in deep-water deposits were transported out to sea after the animal died. Taxa unable to swim (dinosaurs, for example) have been recovered in marine chalks (Langston, 1960; Schwimmer et al., 1993; Schwimmer, 2002), suggesting that postmortem transportation is relatively common in the fossil record.

Although there is some stratigraphic overlap between specimens attributed to *D. schwimmeri* and *D. riograndensis*, the morphological differences separating the species indicates that they were not interbreeding. Additionally, differences in size may suggest species-level separation. Should species of *Deinosuchus* be salt water intolerant like modern alligatorids, the vast distances separating the eastern and western shores of the Western Interior Seaway would have provided an insurmountable barrier for the exchange of genetic information between the species.

A common ancestral population for the taxa is likely. This ancestral population would have been present in North America prior to the Western Interior Seaway cutting the continent into two. The resulting populations created by this event would have continued to evolve in isolation from one another, creating divergent morphologies and body sizes.

CONCLUSIONS

Due to the scarcity of diagnostic characters preserved by the very incomplete holotype specimen, the type species for *Deinosuchus* should be transferred to *D. riograndensis* to promote nomenclatural stability. Additionally, because the holotype specimen for *Deinosuchus rugosus* is undiagnostic to species level, the species is determined to be a nomen dubium. A new species, *D. schwimmeri*, is erected upon a cranial specimen from Mississippi.

A phylogenetic analysis finds *D. riograndensis* and *D. schwimmeri* to be sister taxa. A complete skull and relatively complete postcranial material are known for *D. riograndensis*

(TMM 43620-1 and TMM 43632-1, respectively), whereas a complete snout (TMM 40571-1), posterior skull (MMNS VP-256), and relatively complete postcranial material (ALMNH 1002) are known for *D. schwimmeri*.

The addition of *D. hatcheri* in the phylogenetic analysis results in a polytomy among the *Deinosuchus* clade. *Deinosuchus hatcheri* is differentiated from *D. riograndensis* and *D. schwimmeri* by one character—lateral-most dorsal shield osteoderms of *D. hatcheri* bear an indentation along their margins. Only 7 characters are coded for *D. hatcheri*, as opposed to 81 and 74 characters for *D. riograndensis* and *D. schwimmeri*, respectively. The result is equally parsimonious placements of *D. hatcheri* as sister to *D. riograndensis* or *D. schwimmeri*.

The phylogenetic analysis is inconclusive regarding the relationships among the species of *Deinosuchus*. It does not solve the underlying taxonomic issue regarding the poorly known *D. hatcheri*, which shares few diagnostic elements in common with the other named species. The result of a poorly known type species is that *D. riograndensis* and *D. schwimmeri* collapse into a single species, although they may be differentiated from one another. A remedy proposed here is the transfer of the type species to *D. riograndensis*, a taxon known from a number of complete individuals. This will allow for broad morphological comparison and the differentiation of the three known species of *Deinosuchus*.

The species of *Deinosuchus* may be differentiated by osteoderm, braincase, maxillary, suborbital fenestra, and premaxillary morphology. In addition to divergent morphologies, the species of *Deinosuchus* are geographically separated by the Western Interior Seaway, with *D. hatcheri*, and *D. riograndensis* found on the western shores and *D. schwimmeri* on the eastern shores and along the Atlantic coast.

Species of *Deinosuchus* are some of the largest crocodylians known. They were the top predators in their environments and are known to have fed on dinosaurs. This work reinforces the identity of the 'terror croc' as an alligatoroid.

ACKNOWLEDGMENTS

We thank C. Mehling (AMNH), M. Norell (AMNH), M. Brown (TMM), C. Sagebiel (TMM), G. Phillips (MMNS), D. Ehret (ALMNH), M. Lamanna (CM), and A. Henrici (CM) for access to collections in their care and for the loan of specimens. Conversations with the University of Iowa Paleontology Working Group greatly improved the manuscript. This work would not be possible without the efforts of many people tirelessly working in the laboratory and the field. In addition to discussions on the stratigraphy of the Big Bend region of Texas, T. Lehman provided this project with new specimens of *D. riograndensis*. These impressive specimens, carefully excavated over a number of field seasons, allowed for a reevaluation of the species from Texas and greatly expanded character coding in phylogenetic matrices. We thank R. Hall, W. S. 'Bill' Rutland, D. Sheffield, and K. Sheffield for their discovery of the *D. schwimmeri* type specimen in the summer of 1978 as well as E. Mancini and D. Jones for leading efforts in the extraction of the specimen. We express our gratitude to E. Manning for discussions on the fauna and stratigraphy of the Coffee Sand Formation. We especially thank G. M. Cidade for pictures of the *Deinosuchus rugosus* type specimen. This work was supported by a T. Anne Cleary International Dissertation Research Fellowship, the University of Iowa Graduate Student Senate, the University of Iowa Department of Earth and Environmental Sciences, and the New York Institute of Technology College of Osteopathic Medicine–Arkansas.

LITERATURE CITED

Aguilera, O. A., D. Riff, and J. Bocquentin-Villanueva. 2006. A new giant *Purussaurus* (Crocodyliformes, Alligatoridae) from the Upper Miocene Urumaco Formation, Venezuela. Journal of Systematic Palaeontology 4:221–232.

Aureliano, T., A. M. Ghilardi, E. Guilherme, J. P. Souza-Filho, M. Cavalcanti, and D. Riff. 2015. Morphometry, bite-force, and paleobiology of the late Miocene Caiman *Purussaurus brasiliensis*. PLoS ONE 10:e0117944. doi: 10.1371/journal.pone.0117944.

Baird, D., and J. Horner. 1979. Cretaceous dinosaurs of North Carolina. Brimleyana 2:1–28.

Barbosa-Rodrigues, B. 1892. Les Reptiles crocodil de la vallée de l'Amazone. Vellosia 2:41–46.

Benton, M. J., and J. M. Clark. 1988. Archosaur phylogeny and the relationships of the Crocodylia; pp. 295–338 in M. J. Benton (ed.), The Phylogeny and Classification of the Tetrapods, Volume 1. Oxford University Press, Oxford.

Bona, P., F. J. Degrange, and M. S. Fernández. 2013. Skull anatomy of the bizarre crocodylian *Mourasuchus nativus* (Alligatoridae, Caimaninae). Anatomical Record 296:227–239.

Bremer, K. 1988. The limits of amino acid sequence data in angiosperm phylogenetic reconstruction. Evolution 42:795–803.

Bremer, K. 1994. Branch support and tree stability. Cladistics 10:295–304.

Brochu, C. A. 1999. Phylogenetics, taxonomy, and historical biogeography of Alligatoroidea. Journal of Vertebrate Paleontology 19(2, Supplement):9–100.

Brochu, C. A. 2004. A new Late Cretaceous gavialoid crocodylian from eastern North America and the phylogenetic relationships of thoracosaurs. Journal of Vertebrate Paleontology 24:610–633.

Brochu, C. A. 2010. A new alligatorid from the Lower Eocene Green River Formation of Wyoming and the origin of caimans. Journal of Vertebrate Paleontology 30:1109–1126.

Brochu, C. A. 2011. Phylogenetic relationships of *Necrosuchus ionensis* Simpson, 1937 and the early history of caimanines. Zoological Journal of the Linnean Society 163:S228–S256.

Brochu, C. A., D. C. Parris, B. S. Grandstaff, R. K. Denton Jr, and W. B. Gallagher. 2012. A new species of *Borealosuchus* (Crocodyliformes, Eusuchia) from the Late Cretaceous–early Paleogene of New Jersey. Journal of Vertebrate Paleontology 32:105–116.

de Broin, F., and P. Taquet. 1966. Découverte d'un Crocodilien nouveau dans le Crétacé inférieur du Sahara. Comptes Rendus de l'Académie des Sciences à Paris, Série D 262:2326–2329.

Busbey, A. B. 1995. The structural consequences of skull flattening in crocodilians; pp. 173–192 in J. J. Thomason (ed.), Functional Morphology in Vertebrate Paleontology. Cambridge University Press, New York.

Cidade, G. M., A. Solórzano, A. D. Rincón, D. Riff, and A. S. Hsiou. 2017. A new *Mourasuchus* (Alligatoroidea, Caimaninae) from the late Miocene of Venezuela, the phylogeny of Caimaninae and considerations on the feeding habits of *Mourasuchus*. PeerJ 5:e3056.

Clark, J. M. 2011. A new shartegosuchid crocodyliform from the Upper Jurassic Morrison Formation of western Colorado. Zoological Journal of the Linnean Society 163:S152–S172.

Colbert, E. H., and R. T. Bird. 1954. A gigantic crocodile from the Upper Cretaceous beds of Texas. American Museum Novitates 1688:1–22.

Cope, E. D. 1871. Observations on the distribution of certain extinct Vertebrata in North Carolina. Proceedings of the American Philosophical Society 12:210–216.

Cossette, A. P., and C. A. Brochu. 2018. A new specimen of the alligatoroid *Bottosaurus harlani* and the early history of character evolution in alligatorids. Journal of Vertebrate Paleontology 38:1–22.

Cushing, E. M., E. H. Boswell, and R. L Hosman. 1964. General Geology of the Mississippi Embayment. U.S. Department of the Interior, Washington, D.C., 32 pp.

Dockery, D. T., and S. P. Jennings. 1988. Stratigraphy of the Tupelo tongue of the Coffee Sand (upper Campanian), northern Lee County, Mississippi. Mississippi Geology 9:1–7.

Erickson, B. R. 1976. Osteology of the Early eusuchian crocodile *Leidyosuchus formidabilis*, sp. nov. Monograph (2): Paleontology. The Science Museum of Minnesota, Saint Paul, Minnesota, 61 pp.

Erickson, G. M., and C. A. Brochu. 1999. How the 'terror crocodile' grew so big. Nature 398:205.

Erickson, G. M., A. K. Lappin, and K. A. Vliet. 2003. The ontogeny of bite-force performance in American alligator (*Alligator mississippiensis*). Journal of Zoology 260:317–327.

Erickson, G. M., P. M. Gignac, S. J. Steppan, A. K. Lappin, K. A. Vliet, J. D. Brueggen, B. D. Inouye, D. Kledzik, and G. J. Webb. 2012. Insights into the ecology and evolutionary success of crocodilians revealed through bite-force and tooth-pressure experimentation. PLoS ONE 7:e31781.

Efron, B. 1979. Bootstrapping methods: another look at the jackknife. Annals of Statistics 7:1–26.

Emmons, E. 1858. Report of the North Carolina Geological Survey. Agriculture of the Eastern Counties; Together with Descriptions of the Fossils of the Marl Beds. H. D. Turner, Raleigh, North Carolina, 314 pp.

Felsenstein, J. 1985. Confidence limits on phylogenies: an approach using the bootstrap. Evolution 39:783–791.

Gilmore, C. W. 1911. A new fossil alligator from the Hell Creek Beds of Montana. Proceedings of the United States National Museum 41:297–302.

Gmelin, J. 1789. Linnei Systema Naturae. Leipzig, 1057 pp.

Goloboff, P. A., J. S. Farris, and K. C. Nixon. 2008. TNT, a free program for phylogenetic analysis. Cladistics 24:774–786.

Goloboff, P. A., J. S. Farris, M. Källersjö, B. Oxelman, and M. J. Ramírez. 2003. Improvements to resampling measures of group support. Cladistics 19:324–332.

Gray, J. E. 1844. Catalogue of Tortoises, Crocodilians, and Amphisbaenians in the Collection of the British Museum. London, British Museum (Natural History), 80 pp.

Grigg, G., and D. Kirshner. 2015. Biology and Evolution of Crocodylians. CSIRO Publishing, Clayton, Queensland, Australia, 672 pp.

Hastings, A. K., M. Reisser, and T. M. Scheyer. 2016. Character evolution and the origin of Caimaninae (Crocodylia) in the New World Tropics: new evidence from the Miocene of Panama and Venezuela. Journal of Paleontology 90:317–332.

Hay, O. P. 1902. Bibliography and Catalogue of Fossil Vertebrata of North America. Geological Survey Bulletin 179. United States Government Printing Office, Washington, D.C., 868 pp.

Holland, W. J. 1909. *Deinosuchus hatcheri*, a new genus and species of crocodile from the Judith River Beds of Montana. Annals of the Carnegie Museum 6:281–294.

Holliday, C. M., and N. M. Gardner. 2012. A new eusuchian crocodyliform with novel cranial integument and its significance for the origin and evolution of Crocodylia. PLoS ONE 7:e30471.

Holliday, C. M., and L. M. Witmer. 2007. Archosaur adductor chamber evolution: integration of musculoskeletal and topological criteria in jaw muscle homology. Journal of Morphology 268:457–484.

Iordansky, N. N. 1973. The skull of the Crocodylia; pp. 201–262 in C. Gans and T. S. Parsons (eds.), Biology of the Reptilia, Volume 4. Academic Press, New York.

Irmis, R. B., J. H. Hutchison, J. J. W. Sertich, and A. L. Titus. 2013. Crocodyliforms from the Late Cretaceous of Grand Staircase–Escalante National Monument and vicinity, southern Utah, U.S.A.; pp. 424–444 in A. L. Titus and M. A. Loewen (eds.), At the Top of the Grand Staircase: The Late Cretaceous of Southern Utah. Indiana University Press, Bloomington, Indiana.

Lambe, L. M. 1907. On a new crocodilian genus and species from the Judith River Formation of Alberta. Transactions of the Royal Society of Canada 4:219–244.

Langston, W. 1960. The vertebrate fauna of the Selma Formation of Alabama. Part IV. The dinosaurs. Fieldiana: Geology Memoirs 3:317–361.

Langston, W. 1973. The crocodilian skull in historical perspective; pp. 263–284 in C. Gans and T. S. Parsons (eds.), Biology of the Reptilia, Volume 4. Academic Press, New York.

Lillegraven, J. A., and L. M. Ostresh. 1990. Late Cretaceous (earliest Campanian/Maastrichtian) evolution of western shorelines of the North American Western Interior Seaway in relation to known mammalian faunas; pp. 1–30 in T. M. Brown and K. D. Rose (eds.), Dawn of the Age of Mammals in the Northern Part of the Rocky Mountain Interior, North America. Geological Society of America Special Paper 243. Boulder, Colorado.

Lucas, S. G., R. M. Sullivan, and J. A. Spielmann. 2006. The giant crocodylian *Deinosuchus* from the Upper Cretaceous of the San Juan Basin, New Mexico. Late Cretaceous Vertebrates from the Western Interior. New Mexico Museum of Natural History and Science Bulletin 35:245–248.

Maddison, W. P., and D. R. Maddison. 2015. Mesquite: a modular system for evolutionary analysis. Version 3.04. Available at mesquiteproject.org. Accessed January 2, 2018.

Martin, J. E. 2010. A new species of *Diplocynodon* (Crocodylia, Alligatoroidea) from the Late Eocene of the Massif Central, France, and the evolution of the genus in the climatic context of the Late Palaeogene. Geological Magazine 147:596–610.

Martin, J. E., T. Smith, F. Lapparent de Broin, F. Escuillié, and M. Delfino. 2014. Late Palaeocene eusuchian remains from Mont de Berru, France, and the origin of the alligatoroid *Diplocynodon*. Zoological Journal of the Linnean Society 172:867–891.

Martin, J. E., M. Delfino, G. Garcia, P. Godefroit, S. Berton, and X. Valentin. 2015. New specimens of *Allodaposuchus precedens* from France: intraspecific variability and the diversity of European Late Cretaceous eusuchians. Zoological Journal of the Linnean Society 176:607–631.

Meyer, H. von. 1832. Paleologica zur Geshichte der Erde und irher Geschöpfe. S. Schmerber, Frankurt-am-Main, 560 pp.

Miller, H. W. 1967. Cretaceous vertebrates from Phoebus Landing, North Carolina. Proceedings of the Academy of Natural Sciences of Philadelphia 119:219–239.

Moreno-Bernal, J. W. 2007. Size and paleoecology of giant Miocene South American crocodiles (Archosauria: Crocodylia). Journal of Vertebrate Paleontology 27(3, Supplement):120A.

Nesbitt, S. J. 2011. The early evolution of archosaurs: relationships and the origin of major clades. Bulletin of the American Museum of Natural History 352:1–292.

Porter, W. R., J. C. Sedlmayr, and L. M. Witmer. 2016. Vascular patterns in the heads of crocodilians: blood vessels and sites of thermal exchange. Journal of Anatomy 229:800–824.

Price, L. I. 1964. Sobre o cranio de um grande crocodilideo extinto do Alto Rio Jurua, Estado do Acre. Anais da Academia Brasileira de Ciência 36:59–66.

Rivera-Sylva, H. E., E. Frey, and J. R. Guzmán-Gutiérrez. 2009. Evidence of predation on the vertebra of a hadrosaurid dinosaur from the Upper Cretaceous (Campanian) of Coahuila, Mexico. Carnets de Géologie, Letter 2:1–6.

Rogers, R. R., S. M. Kidwell, A. L. Deino, J. P. Mitchell, K. Nelson, and J. T. Thole. 2016. Age, correlation, and lithostratigraphic revision of the Upper Cretaceous (Campanian) Judith River Formation in its type area (north-central Montana), with a comparison of low-and high-accommodation alluvial records. The Journal of Geology 124:99–135.

Schwimmer, D. R. 2002. King of the Crocodylians: The Paleobiology of *Deinosuchus*. Indiana University Press, Bloomington, Indiana, 240 pp.

Schwimmer, D. R. 2010. Bite marks of the giant crocodilian *Deinosuchus* on Late Cretaceous (Campanian) bones; pp. 183–190 in J. Milàn, S. G. Lucas, M. G. Lockley, and J. A. Spielmann (eds.), Crocodyle Tracks and Traces. New Mexico Museum of Natural History and Science Bulletin 51. Albuquerque, New Mexico.

Schwimmer, D. R., G. D. Williams, J. L. Dobie, and W. G. Siesser. 1993. Late Cretaceous dinosaurs from the Blufftown Formation in western Georgia and eastern Alabama. Journal of Paleontology 67:288–296.

Seidel, M. R. 1979. The osteoderms of the American alligator and their functional significance. Herpetologica 35:375–380.

Sereno, P. C., H. C. Larsson, C. A. Sidor, and B. Gado. 2001. The giant crocodyliform *Sarcosuchus* from the Cretaceous of Africa. Science 294:1516–1519.

Taplin, L. E. 1988. Osmoregulation in crocodilians. Biological Reviews 63:333–377.

Taplin, L. E., and G. C. Grigg. 1989. Historical zoogeography of the eusuchian crocodilians: a physiological perspective. American Zoologist 29:885–901.

Trutnau, L., and R. Sommerlad. 2006. Crocodilians: Their Natural History and Captive Husbandry. Edition Chimaira, Frankfurt am Main, Germany, 646 pp.

Wheatley, P. V. 2010. Understanding saltwater tolerance and marine resource use in the Crocodylia: a stable isotope approach. Ph.D. dissertation, University of California, Santa Cruz, California, 175 pp.

Williamson, T. E. 1996. ?*Brachychampsa sealeyi*, sp. nov. (Crocodylia, Alligatoroidea) from the Upper Cretaceous (lower Campanian) Menefee Formation, northwestern New Mexico. Journal of Vertebrate Paleontology 16:421–431.

Wu, X. C., D. B. Brinkman, and A. P. Russell. 1996. A new alligator from the Upper Cretaceous of Canada and the relationship of early eusuchians. Palaeontology 39:351–376.

Submitted October 10, 2018; revisions received December 19, 2019; accepted January 28, 2020.
Handling editor: Gabriel Bever.